An investigation of neurochemical, structural and functional characteristics in the murine model of collagen induced arthritis.

© Kerrie A. Mulloy B.Sc (Hons)

October 2010

A thesis submitted to the University of Glasgow, Institute of Neuroscience and Psychology, College of Medical, Veterinary and Life Sciences, for the degree of Doctor of Philosophy.

Wellcome Surgical Institute,
Garscube Estate,
Glasgow G61 1QH

UNIVERSITY
of
GLASGOW

Declaration

I solemnly declare that this thesis comprises my own original work and has not been accepted in any previous application for a degree. All sources of information have been referenced.

Kerrie A. Mulloy

Acknowledgements.

I would like to thank my supervisors Debbie Dewar and Mhairi Macrae for taking the time and effort, even before I arrived to meet with Immunologists and Psychiatrists to discuss collaborative areas of research and come up with the concept of my PhD. I would also like to thank them for their support and guidance through out my time here in the department.

Due to my supervisors wide network of connections I was able to meet and learn valuable skills from other departments and universities. I would like to thank Darren Asquith for teaching me the CIA model as without it I would not have a thesis. I would also like to thank Neil Dawson who demonstrated the semi-quantitative [^{14}C]-2-deoxyglucose autoradiographic technique and his new equation to calculate glucose metabolism.

I would also like to thank all the current and past students who lent a hand and taught me the techniques I required. In particular I would like to thank Dave Tarr who was invaluable during the [^{14}C]-2-deoxyglucose autoradiographic experiments and the experiments would not have been as successful without him.

Finally I would like to thank all the people in the background, including the technicians who have become like surrogate mothers during the course of my time here and my friends and family for supporting me and being there during my the much needed periods of time out.

Summary.

Depression and rheumatoid arthritis have an estimated co-morbidity of 13-20%. However, the mechanisms whereby peripheral inflammation might alter brain function are unknown. We hypothesised that pro-inflammatory cytokines released in the periphery will result in neurochemical, structural and functional changes related to depression. Therefore, the aim of this thesis was to investigate altered central nervous system function in a rodent model of rheumatoid arthritis, the murine model of collagen induced arthritis (CIA). The CIA model is an established model used to investigate novel anti-inflammatory agents and resembles rheumatoid arthritis as the model is chronic and involves an autoimmune response to type II collagen. To our knowledge brain function in the CIA model has not previously been examined. Therefore, we began by identifying key neurochemical, cellular and functional changes associated with depression which had the greatest likelihood of being influenced by pro-inflammatory cytokines.

Serotonin and dopamine transporter densities.

The serotonergic system is implicated in the pathology of depression and there is evidence that pro-inflammatory cytokines may influence the serotonin transporter (SERT) *in vitro*. *In vitro* autoradiography binding of [^{125}I]-β-carbomethoxy-3-β-(4 iodophenyl)tropane ([^{125}I]-β-CIT) in the presence of mazindol and [^{3}H]-citalopram was used to determine SERT binding in mice with CIA and controls. Out of 15 regions of interest investigated a significant change in SERT binding was identified by [^{125}I]-β-CIT binding, in the nucleus accumbens (58%), thalamus (62%), and dentate gyrus (-60%) in CIA mice compared to controls. However, no significant difference in SERT density was detected in any region by [^{3}H]-citalopram binding. Dopamine transporter (DAT) binding sites were also examined using [^{125}I]-βCIT in the presence of displacer fluoxetine and [^{3}H]-WIN 35,428. Out of 14 regions investigated a significant difference in DAT binding was only observed in the caudate putamen (95%) in the CIA group in comparison to the control group. However, no significant difference in DAT binding was detected in any region by [^{3}H]-WIN 35,428 binding. A limitation of this study was the small group sizes and

the degree of clinical symptoms in the CIA group. The data suggest that SERT and DAT transporter densities are not altered by CIA.

[^{14}C]-2-Deoxyglucose autoradiographic study of local cerebral glucose utilisation.

To investigate brain function the [^{14}C]-2-deoxyglucose ([^{14}C]-2-DG) autoradiographic technique and a challenge to the serotonergic system were employed to identify any abnormalities in regional cerebral glucose utilisation. Overall there was no significant difference in the index of cerebral glucose utilization (iLCMRglu) in mice with chronic clinical symptoms of CIA. To investigate altered serotonergic function in the CIA model fenfluramine, a drug which stimulates serotonin release and blocks serotonin re-uptake was employed. Fenfluramine challenge in the CIA group resulted in only 3 out of the 35 regions of interest examined being significantly different from fenfluramine challenged controls. The orbital cortex (-41%) and the molecular level of the hippocampus (-26%) demonstrated a significant difference in iLCMRglu Overall the data suggest minimal influence of CIA on brain function.

Cell proliferation and cell survival in the hippocampus.

Hippocampal atrophy is implicated in the pathology of depression and there is evidence to suggest that pro-inflammatory cytokines reduce cell proliferation *in vitro.* To investigate hippocampal cell proliferation mice were administered 5' –bromo-2'-deoxyuridine (BrdU), a marker of proliferating cells, prior to and after developing chronic clinical symptoms of CIA. There was no significant difference in cell proliferation prior to the development of clinical symptoms. There was a statistically significant increase in cell proliferation after chronic clinical symptoms in the CIA model in one out of two separate experiments. The data has been interpreted cautiously due to the fact the significant increase in cell proliferation was not reproduced. Cell survival was also investigated during the onset of clinical symptoms and the data demonstrated no significant effect of CIA on cell survival.

Conclusion.

The data indicate minimal influence of peripheral inflammation on the central nervous system, at least in the murine CIA model. Two possible explanations are that the CIA murine model is not a suitable model to detect changes in brain function associated with rheumatoid arthritis or that uninvestigated neurochemical systems play a role. This thesis highlights our limited understanding of the CIA model and whether or not it represents the features associated with rheumatoid arthritis other then peripheral inflammation. Further characterisation of the brain and development of the CIA model is required to establish if it is a suitable model to investigate the association between depression and rheumatoid arthritis. This is important as understanding the cause of depression and how the cause influences the brain will allow for the development of more specific treatments.

List of contents.

List of figures

List of tables

Chapter 1

General introduction.

1.1 Depression.

Everyone in their lifetime will have periods of low mood, however depression is characterised as a persistently low mood or a loss of interest in pleasure for an extended period of time (aan het et al., 2009). Other possible symptoms include anorexia, loss of motivation, cognitive decline and neurovegetative symptoms. According to the World Health Organisation (WHO) depression affects approximately 121 million people worldwide and in 2001 was the 4th highest disease in relation to years lost through disability. The WHO also predicts that depression will be the 2nd most prevalent disease world wide by 2020 in all ages and both sexes. It is estimated that in 2000 the cost of depression was £9 billion including the value of lost productivity in society (Thomas and Morris, 2003). As the prevalence of depression is expected to escalate it will become increasingly important to develop effective treatments for depression, to improve patient's welfare and decrease the economic cost.

1.1.1 Serotonergic transmission.

Depression is an extremely complex disorder and the involvement of the serotonergic system is well established in the pathology of depression.
Most serotonergic neuronal pathways originate from the raphe nuclei. The caudal raphe nucleus innervates motorneurons in the ventral horn of the spinal cord and comprise the descending serotonergic pathway. The medial and dorsal raphe nuclei project to forebrain structures and comprise the ascending serotonergic pathways. The ascending serotonergic pathways innervate the sensory system which includes the somatosensory and entorhinal cortex and the limbic system which includes the amygdala and hippocampus, structures involved in emotional and cognitive behaviour (Jacobs and Azmitia, 1992).

Serotonergic neuronal pathways synthesise, store and release serotonin a monoamine neurotransmitter chemically defined as 5-hydroxytryptamine (5-HT, Figure 1.1.1). Serotonin biosynthesis is a two step reaction. The availability of the amino acid tryptophan is the rate limiting step within this reaction. Dietary tryptophan competes with other amino acids to be transported across the blood brain barrier (BBB). Once across the BBB *tryptophan hydrogenase* an enzyme specific for serotonin neurons metabolises tryptophan to the intermediate product 5-hydroxytryptophan, which is further metabolised by amino-acid *decarboxylase* to serotonin (Fuller, 1980). Serotonin is then transported by an adenosine triphosphate (ATP) driven pump into vesicles in preparation for release.

Depolarisation of the nerve terminal by an action potential opens voltage gated calcium channels. The influx of calcium induces calcium dependent exocytosis of serotonin containing vesicles. Following release of serotonin into the synaptic cleft it can be transported back into the pre-synaptic terminal. Once back in the nerve terminal the monoamine can be repackaged into vesicles or can be metabolically degraded. All the monoamines are degraded by the enzyme *monoamine oxidase*. *Monoamine oxidase* is located on the surface membrane of mitochondria and metabolises serotonin to 5-hydroxyindoleactic acid. Alternatively once released serotonin can diffuse across the synaptic cleft where it activates post-synaptic receptors. There are seven types of serotonin receptors (5-HT_{1-7}) which are further subdivided (A-D). There are at least 14 serotonin receptor subtypes that have been differentiated on a genetic basis but the functional characteristics are still unknown (Alexander et al., 2008).

5-HT_{1A} receptors are located both pre- and post-synaptically. Post-synaptic 5-HT_{1A} receptors are localised in limbic regions including the cerebral cortex, hippocampus, amygdala and septum. The majority of 5-HT_{1A} receptors are somatodendritic 5-HT_{1A} autoreceptors which are localised on pre-synaptic membranes of serotonergic neurones. When activated somatodendritic 5-HT_{1A} autoreceptors reduce serotonin neuron firing and serotonin release (Ogren et al., 2008). Chronic exposure to selective serotonin re-uptake inhibitors is believed to desensitise 5-HT_{1A} receptors removing the inhibition on neuronal firing leading to an increase in serotonin in the synaptic cleft (Stahl, 1998).

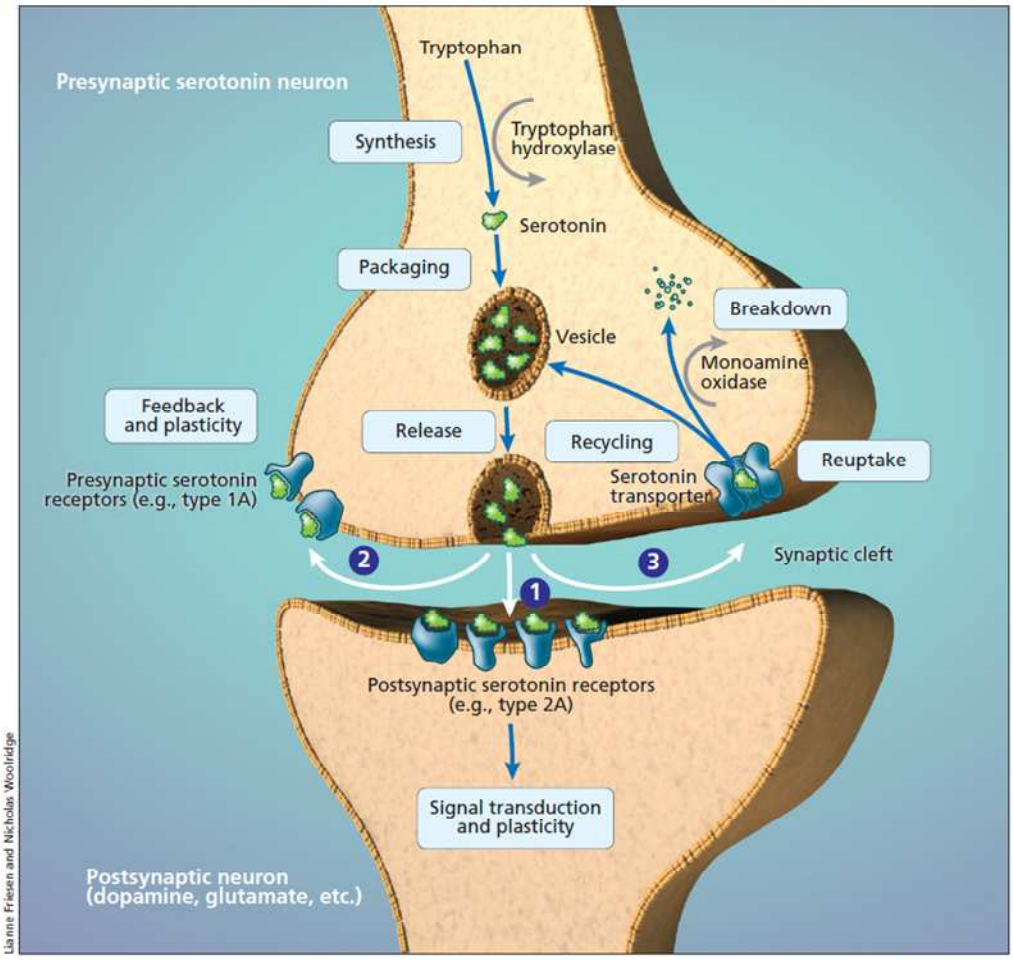

Figure 1.1.1 The serotonin synapse.

Tryptophan hydrogenase synthesises serotonin from the pre-cursor tryptophan. Serotonin is packaged into vesicles and released into the pre-synaptic cleft. 1. Following release, serotonin can diffuse across the synaptic cleft where it activates post-synaptic receptors. 2. Alternatively serotonin can activate 5-HT_{1A} autoreceptors on the neuron it was released from to provide neuronal feedback. 3. Serotonin can also be recycled and transported back into the pre-synaptic terminal and once back in the nerve terminal, serotonin can be repackaged into vesicles or can be metabolically degraded.
From aan het et al. (aan het et al., 2009)

1.1.2 Monoamine hypothesis of depression.

The monoamine hypothesis of depression began to take shape in the 1950s due to the understanding of the mechanism of action of two drugs reserpine and iproniazid. These drugs were only used for a short time as iproniazid was withdrawn due to a possible association with jaundice (Baumeister et al., 2003) and reserpine due to speculation that it did not alleviate the symptoms of depression, but produced them (HARRIS, 1957). Reserpine was shown to block monoamine transporters (Henry and Scherman, 1989) and iproniazid was shown to alleviate the symptoms of depression by inhibition of monoamine oxidase (Baumeister et al., 2003). The problem was the tricyclic antidepressant, imipramine also alleviated the symptoms of depression, but through a different mechanism of action compared to iproniazid. The mechanism of impiramine was later shown using platelets to block serotonin re-uptake (MARSHALL et al., 1960). Joseph Schildkraut became the founder of the monoamine hypothesis of depression by demonstrating that drugs which decreased monoamine levels produced symptoms of depression and the reverse, that drugs which increased monoamine levels alleviated the symptoms of depression (Schildkraut JJ, 1965).

1.1.3 Antidepressant treatment.

To date the majority of medications developed for the treatment of depressive symptoms are monoamine based. At present the conventional treatment for depression are selective serotonin re-uptake inhibitors which have superseded tricyclic antidepressants (Philip et al., 2010). Tricyclic antidepressants and selective serotonin re-uptake inhibitors increase the availability of monoamines in the synapse by blocking the re-uptake of serotonin into the nerve terminal. Antidepressants do not always effectively treat depression and thirty percent of depressed patients are treatment resistant (Sackeim, 2001). There is growing awareness that our knowledge of depression is still very limited and that the monoamine hypothesis of depression is not the complete solution. Recently a meta-analysis study investigated the clinical effectiveness of antidepressant treatment in clinical trials. The study found that according to the National Institute of Clinical Excellence criteria, in moderately depressed patients the attenuation of

clinical symptoms by antidepressant treatment or placebo did not significantly differ. Only in severely depressed patients was there a significant difference between antidepressant treatment and placebo, which was attributed to a decreased response to placebo (Kirsch et al., 2008). This suggests that in clinical trials antidepressants are not always as effective as reported and that the results depend on the degree of the depressive symptoms. In addition depletion of serotonin in healthy volunteers by acute tryptophan depletion does not produce depression (Ruhe et al., 2007) and antidepressant treatment alters the concentration of tryptophan in the synapse within hours of administration. However, it can take weeks before a beneficial effect on depressive symptoms is observed (Baldessarini, 1989). The delay in the beneficial effect of antidepressants may not be due to the change in tryptophan but may be the time required to influence the serotonin transporter. Treatment with antidepressant paroxetine takes over 6 weeks to reduce the level of serotonin transporter binding in the amygdala and dorsal raphe nucleus (Gould et al., 2003). Similarly, radioligand binding assays have shown that fluoxetine, citalopram, or amitriptyline treatment take over 30 days to reduce the levels of serotonin transporter binding in the cortex and hippocampus (Nadgir and Malviya, 2008). The monoamine theory of depression does not completely explain the neurobiology of depression and it is now believed that depression is a heterogeneous disease in which multiple neurochemical systems are interacting.

1.2 Cytokine theory of depression.

During the 1980's there was a gradual realisation that the brain and the immune system were not independent of each other and that there is bi-directional communication (Blalock, 1984; Dantzer R and Kelley KW, 1989). The cytokine theory of depression, also known as the macrophage theory of depression, suggests that systemic pro-inflammatory cytokines are involved in the development of depression (Smith, 1991; Maes et al., 1995). Cytokines are a heterogeneous group of messenger molecules released from immunocompetent cells including T-cells, monocytes and macrophage/microglia in response to infection or tissue damage. There are two distinct classes of cytokines which modulate the immune response in a complementary manner. Pro-inflammatory cytokines including

interleukin (IL) -1β, IL-2, IL-6 tumour necrosis factor-α (TNF) and interferon-γ (IFN) are involved in the inflammatory process. In comparison anti-inflammatory cytokines including IL-4 and IL-10 neutralise the immune response by deactivating monocytes, macrophage/microglia and T-cells.

In response to infection, pro-inflammatory cytokines IL-1β, IL-6 and TNF-α act on their corresponding brain receptors to produce sickness behaviour. Sickness behaviour is the term used to describe an immune response to conserve energy in both humans and a variety of animals and is characterised by fever, fatigue, depression/reduced motivation, anorexia and reduced grooming (Hart, 1988). Infection or endotoxin lipopolysaccharide (LPS) can activate the innate immune response involving the activation of macrophage and microglia, which express IL-1. IL-1β was the first cytokine discovered and has been the most extensively researched due to its role in the inflammatory process (Dinarello, 2005). IL-1β is important in the immune response to infection as microinjection of recombinant IL-1β into the rat ventromedial hypothalamus has been shown to result in anorexia and weight loss (Kent et al., 1994). In comparison, pre-treatment with an IL-1 receptor antagonist into the lateral ventricle prior to intraperitoneal injection of LPS resulted in reduced IL-1β mRNA expression as well as reduced TNF-α and IL-6 mRNA expression within the hypothalamus (Laye et al., 2000). IL-1β is not the only cytokine involved in the immune response as in IL-1 receptor knock out mice, sickness behaviour was still produced in response to systemic administration of LPS and by injecting LPS directly into the lateral ventricle suggesting the involvement of other pro-inflammatory cytokines (Bluthe et al., 2000).

1.2.1 Immune activation in depressed patients.

Depression is believed to be both a psychiatric disease as well as an immune disorder (Miller et al., 2009). There have been consistent reports of increased pro-inflammatory cytokines in depressed patients including elevated serum or plasma levels of TNF-α (Tuglu et al., 2003; Hestad et al., 2003; Suarez et al., 2003; Tsao et al., 2006), IL-1β (Suarez et al., 2003; Thomas et al., 2005; Tsao et al., 2006), IL-6 (Sluzewska et al., 1996) and IFN-γ mRNA expression (Tsao et al., 2006). There is also evidence of increased numbers of cytokine receptors in the serum of

depressed patients including the soluble IL-6 receptor and soluble IL-2 receptor (Sluzewska et al., 1996).

In depressed patients the increase in pro-inflammatory cytokines is believed to occur through cell-mediated immune activation. Cell-mediated immunity involves the interaction between monocytes and T-cells (Figure 1.2.1). Depression is characterised by increased number of leukocytes, a group of immune cells involved in the innate immune response including neutrophils, monocytes and macrophage (Maes et al., 1992; Kronfol and House, 1989). Monocytes secrete the pro-inflammatory cytokines, IL-1β, IL-6 and neopterin. Increased neopterin concentrations (Duch et al., 1984; Dunbar et al., 1992) in depressed patients represent an increase in monocytes. Monocytes migrate from the blood stream to the tissue where they differentiate into macrophage or dendritic cells which act as antigen presenting cells to T-cells. Major histocompatibility complex class II molecules (MCH II) are expressed on the surface of antigen presenting cells which present the antigen to T-cells stimulating activation. The MHC II, HLA-DR is expressed only on mature activated peripheral T cells and is elevated in patients with depression (Maes et al., 1993). Once activated the T-cells produce pro-inflammatory cytokines IFN-γ and IL-2, which can promote T-cell proliferation and activation or provide positive feedback to monocytes (Maes, 2010). In comparison a recent study in the literature found a reduced T regulatory (T_{reg}) cell population, a subtype of T-cell responsible for suppressing the immune response, and reduced anti-inflammatory cytokine IL-10 expression (Li et al., 2010). The overall findings published in the literature provide considerable evidence to confirm an active immune system in patients with depressive symptoms.

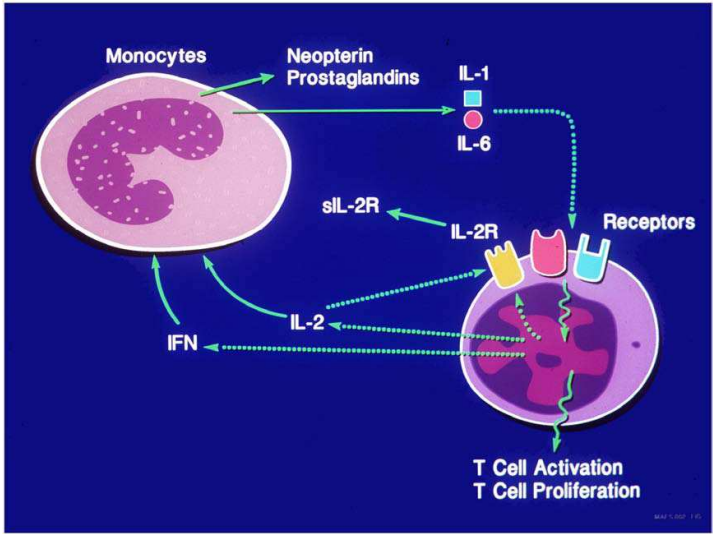

Figure 1.2.1 Cell-mediated immune response.

The innate immune response is characterised by the activation of monocytes/macrophage which increase the expression of pro-inflammatory cytokines IL-1 and IL-6. IL-1 and IL-6 interact with the T-cell, stimulating IFN and IL-2 which can promote T-cell proliferation and activation of monocytes/macrophage. From Maes. (Maes, 2010)

1.2.2 Immune activation causes symptoms of depression.

The cytokine theory was based on evidence of an active immune system in patients with depression along with evidence in rodent behavioural studies which illustrated that immune activation produced symptoms of anhedonia, the key symptom of depression. Two rodent behavioural studies have demonstrated anhedonia. LPS and IL-1 treated rats demonstrated the inability to experience pleasure through decreased sexual behaviour (Yirmiya, 1996; Yirmiya et al., 1995). In addition LPS treated rats also demonstrated reduced saccharine preference in both fluid deprived and non-deprived rodents which was attenuated by chronic treatment with the antidepressant imipramine (Yirmiya, 1996). Animals do not get depressed in the same manner as humans and care is required to disassociate sickness behaviour from possible symptoms of depression or anxiety in rodents. This was highlighted in a study investigating the effect of peripheral IL-1 or LPS on mouse behaviour in the elevated plus maze and open field test. The paper concluded that the sickness behaviour of reduced locomotion made it impossible to determine if the results were due to elevated anxiety or reduced locomotion (Swiergiel and Dunn, 2007).

It was only relatively recently that the first evidence emerged in humans suggesting cytokines are responsible for the development of depression after cancer patients

that received 5 days of IFN-α therapy produced symptoms of depression (Capuron et al., 2000). It has since been shown that patients receiving cytokine therapy develop depressive symptoms along side alterations in the central nervous system (CNS) related to the development of depression. For instance cancer patients undergoing IL-2 and/or IFN-α therapy had clinical symptoms of depression, the severity of which negatively correlated with serum tryptophan concentrations (Capuron et al., 2002). Similarly, IFN-α therapy induced depression which negatively correlated with reduced serum levels of brain-derived neurotrophic factor (BDNF). BDNF regulates neural survival and differentiation and is believed to be required for neurogenesis (Linnarsson et al., 2000). IFN-α therapy in cancer patients has also been shown to increase the cortisol response which correlated with the depressive score (Capuron et al., 2003b). This demonstrates that cytokine therapy may reduce serotonin, may decrease neurogenesis or may stimulate the hypothalamic-pituitary-adrenal axis (HPA-axis) to release glucocorticoids, all of which have been implicated in the pathology of depression.

1.3 Cytokines, depression and the serotonergic system.

1.3.1 Pro-inflammatory cytokines influence tryptophan metabolism.

Pro-inflammatory cytokines are believed to directly alter the serotonergic system by driving indoleamine 2,3- dioxygenase (IDO) activity to metabolise tryptophan to metabolite kynurenine. Kynurenine can then be further metabolised to kynurenic acid or 3-hydroxy kynurenine and quinolinic acid (Figure 1.4.1). This would deprive the serotonin pathway of tryptophan, consistent with the monoamine hypothesis of depression. Cytokine therapy has been shown to reduce tryptophan levels in cancer patients which was directly related to the development and intensity of depressive symptoms (Capuron et al., 2002). IDO is implicated in the mechanism of cytokine induced depression as patients receiving IFN-α therapy also have reduced tryptophan availability, increased plasma kynurenine and an increased kynurenine/tryptophan plasma ratio (Capuron et al., 2003a; Wichers et al., 2005). Similarly in rodents, blockade of IDO inhibits LPS-induced depression and normalised the kynurenine/tryptophan ratio in the brain (O'Connor et al., 2008). There is also evidence of hippocampal atrophy in depressed patients (Sheline et

al., 1996) which may be due to the neurotoxic effects of 3-hydroxy kynurenine and quinolinic acid (discussed in detail in section 1.4).

1.3.2 Pro-inflammatory cytokines influence the serotonin transporter.

There is some evidence that pro-inflammatory cytokines directly alter the serotonergic transporter (Rang et al., 2003). Pro-inflammatory cytokines IL-1β (Ramamoorthy et al., 1995; Mossner et al., 1998) and TNF-α (Mossner et al., 1998) have been shown to increase serotonin uptake *in vitro*. This is consistent with another study which demonstrated increased serotonin uptake in response to TNF-α and IL-1β exposure *in vitro* (Zhu et al., 2006). In a recent study by the same group it has been suggested that increased serotonin uptake by the serotonin transporter is controlled through the IL-1 receptor as this effect is absent in IL-1 receptor deficient mice (Zhu et al., 2010). In comparison, the anti-inflammatory cytokine IL-4 has been shown to decrease serotonin uptake *in vitro* (Mossner et al., 2001). Overall the evidence indicates that pro-inflammatory cytokines may increase the expression of the serotonin transporter, but the majority of these studies are based on serotonin uptake by the serotonin transporter and do not specifically examine the serotonin transporter density. There has been recent interest in the possibility that polymorphisms in the promoter region of the serotonin transporter may result in a pre-disposition to IFN-α induced depression. The evidence so far has been inconclusive with a study showing minimal differences (Bull et al., 2009) and another which suggests that the polymorphism depends on ethnicity (Pierucci-Lagha et al., 2010).

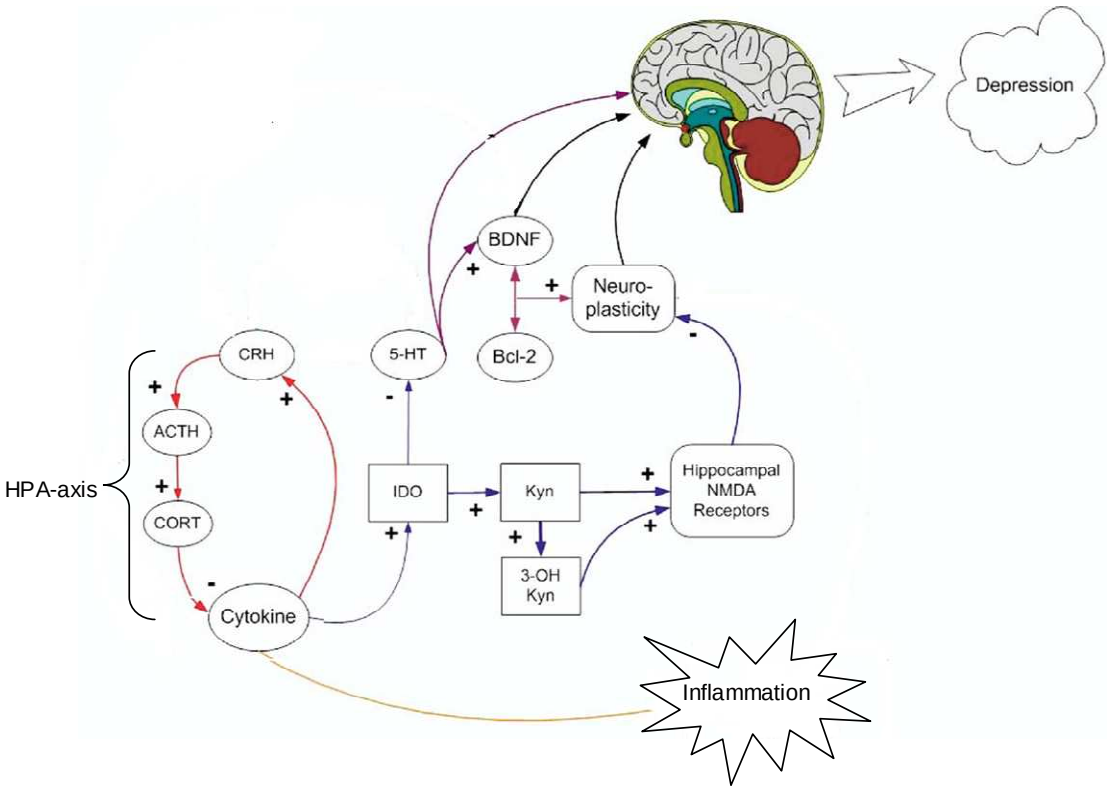

Figure 1.3.1 Mechanism whereby inflammation influences brain systems related to depression.

An inflammatory response releases cytokines which may directly or indirectly influence the serotonergic system. Directly cytokines activate indoleamine 2,3- dioxygenase (IDO) reducing tryptophan availability. Indirectly cytokines can activate the hypothalamic-pituitary-adrenal axis (HPA-axis), which reduces serotonin (5-HT) function. Cytokines can also influence neuroplasticity through different pathways. Cytokines can metabolise tryptophan to neurotoxic metabolites 3-hydroxy kynurenine (3-OH KYN) and quinolinic acid, which alters neuroplasticity. Alternatively cytokines can stimulate the HPA-axis, which reduces hippocampal brain derived neurotrophic factor (BDNF), resulting in altered neuroplasticity. Adapted from Hayley et al (Hayley et al., 2005).

1.3.3 Association between the 5-HT_{1A} receptor and pro-inflammatory cytokines.

There is limited information available about the direct influence of pro-inflammatory cytokines on the 5-HT_{1A} receptor. In lymphatic cells lines IFN-α has been shown to reduce 5-HT_{1A} expression which was attenuated by fluoxetine treatment (Cai et al., 2005). There are also studies which investigated the possibility that the 5-HT_{1A} receptor modulates the immune response. The 5-HT_{1A} receptor is present on T-cells and antagonism of 5-HT_{1A} receptors inhibits the production of T_{h1} cytokines IL-2 and IFN-γ after immune stimulus (Aune et al., 1994). Another study investigating TNF-α found blockade of the 5-HT_{1A} receptor did not prevent the effect of an anti-inflammatory drug on TNF-α expression (Laengle et al., 2006). All these studies investigated different possible roles of the 5-HT_{1A} receptor during an immune response and in the future further investigation is still required to determine how 5-HT_{1A} receptors and pro-inflammatory cytokines interact.

1.3.4 Pro-inflammatory cytokines, serotonergic system and the HPA-axis.

Indirectly, pro-inflammatory cytokines may modulate their effect through the HPA-axis to alter the serotonergic system. The HPA-axis which comprises the parventricular nucleus of the hypothalamus, the anterior lobe of the pituitary gland and the adrenal cortex, is highly responsive to stress. The hypothalamus secretes corticotrophin-releasing hormone and vasopressin that regulate the pituitary to secrete adrenocorticotrophin. Adrenocorticotrophin acts on the adrenal cortex to produce cortisol in humans and corticosterone in rodents. Corticosterone activates two types of receptors mineralcorticoid and glucocorticoid which produces negative feedback to the HPA-axis (Neeck et al., 2002). Under normal physiological conditions the neuroendocrine system restores homeostasis in response to stress. Impaired negative feedback is a characteristic of depression.

Pro-inflammatory cytokines have been shown to activate the HPA-axis resulting in elevated levels of glucocorticoids as IL-1 administration increased secretion of adrenocorticotrophin and corticosterone both *in vivo* and *in vitro* (Besedovsky et al.,

1986). In addition, cancer patients receiving IFN-α therapy had an increased cortisol response which correlated with the depressive score (Capuron et al., 2003b). Glucocorticoids are released during stress and in stressed animals there is an increase in the enzyme tryptophan hydroxylase and an increase in 5-HT_{1A} receptors. Adrenolectomy blocked the increases in tryptophan hydroxylase (Singh et al., 1990) and the increase in 5-HT_{1A} (Mendelson and McEwen, 1992) receptor binding caused by stress. It is therefore possible that pro-inflammatory cytokines increase the secretion of glucocorticoids, increasing the 5-HT_{1A} autoreceptors and thereby resulting in reduced serotonergic neuronal firing.

1.3.5 Antidepressants have anti-inflammatory properties.

Antidepressant treatment can also have anti-inflammatory properties as monoamine uptake-inhibitors have been shown to inhibit T-cell proliferation in a dose dependent manner (Berkeley et al., 1994). Selective serotonin re-uptake inhibitors have also been shown to inhibit the release of TNF-α from T-cells *in vitro* (Taler et al., 2007). Furthermore, 8 weeks of fluoxetine treatment has been shown to normalise serum IL-6 (Sluzewska et al., 1995) and in 3 months decreased IFN-γ mRNA expression in peripheral blood mononuclear cells of depressed patients (Tsao et al., 2006). Similarly, antidepressant treatment was found to reduce serum TNF-α (Tuglu et al., 2003) and serum IL-1β (Himmerich et al., 2010) in depressed patients. Recently the effect of antidepressants on T_{reg} cells was examined, revealing that antidepressant treatment increased T_{reg} cells (Himmerich et al., 2010), which are responsible for releasing anti-inflammatory cytokines.

However, there is also evidence that antidepressants have no affect on the immune system (Kenis and Maes, 2002). Three months of fluoxetine treatment resulted in no significant difference in IL-1β, IL-6 and TNF-α mRNA expression in peripheral blood mononuclear cells compared to previous mRNA expression in the same patient (Tsao et al., 2006). This is possibly due to variations in the subtypes of depression, severity of the depressive symptoms and the different study designs. In the future, further study is still required to determine the difference between subtypes of depression and to examine the mechanisms whereby the immune system may alter the brain.

1.4 Cytokines, depression and neurogenesis.

There is evidence for structural modifications in the hippocampus of depressed patients (Bremner *et al*, 2000; Frodl *et al*, 2002; Sheline *et al*., 1996, 2003). There is also evidence of reduced hippocampal volume in people suffering from depression which is exacerbated with repeated episodes and duration (Sheline *et al*., 1996, 2003). There are 3 possible explanations for reduced hippocampal volume increased cell death, reduced hippocampal neurogenesis or decreased dendritic branching (Stockmeier et al., 2004).

It is possible reduced hippocampal volume results in a pre-disposition to depression. The possibility that reduced hippocampal volume may be a risk factor for psychiatric disorders has been highlighted in a post traumatic stress disorder study in identical twins, one twin with combat experience and an identical twin with no combat experience. The sets of twins were then separated into two study groups depending on whether or not the combat twin developed post traumatic stress disorder. The results ascertained that the sets of twins had similar hippocampal volumes. However, in the set of twins with a twin with post traumatic stress disorder both twins had a smaller hippocampal volume compared to the set of twin which did not have a twin which developed post traumatic stress disorder. This suggests reduced hippocampal volume may be a risk factor for psychiatric disorders including depression and not a result of the psychiatric disorder (Gilbertson et al., 2002). Whether reduced hippocampal volume is a pre-disposition for depression or a result of depression the mechanisms through which neurogenesis may be reduced are still unknown but may include altered serotonin turnover, elevated levels of glucocorticoids, pro-inflammatory cytokines, altered BDNF or a combination of factors.

1.4.1 Neurogenesis.

Neurogenesis is the generation of new neurons from the differentiation of stem cells. Neurogenesis is prevalent during development but it is now established that under normal conditions the generation of new neurons also occurs throughout

adult life in the subgranular zone of the hippocampus and the subventricular zone of the lateral ventricles. Stem cells born in the subgranular zone of the dentate gyrus differentiate and migrate to the cellular level of the dentate gyrus. Stem cells born in the subventricular zone of the lateral ventricles migrate through the rostral migratory stream to the olfactory bulb (Ming and Song, 2005). It remains controversial whether or not adult neurogenesis occurs in brain regions other than the subventricular and subgranular zones.

Neural stem cells by definition are cells with a capacity for self renewal and differentiation. Neural stem cells proliferate, either self renewing to produce two stem cells or progenitor cells which have the potential to differentiate and mature into a specific cell phenotype including neurons, microglia, oligodendrocytes or astrocytes. It takes approximately 3 weeks for progenitor cells to differentiate and mature (Schmidt and Duman, 2007). The developmental time course of progenitor cells labelled with 5-bromo-2-deoxyuridine (BrdU) has been investigated in the dentate gyrus of the adult mouse over a 30 day period. There was a significant decrease in the number of BrdU labelled cells at 30 days after BrdU administration compared to 15 hours after BrdU administration, giving an indication of cell survival (Mandyam et al., 2007). There is limited information about how the internal environment influences progenitor cells. However, it is believed that the internal environment is fundamental in determining the phenotype of the progenitor cell and survival. Progenitor cells which differentiate and mature into new neurons are believed to integrate into neuronal circuitry to both receive synaptic input (Van Praag et al., 2002) and transmit neuronal output to postsynaptic targets (Toni et al., 2008). The function of these new connections is still unknown, although it is believed that hippocampal neurogenesis is required for working and spatial memory (Sahay and Hen, 2007)

1.4.2 Pro-inflammatory cytokines influence neurogenesis.

There is substantial evidence that pro-inflammatory cytokines reduce neurogenesis. Transgenic mice over expressing IL-6 demonstrate reduced neurogenesis (Vallieres et al., 2002). Similarly exposure to IL-6 (Monje et al., 2003) and TNF-α (Ben Hur et al., 2003; Monje et al., 2003) significantly reduces neurogenesis *in*

vitro. IL-6 has also been implicated in reduced cell survival (Monje et al., 2003). Deletion of the TNFα-R1 resulted in increased neurogenesis which suggests TNF-α mediates its effect through the TNFα-R1 to reduce neurogenesis (Iosif et al., 2006). Activation of the immune system by LPS reduces cell proliferation and microglia cells are found in close proximity to proliferating cells in the subgranular zone (Ekdahl et al., 2003). The effect of IFN-γ remains unclear as exposure of proliferating cells *in vitro* to IFN-γ showed no change in neurogenesis (Monje et al., 2003). However, other research groups have shown that IFN-γ reduces cell proliferation and increases apoptosis *in vitro* (Ben Hur et al., 2003). Another group has suggested that IFN-γ decreases neurogenesis through IL-1β as antagonism of the IL-1 receptor attenuated the IFN-γ reduction in neurogenesis (Kaneko et al., 2006).

1.4.3 Pro-inflammatory cytokines, neurogenesis and serotonin system.

There is evidence for an association between the serotonergic system and neurogenesis. For example destruction of serotonin neurons in rodents results in reduced neurogenesis in the subgranular zone of the hippocampus (Brezun and Daszuta, 1999). It has been suggested that pro-inflammatory cytokines reduce neurogenesis through the activation of IDO in microglia, which is believed to produce neurotoxins which inhibit neurogenesis (Figure 1.4.1). Evidence for the involvement of microglia in LPS induced inflammation has been demonstrated by minocycline administration which inhibited microglia activation and restored neurogenesis (Ekdahl et al., 2003). Pro-inflammatory cytokines released during the immune response drive IDO to metabolise tryptophan to kynurenine and quinolinic acid. Quinolinic acid is a selective N-methyl-D-aspartate (NMDA) receptor agonist and kynurenine is an NMDA receptor antagonist. The pro-inflammatory cytokine IFN-γ is a potent mediator of IDO activity (Chiarugi et al., 2001) and microglia cell cultures stimulated by IFN-γ produce quinolinic acid (Heyes et al., 1996). *In vivo* quinolinic acid concentrations and IDO activity are elevated in the cerebral cortex of macaque infected with a retrovirus infection (Heyes et al., 1998). In addition pro-inflammatory cytokines stimulate the enzyme kynurenine-3-monooxygenase to metabolise kynurenine further into 3-hydroxy kynurine which also has neurotoxic properties (Zunszain et al., 2010). Therefore it is possible that pro-inflammatory

cytokines drive IDO, depriving the serotonin system of its precursor tryptophan, which IDO metabolises to neurotoxic metabolites leading to reduced neurogenesis.

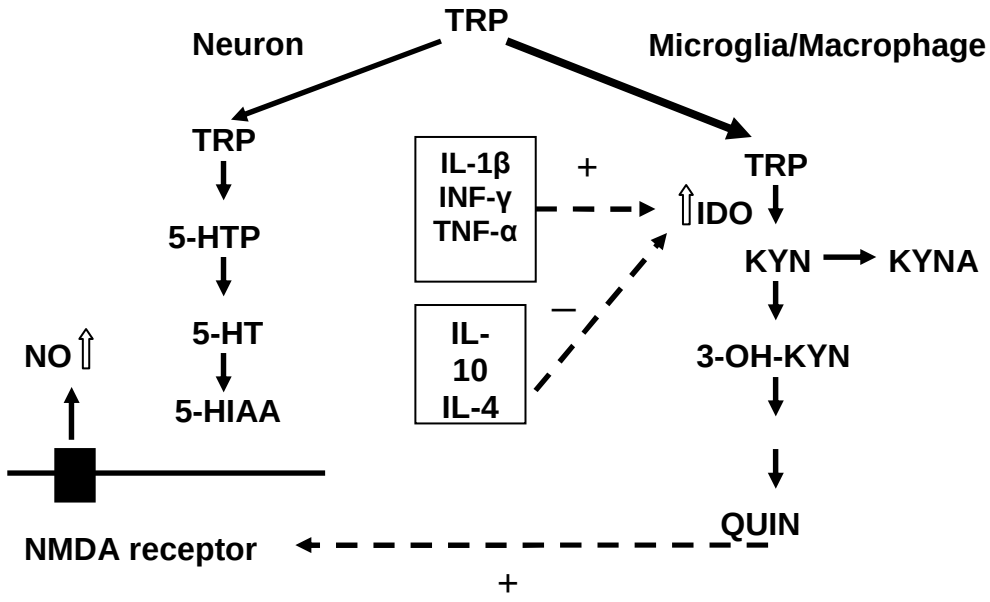

Figure 1.4.1 Tryptophan metabolism.

Under normal physiological conditions tryptophan (TRP) is metabolised by neurons to serotonin (5-HT). However, pro-inflammatory cytokines stimulate indoleamine 2,3- dioxygenase (IDO) activity in microglia to metabolise tryptophan to neurotoxic metabolites 3-hydroxy kynurine (3-OH KYN) and quinolinic acid (QUIN). From Mauri et al. (Mauri et al., 1996)

Antidepressants may influence neurogenesis through the 5-HT_{1A} receptor. Antidepressants take weeks to alleviate the symptoms of depression suggesting that antidepressants possibly alter brain structures and neurochemistry over time. These changes may occur in the hippocampus as chronic antidepressant treatment has been shown to increase neurogenesis in the dentate gyrus (Malberg et al., 2000). Hippocampal neurogenesis is further implicated in the mechanism of antidepressants as irradiation of the rodent hippocampus inhibited the antidepressant increase in neurogenesis. Selective serotonin re-uptake inhibitors block 5-HT_{1A} autoreceptors increasing the availability of serotonin in the synapse.

The 5-HT_{1A} receptor is present in high concentrations in the dentate gyrus of the hippocampus and may be a possible mechanism through which selective serotonin re-uptake inhibitors increase neurogenesis as fluoxetine induced increase in neurogenesis was absent in 5-HT_{1A} receptor knock out mice. Similarly, administration of 5-HT_{1A} receptor selective agonist resulted in an increase in neurogenesis in wild type mice which was absent in 5-HT_{1A} receptor knock out mice (Santarelli et al., 2003).

1.4.4 Pro-inflammatory cytokines, neurogenesis and the HPA-axis.

Indirectly pro-inflammatory cytokines may modulate their effect through the HPA-axis to decrease neurogenesis. Pro-inflammatory cytokines stimulate the HPA-axis resulting in elevated levels of glucocorticoids. This has been illustrated in cancer patients receiving IFN-α therapy (Capuron et al., 2003b) and in both *in vivo* and *in vitro* studies involving administration of IL-1 (Besedovsky et al., 1986). Glucocorticoids have been shown to decrease neurogenesis. Evidence for this has been demonstrated in adrenalectomized rats which had increased neurogenesis which was attenuated by administration of glucocorticoids (Gould et al., 1992). It is still undetermined how glucocorticoids inhibit neurogenesis but a possible mechanism of action is by increasing NMDA receptors resulting in neuronal excitotoxicity. This is supported by the evidence that chronic glucocorticoid administration up-regulation NMDA receptor subunit mRNA expression in the hippocampus (Weiland et al., 1997). Furthermore blockade of NMDA receptors has been shown to attenuate glucocorticoid induced reduction of cell proliferation (Cameron et al., 1998).

1.4.5 Brain-derived neurotrophic factor and neurogenesis.

There is growing interest in BDNF as it is influenced by a number of neurochemical systems and has a pivotal role in neurogenesis. Neurotrophins support neurogenesis and BDNF knock out mice do not survive past post natal day 8, have a smaller brain mass and neural deficits (Conover et al., 1995). In BDNF heterozygous knock out mice impaired neurogenesis has been observed (Lee et

al., 2002). In comparison BDNF administration into the dentate gyrus had a beneficial effect increasing neurogenesis (Scharfman et al., 2005). There have been a limited number of studies which have investigated the influence of the serotonergic system, HPA-axis and cytokines on BDNF function. Antidepressant treatment has been shown to increase the level of BDNF in the rat hippocampus, and this may be a potential mechanism through which antidepressants increase neurogenesis (Nibuya et al., 1995). Glucocorticoids suppress BDNF mRNA in the hippocampus because in adrenalectomized animals there is an increase in BDNF mRNA expression which is attenuated by administration of aldosterone (Chao et al., 1998). Finally, pro-inflammatory cytokines may also influence BDNF directly as IL-1β administration reduces BDNF mRNA which is attenuated by antagonism of the IL-1 receptor (Barrientos et al., 2003). Alternatively, pro-inflammatory cytokines may influence BDNF indirectly through the serotonergic system or HPA-axis. Overall BDNF appears to be a potential target through which the serotonergic system, HPA-axis and cytokines may modulate neurogenesis, possibly leading to the development of depression.

1.5 Rheumatoid arthritis.

Rheumatoid arthritis is an autoimmune disease where a compromised immune system can no longer differentiate between self and non-self molecules. According to WHO rheumatoid arthritis was the 31st leading cause of years lived with disability globally in 2000 and the prevalence of rheumatoid arthritis in industrialised countries is 0.3-1%. There is a greater prevalence of depression in the medically ill compared to the general population. A systemic review has reported a 13-17% co-morbidity (Dickens et al., 2002) between rheumatoid arthritis and depression and a recent study in 62 rheumatoid arthritis patients reported a 52% co-morbidity (Mella et al., 2010). Depression in rheumatoid arthritis patients has been noted as far back as 1969 (Annon.,1969). There are two possible explanations for the co-morbidity between depression and rheumatoid arthritis. The first is the concept that a medically ill person would have a depressed mood as they are unwell, which in time may alter the brain to reflect the reduced mood. The second theory is that the systemic inflammatory response influences the CNS in neurological pathways which relate to the symptoms of depression. Recently a publication in the literature

compared two rheumatic diseases in order to draw a distinction between the prevalence of depression in a rheumatic disease with and without an inflammatory response. Both diseases displayed similar degrees of pain however, there was a higher prevalence of depressive mood in patients with rheumatoid arthritis which involved an inflammatory response compared to osteoarthritis which does not (Mella et al., 2010). This is data from only one study which had limitations. However, it contributes to the cytokine theory of depression by demonstrating clinically that that depression may not be just due to the emotional aspect of a disease associated with suffering and physical disability.

There is *in vivo* evidence for an association between depression and immune activation (Capuron et al., 2000; Yirmiya, 1996). However, there is limited evidence as to how immune activation in these disorders trigger depression. Recently the effect of pro-inflammatory cytokines on the serotonin transporter was investigated in rheumatoid arthritis patients. Adalimumab, a TNF blocker was prescribed to patients with rheumatoid arthritis and [^{123}I]- β-carbomethoxy-3-β-(4 iodophenyl)tropane (βCIT) binding in the midbrain measured before and after 4 weeks on adalimumab. The results found a significant decrease in serotonin transporter binding after 4 weeks on adalimumab (Cavanagh et al., 2010). This study suggests that the serotonin transporter is increased in the midbrain of rheumatoid arthritis patients and by inhibiting TNF, serotonin transporter binding is decreased. The limitation of the study was the small number of participants (6) and further study with a greater number of patients is required to make this finding more robust.

There are also a limited number of studies which have investigated the effect of systemic inflammation on the CNS in rodent models of rheumatoid arthritis. The majority of studies employ LPS or individual cytokine administration to examine the influence of the immune response on the CNS *in vitro* (Monje et al., 2003; Ekdahl et al., 2003; Zhu et al., 2006). The limitation of these studies is that LPS administration results in transient activation of the innate immune system. Similarly, administration of only a single pro-inflammatory cytokine results in an acute immune response and may not represent the immune state observed in inflammatory disorders. It is for this reason that it is important to use animal models

of rheumatoid arthritis which has a priming stage and a chronic inflammatory response to investigate the effect of the peripheral immune response on the CNS. There are a limited number of studies which have investigated altered CNS function in a rodent model of rheumatoid arthritis. These studies have investigated altered cerebral metabolic function, the serotonergic system, HPA-axis and neurogenesis in different rodent models of rheumatoid arthritis (Wolf et al., 2009b; Holmes et al., 1995; Sternberg et al., 1989; Neto et al., 1999).

1.5.1 Collagen induced arthritic model.

To date no studies have examined the CNS in the murine model of collagen induced arthritis (CIA). The murine model of CIA is frequently employed as a model of rheumatoid arthritis to investigate possible cellular mechanisms and anti-inflammatory drug treatments. On day 0 of the murine CIA model, naïve mice are immunised with type II collagen and complete Freund's adjuvant an endotoxin similar to LPS which activates the innate immune response. On day 21 mice are challenged with type II collagen and phosphate buffer saline after which clinical symptoms of swelling and eyrethma appear.

No animal model will ever reflect all cellular and molecular aspects of the human form of the disease. However, there are a number of similarities between the CIA model and rheumatoid arthritis. Both the human and murine model are genetically susceptible (Rosloniec et al., 1998; Rosloniec et al., 1997; Wooley et al., 1981) and both CIA and rheumatoid arthritis produce an autoimmune response to type II collagen. This results in inflammatory cell infiltration of the joint and eventually destruction and erosion of the joint (Cho et al., 2007). The similarities between the CIA model and rheumatoid arthritis make this a possible model in which to further our understanding of the effect of the autoimmune response on systemic and central function.

CIA is initiated in a genetically susceptible strain of mice (DBA/1) by a subcutaneous injection of type II collagen emulsification in complete Freund's adjuvant. A booster is then given on day 21 post immunisation after which clinical symptoms of swelling and erythema may appear in all 4 limbs (Brand et al., 2004).

At the later stages of the CIA model 40-50 days post immunisation the disease begins to go into remission with the resolution of clinical symptoms and decrease in the pro-inflammatory cytokines IL-1β, TNF-α and IFN-γ. In CIA mice with severe limb swelling by day 40 post immunisation there may be neutrophil infiltration in the joint space and synovial tissue (Thornton et al., 1999).

The CIA model is characterised by an active immune system involving monocytes/macrophage, T-cells and B- cells. Once activated these immunocompetent cells release pro-inflammatory cytokines IL-1β, IL-6, IL-17, IL-23, TNF-α and IFN-γ at varying times during the temporal evolution of the murine CIA model (Figure 1.5.1). The CIA model is dependent on the activation of CD4+ T-cells as antagonism reduces disease expression (Ranges et al., 1985). There are two subtypes of CD4+ T-cell, T_{h1}-cells secrete IL-2 and IFN-γ and is involved in cell-mediated immunity and T_{h2}-cells which secrete IL-4 and IL-10 and is involved in humoral immunity. The development and maintenance of CIA is dependent on the synergistic expression of cytokines to produce a biological effect. Both cell-mediated immunity and humoral immunity are required for the establishment of clinical symptoms (Seki et al., 1988) as T_{h1}-cells secrete IFN-γ and IL-2 during the early development of the disease and T_{h2}-cells secrete anti-inflammatory cytokines IL-4 and IL-10 towards the end of the CIA experiment (Mauri et al., 1996).

1.5.2 Interleukin-1 and the CIA model.

IL-1 is implicated in the induction of clinical symptoms e.g swelling and erythema of the joints. This is demonstrated by increased IL-1 expression during the development of clinical symptoms which peaks after the development of the clinical symptoms then declines (Mauri et al., 1996; Thornton et al., 1999). Recombinant IL-1β has been shown to accelerate the onset of CIA and increased the incidence of disease in genetically susceptible rodent strains (Hom et al., 1992). In comparison there is reduced incidence of disease in CIA immunised IL-1α and IL-1β knock out mice. However, IL-1α knock out mice had normal disease severity in comparison to IL-1β knock out mice which displayed disease suppression. This suggests that IL-1α and IL-1β have different roles in the development of arthritis and that IL-1β may have a role in the development of clinical symptoms (Saijo et

al., 2002). IL-1 is also implicated in the destruction of the joint (Pettipher et al., 1986). Anti-IL-1 treatment has been shown to suppress the development of disease and reduce cartilage destruction (Joosten et al., 2008; van den Berg et al., 1994). IL-1 is an important mediator of CIA, however is not the only cytokine elevated during the inflammatory response.

1.5.3 Tumour-necrosis-factor-α and the CIA model.

There is increased TNF-α expression throughout the evolution of CIA which declines during disease remission (Mauri et al., 1996). The expression of TNF- α is consistent with the belief that TNF- α is important in initiation, progression and maintenance of CIA. TNF-α is believed to be involved in the development of inflammation during the development of rheumatoid arthritis. TNF- α accelerates the incidence and severity of CIA (Thorbecke et al., 1992). In comparison anti-TNF-α suppresses the development of CIA however, it does not have a beneficial effect on existing clinical symptoms (Thorbecke et al., 1992; Piguet et al., 1992). Blockade of TNF-R1, a TNF-α receptor suppresses the development of CIA (Shibata et al., 2009). TNF- α is also implicated in bone erosion and blockade of TNF-α has been shown to protect the joint (Williams et al., 2000).

1.5.4 Interleukin-6 and the CIA model.

There is increased IL-6 expression in the sera of CIA mice (Takai et al., 1989) and a rapid increase in IL-6 mRNA expression which peaks on day 26 post immunisation after which IL-6 mRNA expression declines (Thornton et al., 1999). IL-6 is believed to be important in the development of CIA as there is no inflammatory response to type II collagen in the limbs of IL-6 deficient mice (Alonzi et al., 1998). Similarly blockade of the IL-6 receptor on day 0 or 3 post immunisation inhibits the onset of disease. However, blockade of IL-6 at later time points had no effect on the disease expression (Takagi et al., 1998).

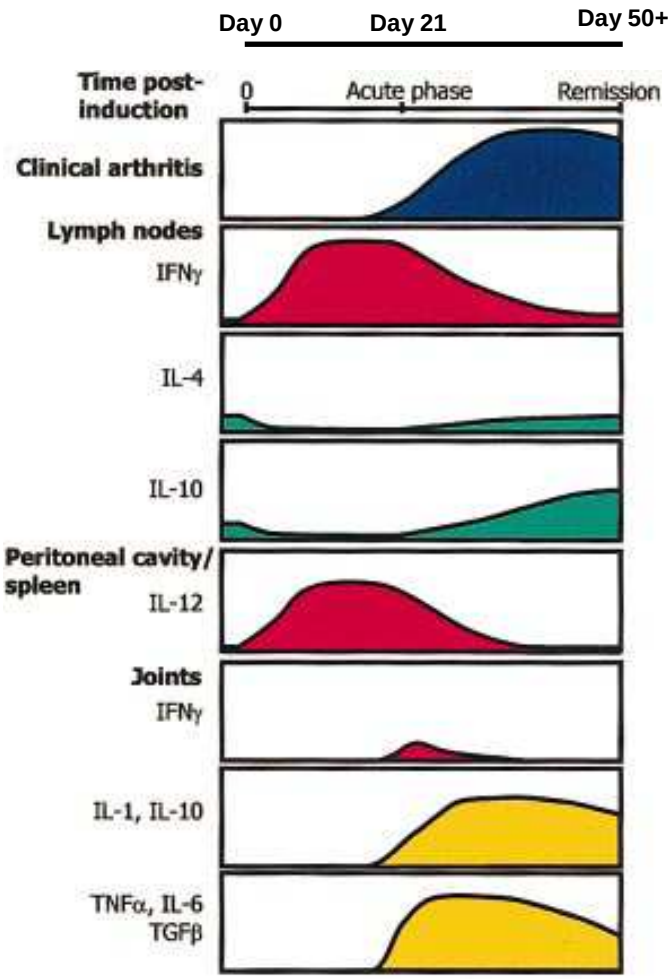

Figure 1.5.1 Cytokine expression during the temporal evolution of CIA.

The top panel represent the progression of disease which develops approximately 3-4 weeks after initial CIA immunisation. The panels below illustrate the evolution individual cytokines examined in the lymph node, peritoneal cavity/spleen or in the joints. From Luross et al. (Luross and Williams, 2001)

1.5.5 Interferon-γ and the CIA model.

There is conflicting evidence for the role of IFN-γ in the development of clinical symptoms in the CIA model. IFN-γ is reported to only be present during the initial phase of CIA, with the greatest peak of IFN-γ on the day of immunisation, suggesting a role in the development of arthritic symptoms (Mauri et al., 1996; Thornton et al., 1999). Treatment with monoclonal antibodies to IFN-γ delayed the onset of the disease and reduced disease incidence and severity (Cooper et al.,

1988; Boissier et al., 1995). However, in IFN-γ receptor knock out mice the disease is accelerated appearing earlier with greater severity and incidence (Vermeire et al., 1997; Manoury-Schwartz et al., 1997). A possible explanation for the observed differences is that IFN-γ plays a role in the induction of CIA as well as modulating the inflammatory response once clinical symptoms begin to appear (Boissier et al., 1995).

1.5.6 Interleukin-10 and the CIA model.

IL-10 is an anti-inflammatory cytokine released from T_{h2}-cells. IL-10 has been shown to inhibit a number of pro-inflammatory cytokines including IL-1, IL-6 and TNF-α (Fiorentino et al., 1991). Increased expression of IL-10 has been noted at the later time points of the CIA model particularly during the remission of the disease (Kasama et al., 1995; Mauri et al., 1996). The inhibitory properties of IL-10 have also been demonstrated during the
evolution of the CIA model, as daily administration of IL-10 attenuated the clinical symptom of arthritis (Walmsley et al., 1996). Inversely, anti-IL-10 accelerated the development and intensified the severity of the clinical symptoms (Kasama et al., 1995).

1.5.7 Blood brain barrier.

It is not disputed that cytokines influence the CNS as cytokine receptors are present throughout the brain (Ericsson et al., 1995) and are influenced by the systemic immune response. For instance, LPS or IL-1 administration induces fever which is regulated by the hypothalamus and attenuated by IL-1 receptor antagonist (Opp and Krueger, 1991; Luheshi et al., 1996). Cytokines are large hydrophilic molecules and the mechanisms whereby cytokines cross the BBB are still debated. There are two possible pathways in which the immune system may communicate with the brain: the humoral and the neural pathways.

The humoral pathway includes diffusion at the site of the circumventricular organs (CVO), carrier mediated transport or by secondary messengers such as prostaglandins. Cytokines may directly cross the BBB at the circumventricular

organs (CVO) which is less restricted but cytokines are too large to diffuse further than the structure organum vasculosum of the lamina terminalis (OVLT). It has been suggested that cytokines influence the CNS via prostaglandins within the OVLT. Evidence to support this has been demonstrated by directly injecting a prostaglandin antagonist into the OVLT which resulted in inhibition of the IL-1β induced increase in plasma adrenocorticotropic hormone (Katsuura et al., 1990).

Prostaglandins are small lipophilic second messenger molecules which are activated by cytokines. Prostaglandins are part of a fundamental mechanism through which cytokines are believed to induce fever by diffusing to the hypothalamus. Evidence for this comes from genetically modified mice with altered prostaglandin E-synthase-1 which did not develop a fever after LPS or IL-1β administration (Engblom et al., 2003; Saha et al., 2005). This suggests cytokines bind directly to cerebral vascular endothelial cells to release prostaglandins or activate astrocytes within the OVLT to release prostaglandins. In either case they have an important role in mediating the biological effect of cytokines. In addition, another study has suggested that transport into the brain depends on the route of administration. An intracerebroventricular injection of [^{125}I] IL-1α suggested transport via the CVO. However, intravenous injection suggested IL-1α crossed the BBB via carrier mediated transport (Plotkin et al., 1996). There is also evidence that IL-6 and TNF-α cross the BBB via carrier mediated transport (Banks et al., 1994; Gutierrez et al., 1993).

Another way in which cytokines may influence the brain is via the neural pathway which involves the vagus nerve. The vagus nerve connects to the vagal nucleus in the brainstem and the nucleus tractus solitarius. This pathway is activated by LPS and IL-1 administration (Bluthe et al., 1996; Bluthe et al., 1994). From the nucleus tractus solitarius the signal is transmitted to regions of the brain involved in mood including amygdala, hippocampus and locus coeruleus (O'Keane et al., 2005). Signalling via the vagus nerve appears to be dose dependent as vagotomy attenuates LPS induced fever at low doses. However, at a higher dose of LPS fever is not inhibited in vagotomised rodents (Romanovsky et al., 1997). This suggests that at higher concentrations LPS possibly influences the brain via the CVO, prostaglandins or carrier mediated transport.

It is also possible that the BBB is compromised during the disease state and it has recently been suggested that this is the case during CIA. The sodium fluorescein content was measured at day 21-50 post immunisation and day 51-100 post immunisation. The results suggest that there is increased permeability of the BBB at day 21-50 post immunisation which improved at the later time point 51-100 post immunisation but was still permeable (Nishioku et al., 2010b). This increases the likelihood that elevated pro-inflammatory cytokines in the periphery may enter the brain via passive diffusion. The same group also investigated the influence of anti-TNF-α on the increased permeability observed in cell cultures after LPS administration. The results suggested that TNF-α is responsible for increased BBB permeability (Nishioku et al., 2010a). However, this study only investigated the effect of anti- TNF-α on LPS induced permeability and other cytokines may also be involved. Further evidence is required in both clinical and non-clinical studies to confirm that cytokines can enter the brain.

1.6 Aims.

There is evidence for an association between depression and rheumatoid arthritis. However there is no information available which has investigated how rheumatoid arthritis may influence the brain and what neurochemical systems rheumatoid arthritis affects to bring about symptoms of depression. Therefore the hypothesis of this thesis is that chemical mediators released during a chronic peripheral inflammatory response will alter the brain. The overall aim of this thesis was to investigate if there were alterations in brain function in a model of collagen induced arthritis. To achieve this neurochemical, structural and functional characteristics were investigated in the murine model of CIA as described in the aims below.

I. To establish the CIA model during which the clinical symptoms and temporal evolution of the disease were characterised (chapter 3).

II. Using the brain tissue derived from the animals in chapter 3, study 1, serotonin and dopamine transporter distribution was determined using *in vitro* autoradiography (chapter 4).

III. Evidence for any change in brain function was investigated in the CIA model, after development of clinical symptoms, using [^{14}C]-2-deoxyglucose (DG) autoradiography. To examine serotonergic function, CIA mice were challenged with fenfluramine, a serotonergic specific drug which depletes central stores. Changes in serotonergic transmission were detected by [^{14}C]-2-DG autoradiography. Prior to this the effect of fenfluramine challenge on brain function in naïve mice was characterised (chapter 5).

IV. Investigation of cell proliferation in the subgranular zone of the hippocampus during the temporal evolution of the CIA model. Cell survival during the development of the clinical symptoms was also examined to determine if peripheral inflammation decreases cell survival (chapter 6).

Chapter 2

Materials and methods.

2.1 *In vivo* murine models of arthritis.

2.1.1 Induction of collagen induced arthritis (CIA).

The CIA model is established within the University of Glasgow and the schematic of the CIA experiment is illustrated in Figure 2.1.1 (Asquith et al., 2009a). Male DBA/1 mice (13-15g, Harlan) aged 7-8 weeks are more susceptible to the development of disease than female or older mice. All animals were housed in a controlled environment with free access to food and water. On day 0, all mice were lightly anesthetised with 4% isofluorane in a mixture of 30% oxygen/ 70% nitrogen and the fur at the base of the tail shaved. Under anaesthetic the CIA group were subcutaneously (s.c) injected with 0.1ml of collagen emulsification. The collagen emulsification was made fresh on day of immunisation consisting of 2mg/ml bovine type II collagen in dilute acetic acid, (MDbioscience cat 804001-sol) emulsified in an equal volume of complete Freund's adjuvant (MDbioscience cat 501009) using a homogeniser.

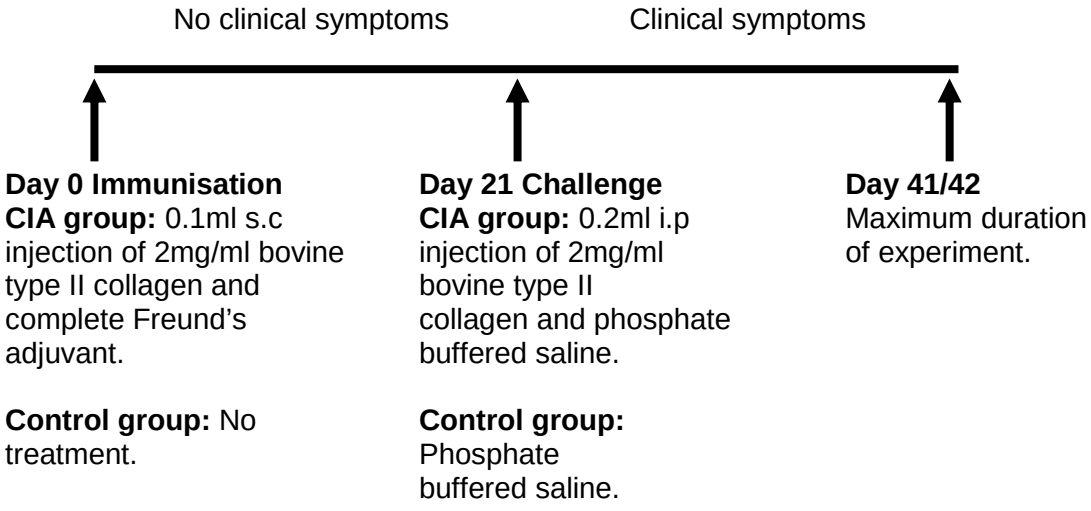

Figure 2.1.1 Schematic of the collagen induced arthritic model.

To check the consistency of the emulsification, a droplet of emulsion was placed in a beaker of water. If it formed an iceberg within the water the collagen emulsification was determined to be correctly prepared however, if the droplet dispersed readily in the water then further homogenisation was required. The collagen emulsification was administered to the CIA group as two 0.05ml subcutaneous injections on either side of the tail base. Complete Freund's adjuvant is an endotoxin which stimulates an immune response. It is for this reason on day 0 no further treatment was administered to the control group after the base of the tail was shaved.

On day 21 post immunisation, the CIA group were injected intraperitoneally (i.p) with 0.2ml bovine type II collagen (2mg/ml in dilute acetic acid in equal volume of sterile phosphate buffered saline). At this same time point the control group were injected intraperitoneally with 0.2ml sterile phosphate buffered saline.

Brains were harvested in all experiments; in Chapter 3 brains were harvested on day 42 post immunisation; in Chapter 5 brains were harvested on day 41 or 42 post immunisation; and in Chapter 6 brains were harvested on day 6 and day 42 post immunisation.

Hind legs were harvested for histological assessment of the joint in Chapter 3 from animals generated for study 2 as this was the first study that had a disease incidence greater than 75%.

2.1.2 Termination criteria.

For the first study using the CIA model (Chapter 3/4) in accordance with the Home Office project licence held at the time, any mouse with a decrease in body weight of 20% or greater compared to their body weight pre-immunisation were terminated by a Schedule 1 method. Alternatively any mouse with a clinical score of twelve or over was also terminated by a Schedule 1 method.

Due to a change in project licence after the initial study, in all subsequent experiments (Chapter 3, Study 2, Chapter 5 and Chapter 6), animals were assigned

a score of ill-health and any mouse with an ill-health score of 7 or greater was killed by a Schedule 1 method. Animals were assigned an ill-health score of 1 for each of the following: reduced movement, decreased inquisitiveness, a hunched over appearance or encrusted eyes. A score of 4 was assigned if an animal was non-responsive to touch and a score of 7 was assigned for a decrease in body weight of 20% or greater compared to their starting body weight.

2.1.3 Clinical score.

From day 20 post immunisation, both CIA immunised mice and controls were monitored daily for clinical signs of the disease by scoring each of the 4 limbs. The sum score of the four limbs was calculated on each day for each animal and the median clinical score for each limb was calculated each day per group of animals.

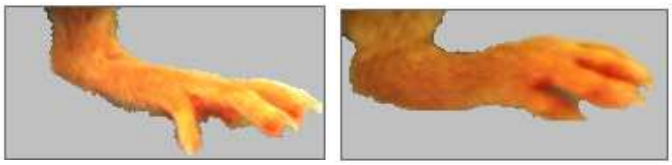

Control group: no clinical symptoms. **CIA group: clinical symptoms.**

Figure 2.1.2 Image of a hind limb from a control and CIA animal.

In the control group there was no sign of clinical symptoms and the hock joints and digits were clearly defined. In the CIA group some limbs displayed clinical symptoms of swelling and erythema of the limb.

In the CIA experiment used to establish the CIA model within the department (described in Chapter 3, study 1) the clinical scoring system described below was used (Table 2.1.1).

Clinical score	Description
0	No disease/ normal.
1	Erythema of hock joint.
2	Erythema from hock to the limb.
3	Erythema and swelling of hock and limb.
4	Loss of function in the limb.

Table 2.1.1 Clinical scoring employed in Study 1 only (Chapter 3).

After the first CIA experiment, a scoring system which included a more detailed description of the clinical symptoms was used. This scoring system in Table 2.1.2 was used in all other experiments (Chapter 3 (study 2), chapter 5, and chapter 6).

Clinical score	Description
0	No disease/ normal.
1	Erythema and mild swelling of hock joint.
2	Erythema and mild swelling from the hock to the metacarpal articulations or metatarsal articulations.
3	Erythema and moderate swelling from the hock to phalangeal articulations.
4	Erythema and severe swelling of the limb.

Table 2.1.2 Clinical scoring system used in the majority of CIA experiments.

2.1.4 Disease severity and hock/paw summary measure.

The sum clinical score/ calliper measurement of the four limbs was calculated on each day per animal and plotted over time. From this graph the area under the curve was calculated and used as a summary measure of disease severity or hock/paw thickness for each animal.

2.1.5 Disease incidence.

The incidence of disease was calculated as the percentage of all mice initially immunised which demonstrated clinical symptoms of swelling and erythema

2.1.6 Calliper measurements.

In the CIA model, from day 20 post immunisation calliper measurements of the hock or paw were recorded every second day. Manual callipers were used to measure hock thickness and were placed between the hock joint and the paw on each of the 4 limbs per mouse (Figure 2.1.3). Manual callipers were used in the first CIA experiment only (Chapter 3, study 1).

Subsequent to the initial CIA experiment spring callipers were used to measure paw thickness and were placed above and below the paw. Spring callipers were used in the CIA experiments used in Chapter 3 (study 2), 5 and 6 (Figure 2.1.3). When released the spring callipers apply the same pressure to all paws within the same animal and within the group. In comparison manual callipers rely on the experimenter to judge the degree of pressure applied when measuring hock thickness. Spring callipers therefore allow consistent measurements between animals and for this reason were favoured over manual callipers.

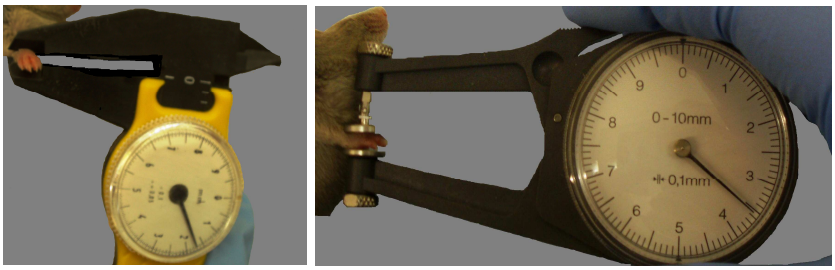

Manual callipers **Spring callipers**

Figure 2.1.3 Image of manual and spring callipers.

2.1.7 Perfusion fixation and tissue processing.

Animals were deeply anaesthetised in a perspex box containing 4% isofluorane in a mixture of 30% oxygen /70% nitrogen. Using a pair of forceps, the animal was given a reflex test to determine the depth of anaesthesia, if there was no reflex then the animal was deemed ready to be moved to a facemask where the flow was reduced to 2.5-3%. Again a pair of forceps was used to give a reflex test before an incision was made below the sternum, to reveal the diaphragm. An incision was then made carefully through the diaphragm and the ribs cut to expose the heart. To perfuse 10ml of heparinised saline followed by 10ml 4% formaldehyde in phosphate buffer (PAM) a needle attached to a syringe pump was inserted into the left ventricle and clamped in place. The right atrium was then incised to allow circulation of the solutions.

Following fixation the head was removed and placed in PAM for 24 hours. The brain was then removed from the skull and post fixed for a further 48 hours before being transferred to 30% sucrose in phosphate buffer. Over a period of five days the brain sank and was then frozen in isopentane at -45 ºC, and stored at -50 ºC until ready to be cut. Sections (30µm thick) were cut on a cryostat at -20 ºC, and stored in individual cell wells containing cryoprotectant at -20 ºC (Appendix 1). Sections were mounted on poly-L-lysine coated slides 24 hours prior to immunohistochemical staining (Appendix 1).

2.1.8 Histological assessment of joint pathology.

On day 42 post immunisation, hind limbs were harvested and fixed in neutral-buffered formalin (Appendix 1) for histological assessment of joint pathology (Appendix 1). Both the right and left hind limbs from the control group (n=12) and the CIA group (n=12) were contracted out to the Pathology department to be decalcified, paraffin embedded and cut on a microtome before haematoxylin and eosin staining. One section from each hind limb was examined under a light microscope to determine if cell infiltration was present in either the hock or digit joints.

2.2 Ligand binding autoradiography.

2.2.1 Theory.

In vitro ligand binding autoradiography involves the interaction between radiolabelled ligands and target receptor sites which form reversible ligand-receptor complexes. The bound radiolabelled ligands then emit energy which creates an autoradiographic image when apposed to radiation sensitive film. The optical density can be quantified from autoradiograms using an image analyser. By co-exposing the sections to film with calibrated radioactive standards a standard curve of optical density versus radioactivity can be plotted and used to calculate the amount of radioligand bound to receptors in the tissue section. The binding of the radiolabelled ligand to components in the tissue other then the receptor is termed non-specific binding and is determined by displacement of the radiolabelled ligand from the receptor. This technique allows anatomical mapping of the distribution of ligand binding with a high degree of spatial resolution in discrete anatomical locations.

2.2.2 Tissue processing.

On day 42 post immunisation, brains were removed from the skull and frozen in isopentane at -45ºC. Coronal sections (20µm thick) were cut on a cryostat set at -20ºC, and mounted on poly-L-lysine coated slides (Appendix 1). Sections were stored at -20ºC prior to use.

2.2.3 Autoradiographic protocol for [^{125}I]-βCIT.

[^{125}I]-βCIT is a radioligand which binds to both the serotonin transporter (SERT) and the dopamine transporter (DAT). [^{125}I]-βCIT was synthesised by Dr Sally Pimlott at the West of Scotland Radionuclide Dispensary as previously described (Baldwin et al., 1993). At any point during the experiment that [^{125}I] -βCIT was handled the handler was double gloved and all steps were performed in a fume hood up until the slides had dried.

The protocol for [^{125}I] -βCIT autoradiography was derived from that of (McGregor et al., 2003) with modification. Tris-buffer was substituted for phosphate buffer and instead of using two separate sections to define non-specific binding for SERT and DAT one section was incubated with both displacers for both transporters.

Slides were removed from storage at -20ºC, brought to room temperature and tissue sections circled with a hydrophobic pen. Sections were pre-incubated in Tris HCl buffer (pH 7.4) containing 50mM Tris HCl, 120mM NaCl and 5mM KCl for 30 minutes at room temperature, prior to incubation with 50pM [^{125}I]-βCIT (specific activity 1.47-6.0 Ci/μmol) in the presence of appropriate displacers to determine SERT, DAT and non-specific binding (Table 2.2.1). To determine [^{125}I]-βCIT binding to both SERT and DAT (defined as total binding) sections were incubated for 60 minutes at room temperature, with 50pM [^{125}I]-βCIT (West of Scotland Radionuclide Dispensary). To determine binding of [^{125}I]-βCIT to SERT, sections were incubated for 60 minutes at room temperature with 50pM [^{125}I]-βCIT in the presence of 1μM mazindol, which binds specifically to DAT (Tocris). To determine [^{125}I]-βCIT binding to DAT, sections were incubated for 60 minutes at room temperature in 50pM [^{125}I]-βCIT in the presence of 50nM fluoxetine, which specifically binds to SERT (Tocris). Tissue sections were also incubated in both 10μM fluoxetine and 1μM mazindol to determine non-specific binding. At the end of the incubation the sections were washed in buffer at 4 ºC for 1 minute and then for two x 20 minute, followed by a dip in distilled water. Tissue sections were left to dry overnight before being mounted on a card along with a set of pre-calibrated [^{125}I]-standards (Sigma-Aldrich). The tissue sections and standards were apposed to Kodak Biomax MR film between 2-48 hours, depending on the magnitude of decay. At the end of the exposure time films were developed using an x-ray film processor.

	SERT and DAT	SERT or DAT	Non - Specific	SERT	DAT
Ligand	**50pM [^{125}I]-β-CIT**			**2nM [^{3}H]-citalopram**	**10nM [^{3}H]-WIN-35,428**
Specific activity	1.47-6 Ci/μmol			83-84 Ci/mmol	83.6-85.9 Ci/mmol
Radioliagnd source	West of Scotland Radionuclide dispensary			Amersham	PerkinElmer
Assay Buffer	Tris-buffer 50mM Tris HCl 120mM NaCl 5mM KCl pH 7.4			Tris-buffer 50mM Tris HCl 120mMNaCl 5mM KCl pH 7.4	Phosphate-buffer: 25mM Na_2HPO_4 25mM NaH_2PO_4 50mM NaCl pH 7.7
Pre-incubation	30min (25ºC)			15 min (25ºC)	20min (25ºC)
Incubation Time	60 min (25ºC)			120min (25ºC)	120 min (4ºC)
Displacer final conc.	N/A	50nM fluoxetine or 1 μM mazindol	1 μM mazindol and 10 μM fluoxetine	20 μM fluoxetine	30 μM nomifensine
Displacer source	Tocris			Tocris	Sigma-Aldrich
Wash	1X 1min 2X20 min buffer 1 dip dH_2O All at (4ºC)			4X 2min buffer 1 dip dH_2O All at(4ºC)	3X 30 sec buffer 1 dip dH_2O All at(4ºC)
Film exposure time	2-48 hours			6 weeks	12 weeks
Reference	McGregor *et al*., (2003)			Hébert *et al*., (2001)	Andersen *et al*., (2005)

Table 2.2.1 *In vitro* autoradiography protocol for [^{125}I]-βCIT, [^{3}H]-citalopram and [^{3}H]-WIN-35,428.

2.2.4 Autoradiographic protocol for [^{3}H]-citalopram and [^{3}H]-WIN-35,428.

[^{3}H]-Citalopram is a radioligand which binds to SERT and [^{3}H] WIN-35,428, is a radioligand which binds to DAT. For both radioligands slides were removed from storage at -20ºC, brought to room temperature and tissue sections circled with a hydrophobic pen.

To quantify SERT binding, sections were pre-incubated in a Tris HCl buffer (pH 7.4) containing 50mM Tris HCl, 120mM NaCl and 5mM KCl for 15 minutes at room temperature (25℃). Sections were then incubated fo r 120 minutes at room temperature with 2nM [^{3}H]-citalopram (specific activity 83-84 Ci/mmol; Amersham). Non-specific binding was determined by incubating adjacent sections with 2nM [^{3}H]-citalopram in the presence of 20µM fluoxetine. At the end of the incubation sections were washed in buffer at 4 ºC for four x 2 minutes, followed by a dip in distilled water (Table 2.2.1).

To quantify DAT binding, sections were pre-incubated in 25mM Na_2HPO_4, 25mM NaH_2PO_4 and 50mM NaCl buffer (pH 7.7), for 20 minutes at room temperature. Sections were then incubated for 120 minutes at 4 ºC with 10nM [^{3}H]-WIN-35,428 (specific activity 83.6-85.9 Ci/mmol; PerkinElmer). Non-specific binding was determined by incubating adjacent sections with 10nM [^{3}H]-WIN-35,428 in the presence of 30µM nomifensine (Sigma-Aldrich). At the end of the incubation sections were washed in buffer at 4 ºC for three x 30 seconds followed by a dip in distilled water (Table 2.2.1).

For both [^{3}H]-citalopram and [^{3}H]-WIN-35,428 autoradiography tissue sections were left to dry overnight before being mounted on a card along with a set of pre-calibrated [^{3}H]-standards (Sigma-Aldrich) and then apposed to Kodak Biomax MR film for 6 or 12 weeks ([^{3}H]-citalopram and [^{3}H]-WIN-35,428 respectively; Table 2.2.1). At the end of the exposure time films were developed using an x-ray film processor.

One alteration was made from the original [^{3}H]-WIN-35,428 autoradiographic protocol (Andersen et al., 2005) which used cocaine to determine non-specific binding while I used nomifensine.

2.2.5 Densitrometric analysis.

Densitometric analysis of autoradiograms was performed using an MCID basic system (7.0 Rev 1.0, build 207; Imaging Research Inc) by converting measured grey level values (0-255) into optical density values. The MCID system was calibrated at the start of each session to standardise the film background. The optical densities of the pre-calibrated [^{3}H]-standards or [^{125}I]-standards were measured to produce a calibration curve. Decay correction was applied to [^{125}I] and [^{3}H]-standards. Optical densities measured in brain regions of interest were converted to fmol/mg using the standard curve. Optical density measures of pre-determined brain structures were made by placing a measuring frame over defined regions. The size of the measuring frame was adjusted depending on the region of interest sampled and the same region was measured bilaterally in 3 tissue sections from the same animal. Structures were defined by reference to a stereotaxic atlas (Franklin K.B.J and Paxinos G., 2007)

2.3 *In vivo* [^{14}C]-2-deoxyglucose autoradiography.

2.3.1 Theory.

The [^{14}C]- 2-deoxyglucose autoradiographic technique ([^{14}C]-2-DG) measures *in vivo*, the relationship between functional activity and energy metabolism at the synapses of discrete structural components of the nervous system (Sokoloff, 1977). Under normal physiological conditions oxidative catabolism of glucose predominantly provides the energy required for cerebral function. Therefore glucose phosphorylation is directly related to the level of functional activity in discrete neural subunits of cerebral tissue. Due to the biochemical properties of glucose it passes through the glycolytic pathway and is broken down into water and carbon dioxide which freely diffuse away. 2-Deoxyglucose is an analogue of glucose and structurally similar except for the replacement of the hydroxyl group on the second carbon by a hydrogen atom making it a suitable radioisotope to measure cerebral functional activity. [^{14}C]-2-DG method has been designed so that the radiolabelled concentration of [^{14}C]-2-DG is proportionate to rate of glucose utilisation. Both [^{14}C]-2-DG and glucose compete equally for the same carrier across the BBB and are metabolised by the enzyme hexokinase. Glucose-6-phosphate then continues through the glycolytic pathway and is further metabolised, however [^{14}C]-2-deoxyglucose-6-phosphate becomes trapped in the tissue as it is not a substrate for the next step in the glycolytic pathway. The trapped [^{14}C]-2-deoxyglucose-6-phosphate gives a measure of glucose utilisation and therefore in turn is a measure of functional activity.

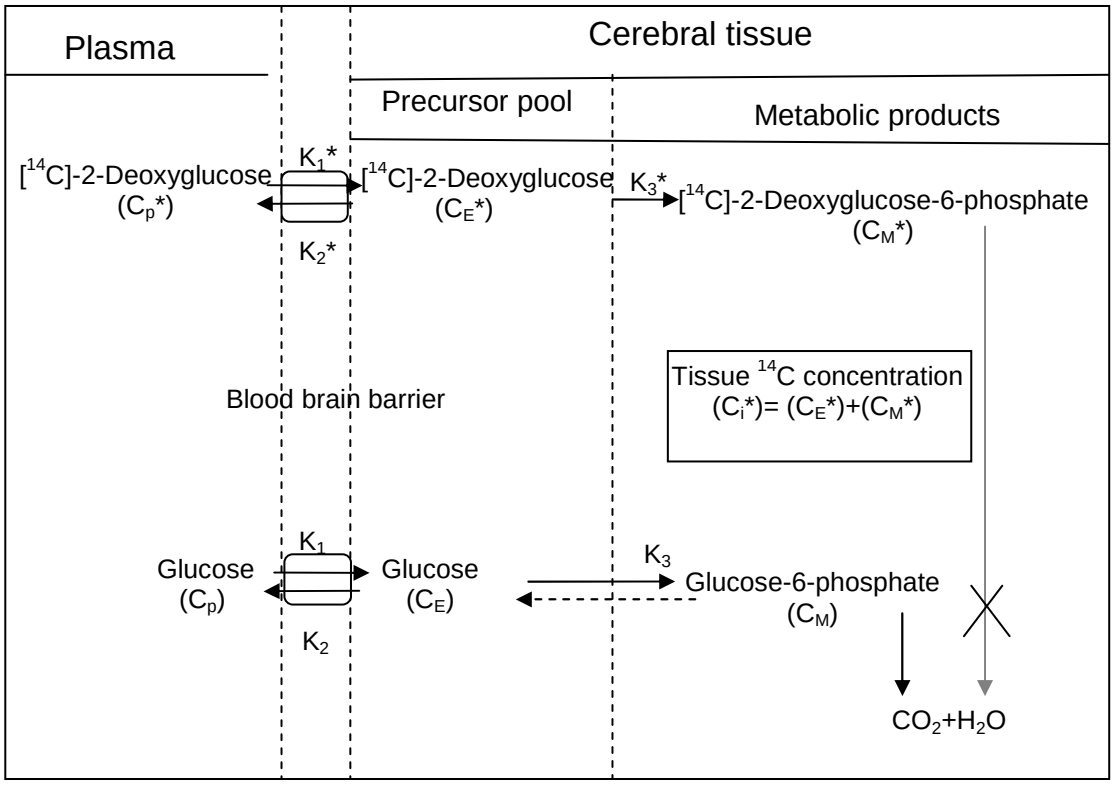

Figure 2.3.1 Schematic of theoretical model of [^{14}C]-2-deoxyglucose autoradiographic technique.

C_i* represents the total [^{14}C] in a single homogenous tissue of the brain.

C_p and **C_p*** represents the concentration of glucose and [^{14}C]-2-deoxyglucose in the arterial plasma respectively.

C_E and **C_E*** represents the concentration of glucose and [^{14}C]-2-deoxyglucose in the precursor tissue pool.

C_M and **C_M*** represents the tissue concentration of glucose-6-phosphate and [^{14}C]-2-deoxyglucose-6-phosphate respectively.

K_1* and **K_2*** are the rate constant for carrier mediated transport of [^{14}C]-2-deoxyglucose from plasma to tissue and from tissue to plasma respectively.

K_3* is the rate constant for hexokinase phosphorylation.

K_1, **K_2** and **K_3** are the equivalent rate constants for glucose

(Sokoloff, 1977)

2.3.2 Quantitative and semi-quantitative [^{14}C]-2-deoxyglucose autoradiography.

Based on the biochemical behaviour of glucose and deoxyglucose (Figure 2.3.1), Sokoloff *et al*. (1977) developed a mathematical model, the operational equation, that allows for the rate of local cerebral glucose utilisation (LCMRglu) to be calculated in discrete structural components of cerebral tissue. The operational equation describes LCMRglu by taking into account the relationship between the arterial plasma concentration of both glucose (C_p) and 2-DG (C_p*) and the total [^{14}C] present in the cerebral tissue (C_i*). These are mathematically defined by the operational equation and depend on three assumptions:

1. Steady state of glucose concentration and utilisation.
2. Tracer concentrations of [^{14}C]-2-DG and [^{14}C]-2-deoxyglucose-6-phosphate.
3. [^{14}C]-2-DG and glucose are uniform in homogeneous tissue that exchanges directly with the plasma.

The operational equation is used in the fully quantitative [^{14}C]-2-DG autoradiographic technique to measure LCMRglu. This method requires multiple blood samples over a 45 minute time period. However, it is not possible in smaller animals such as mice to produce the plasma glucose and [^{14}C] profiles required without the risk of hypoglycaemia. The semi- quantitative (SQ) [^{14}C]-2-DG autoradiographic method has been derived from the fully quantitative 2-DG autoradiographic technique as a way of investigating LCMRglu in mice, which is performed in conscious unrestrained mice and requires only a terminal blood sample (Cuthill et al., 2006). The disadvantage of this method is there are no plasma profiles so it is not possible to use the operational equation to calculate LCMRglu. Previously to estimate LCMRglu in the SQ 2-DG technique densitometric readings from a region of interest on an autoradiogram were measured and compared to a reference region (Jordan et al., 2005). However, the choice of reference region impacts on the accuracy of the result. Recently terminal plasma samples have been shown to provide an accurate plasma glucose and [^{14}C] profile. This allowed for the simplification of the operational equation for use in the SQ 2-DG method (Dawson et al., 2008).

To simplify the operational equation the rate constants were removed as over a period of 45 minutes the [^{14}C]-2-DG left in the plasma or in the unphosphorylated state in the cerebral tissue approaches zero and therefore so do the rate constants. A detailed plasma profile is not examined in the semi-quantitative 2-DG technique so removal of the plasma glucose and [^{14}C]-2-deoxyglucose profiles simplified the equation further. Finally the lumped constant describes differences in glucose and [^{14}C]-2-DG kinetics and volume distributions and is influenced by factors which alter glucose supply and utilisation. The lumped constant is the same between all brain regions and animals so can also be removed from the equation. The new equation (Equation 1, Figure 2.3.2) describes the relationship between the [^{14}C]/[glucose] ratio of an individual animal and other experimental animals both within the same experimental group and between experimental groups. This equation can then be simplified further into the final equation (Equation 2, Figure 2.3.2) and was used in the current studies to provide an index of LCMRglu (iLCMRglu).

$$R_i = \left(\frac{C_i^*(T)}{(C_p^*/C_p)_{individual}}\right)\left(\frac{(C_p^*/C_p)_{individual}}{mean(C_p^*/C_p)_{group}}\right)\left(\frac{mean(C_p^*/C_p)_{group}}{mean(C_p^*/C_p)_{control\ group}}\right)$$

Equation 1

$$R_i = \left(\frac{C_i^*(T)}{mean(C_p^*/C_p)_{control\ group}}\right)$$

Equation 2

Figure 2.3.2 Simplification of the operational equation in the semi-quantatative [^{14}C]-2-deoxyglucose autoradiographic method.

C_i* represents the total [^{14}C] in a single homogenous tissue of the brain.
C_p and **C_p*** represents the concentration of glucose and [^{14}C]-2-deoxyglucose in the arterial plasma respectively.
T represents time at the end of experiment.
(Sokoloff, 1981)

2.3.3 Experimental protocol for semi-quantitative [^{14}C]-2-deoxyglucose autoradiography.

[^{14}C]-2-DG (5μCi in 0.4mls sterile saline; specific activity 50-57.7 mCi/mmol; Tocris) was injected intraperitoneally to mice at a steady rate over 10 seconds. 42.5 minutes later after the [^{14}C]-2-DG injection mice were anesthetised with 4% isofluorane in a mixture of 30% oxygen /70% nitrogen for 2.5 minutes. Then at exactly 45 minutes after the [^{14}C]-2-DG injection mice were decapitated and a terminal blood sample taken by torso inversion and immediately centrifuged. Plasma glucose levels were analysed using a semi-automated glucose oxidase enzyme assay (Glucose analyser 2, Beckman) and plasma [^{14}C] was measured using the liquid scintillation counter. Brains were rapidly dissected from the skull and frozen in isopentane at -45ºC. Brain coronal sections (20μm thick) were cut in a cryostat at -15 ºC. Three out of every six brain sections were collected on coverslips and dried quickly on a hotplate at 60 ºC. The sections were then exposed to Kodak Biomax MR film for 4 days along with a set of [^{14}C]-standards and developed using an x-ray film processor. Densitometric analysis was used to determine the [^{14}C] isotope concentration present in discrete regions of interest and the data was analysed using Equation 2 as described above.

2.3.4 Intraperitoneal injections of fenfluramine.

Naïve balb/c mice were injected intraperitoneally with 10mg/kg fenfluramine in sterile saline (Tocris) 30 minutes prior to [^{14}C]-2-DG administration. The control group were injected intraperitoneally with saline. In a separate experiment on day 41/42 post immunisation, both the CIA group and the control group were intraperitoneally injected with 10mg/kg fenfluramine 30 minutes prior to intraperitoneal injection of [^{14}C]-2-DG.

2.4 Immunohistochemistry.

2.4.1 Theory.

Immunohistochemistry involves antigen-antibody interactions which can be labelled to allow anatomical mapping of the antigen in discrete anatomical locations. The antigen detection method used in this thesis is the Avidin-Biotin Complex (ABC) method involving multiple incubation steps which amplify the signal. The first incubation introduces an unlabelled primary antibody that reacts with the antigen. The second incubation involves biotinylated secondary antibody raised against the species of the primary antibody, which attaches itself to the primary antibody. This step introduces biotin into the section which is used to label nucleic acids and proteins that may be detected by avidin. After the tissue is repeatedly washed avidin biotinylated enzyme complex (ABC) is added to the tissue and binds to the biotinylated secondary antibody, during this step the biotin present on the secondary antibody interact with the free biotin binding sites on the ABC. The final stage is to incubate the tissue with Perixodase and diaminobenzidine (DAB) which reacts to form the brown chromagen colour on the tissue section after exposure.

2.4.2 Intraperitoneal injections of BrdU.

BrdU in sterile saline was made fresh on the day of administration. Mice were injected intraperitoneally with either 150 mg/kg BrdU once or 100mg/kg BrdU (Sigma-Aldrich) twice daily at 10am and then again at 4 pm for 3/5 days. After the final injection, mice were culled the following day. A schematic of BrdU administration is illustrated for each study in the results section in either Chapter 3 or Chapter 6. A mouse embryonic brain from mouse line $Fgfr3^{+/K644E}$ was a gift from Tomoko Iwata and was used as a positive control for BrdU staining. This was derived from a pregnant female mouse which was injected intraperitoneally with BrdU (50µg/g) 1 hour prior to termination.

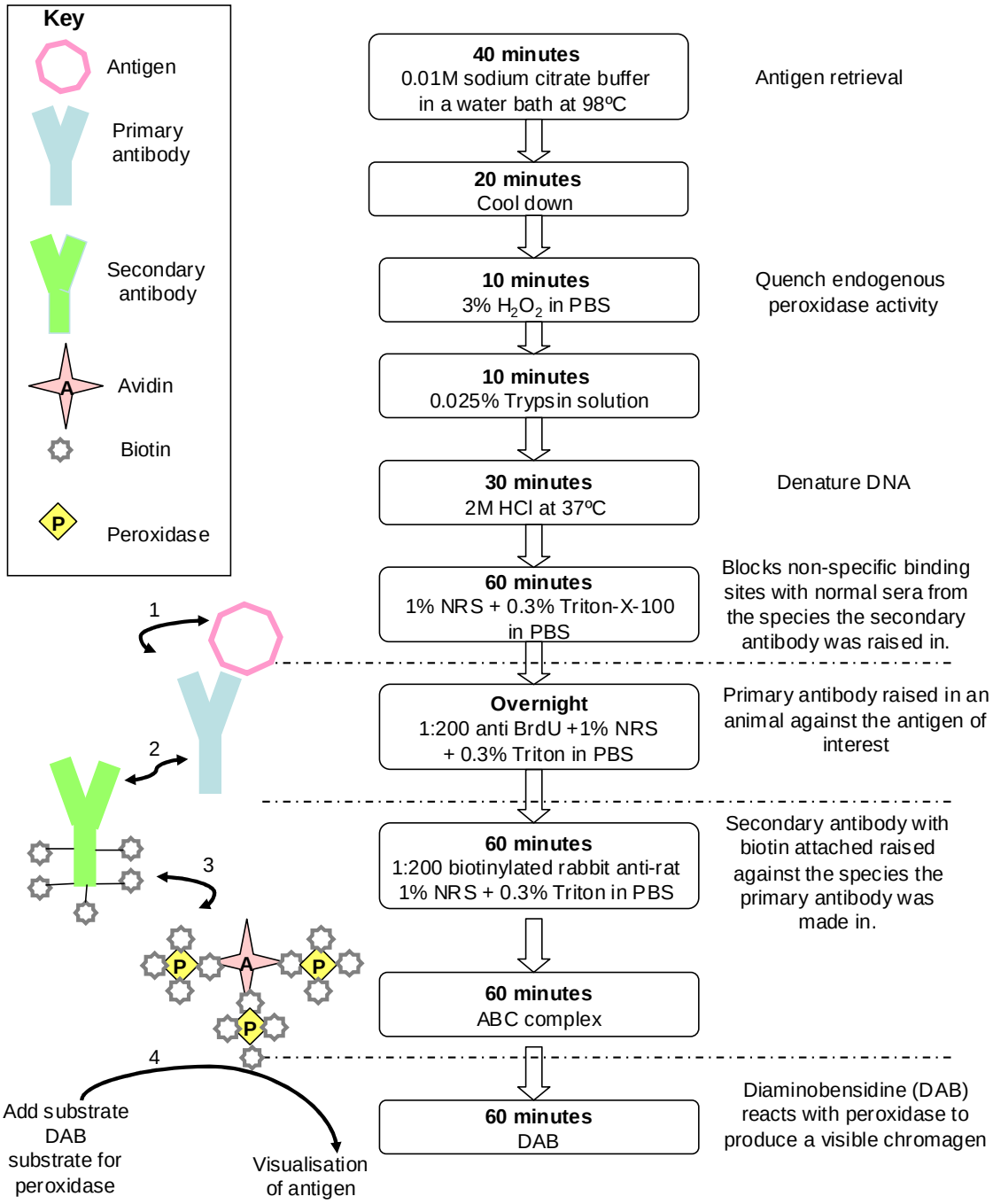

Figure 2.4.1 Immunodhistochemistry protocol for BrdU staining and diagram explaining ABC detection method.

2.4.3 Experimental protocol for BrdU immunohistochemistry.

5' –Bromo-2'-deoxyuridine (BrdU) is a marker of proliferating cells which is integrated into DNA during synthesis and can be detected using immunohistochemistry. Sections were removed from storage at -20 ℃ in cryoprotectant. Every 6th section through the full extent of the hippocampus (Bregma -0.82mm to-4.72; (Franklin K.B.J and Paxinos G., 2007) was mounted on a poly-L-lysine- coated slide and left to dry over night (Appendix 1). Sections were circled with a hydrophobic pen before being placed in two 5 minute phosphate buffer saline (PBS) washes. Sections were then placed in sodium citrate buffer (pH6) and incubated in a water bath at 98ºC for 40 minutes before being cooled by placing the containers in a sink of cold water for 20-30 minutes. Once cooled endogenous peroxidise activity was quenched by incubating sections with 3% hydrogen peroxide (H_2O_2) in PBS for 10 minutes. Sections were then incubated in 0.025% trypsin (Sigma-Aldrich) solution for 10 minutes and then DNA was denatured with 2M hydrochloric acid (HCl) at 37 ºC for 30 minutes. Non-specific binding sites were blocked by incubating sections for 60 minutes in a blocking solution of 1% normal rabbit serum (NRS, Vector Laboratories) in PBS and 0.3% Triton X-100. Sections were incubated with primary antibody (rat-anti-BrdU; 1:200, Serotec) diluted in blocking solution at 4ºC overnight. Sections were then incubated in secondary antibody (biotinylated rabbit anti-rat; 1:200, Vector Laboratories) in blocking solution for 60 minutes. This was followed by incubation in ABC (Vector Laboratories) for 60 minutes and visualisation with DAB (Vector Laboratories, Figure 2.4.1). Between each step in the protocol described above sections were rinsed in two 5 minute washes in PBS on a shaker. The only exception was between the non-specific block and the primary antibody incubation, there was no rinse step. Following incubation with DAB sections were rinsed in distilled water for 30 minutes prior to counterstaining with haematoxylin. Negative and positive controls were performed at the same time as the first run of BrdU immunohistochemistry to determine if the protocol was successful. Negative controls underwent the same procedure in the absence of primary antibody. No BrdU staining was detected in these sections. Embryonic brain sections were used for a positive control which displayed a high level of BrdU staining (Figure 2.4.2).

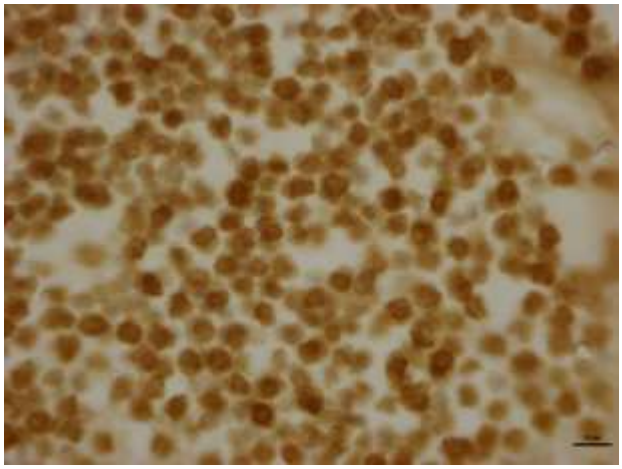

Figure 2.4.2 BrdU positive staining in sections of embryonic brain.

There is substantial cell proliferation throughout the embryonic brain and was used as a positive control. Scale bar =10μm.

2.4.4 Quantification of BrdU positive cells.

Prior to quantification sections were anonymised so that mouse identity was concealed until quantification was complete. The total number of BrdU-positive cells in the subgranular zone (SGZ), granule cell layer (GCL) and hilus of each section examined was determined using light microscopy (x400). In the SGZ a BrdU-positive cell was counted if it was touching the GCL and in the hilus if it was more then one cell away from the GCL (Figure 2.4.3). BrdU labelled cells were counted in every 6 section through the hippocampus therefore the total number of BrdU cells in the whole hippocampus was estimated by multiplying the number of cells in each section by 6.

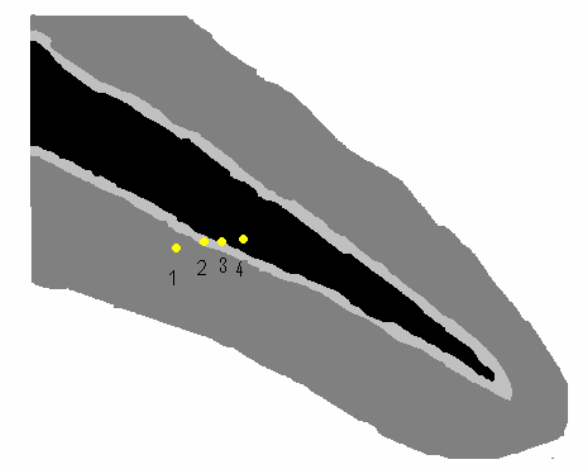

Figure 2.4.3 Diagram representing BrdU staining in the hippocampus.

The granule cell layer is dark grey, the subgranular zone is light grey and the hilus is black. Reference point 1 represents a BrdU positive cell in the granule cell layer. Reference points 2 and 3 represent a BrdU positive cell touching the granule cell layer and within one cell distance from the granule cell layer respectively. Reference point 4 represents a BrdU positive cell in the hilus.

Chapter 3

Establishing the murine model of collagen induced arthritis.

3.1 Introduction.

There are various animal models of arthritis that have diverse etiologies and pathogenic mechanisms which result in a similar outcome of inflammation and bone erosion within the joint (Asquith et al., 2009b). The murine models of collagen induced arthritis (CIA) resemble the human form of rheumatoid arthritis as they both produce an autoimmune response to type II collagen, one of the main autoantigens found in human rheumatoid arthritis patients (Kim et al., 1999; Londei et al., 1989).

The CIA model is a chronic arthritic model used to investigate the development of arthritis and is particularly useful in assessing the therapeutic potential of novel agents. In both human rheumatoid arthritis and the CIA model there are specific major histocompatibility complex class II (MHC II) antigens associated with the development of the disease. The human MHC II antigens are HLA-DR1 (Rosloniec et al., 1997) and HLA-DR4 (Rosloniec et al., 1998) and in the CIA model I-A^q haplotype mice are more susceptible to the disease (Wooley et al., 1981). In the murine CIA model, mice are immunised with type II collagen which binds to a stretch of amino acids in the MHC II which present the arthritogenic epitopes to T-cells. The immune response in the CIA model is dependent on the activation of T-cells as antagonism with anti-L3T4 reduced disease expression by specifically blocking MHC II binding by T-cells (Ranges et al., 1985). Furthermore T-cells generated in arthritic DBA/1 mice can induce arthritis when injected into naïve mice. These naïve mice immunised with T-cell generated from arthritic DBA/1 mice have less sever arthritis, possibly due to reduced B-cell activation (Holmdahl et al., 1985). B-cell deficient mice have an unaltered T-cell response to type II collagen but are resistant to the development of CIA (Svensson et al., 1998). This evidence suggests that both T and B-cells are important in the development of CIA.

3.1.1 Aims.

The main aim of this thesis is to investigate the effect of arthritis and systemic inflammation on the brain at the cellular, molecular and functional levels. Therefore the objective of this first results chapter to establish the murine CIA model in our lab as this has previously not been done before. To achieve this, an initial CIA study was performed (study 1) followed by a second more successful CIA experiment (study 2).

3.2 Methods.

Day “x” in the thesis refers to the number of days after the first immunisation on day 0.

3.2.1 Induction of CIA.

The timeline of the CIA model is illustrated in Figure 3.2.1. On day 0, male DBA/1 mice aged 7-8 weeks (13-15g, Harlan) were anaesthetised and the fur at the base of their tails shaved. Under anaesthetic the CIA group (n=9 or 12) were injected subcutaneously (s.c) with 0.1ml of collagen emulsification at 2 sites just above the base of the tail of 0.05ml each. The collagen emulsification was made up of equal volumes of bovine type II collagen and complete Freund’s adjuvant. At this time point the control group (n=7 or 12) received no treatment. On day 21 post immunisation, the CIA group were injected intraperitoneally with 0.2ml bovine type II collagen 2mg/ml in an equal volume of sterile phosphate buffered saline. At this time point the control group received an intraperitoneal (i.p) injection of 0.2ml sterile phosphate buffered saline. On day 42 post immunisation, all brains were harvested (Section 2.1.1).

Study 1.

An initial CIA experiment was performed in a CIA group (n= 9) and control group (n=7). During this study manual callipers were employed (Section 2.1.6).

Study 2.

The CIA experiment was repeated in a separate CIA group (n=12) and control group (n=12) during which improvements were made to the preparation of the emulsification of bovine type II collagen and complete Freund’s adjuvant. Improvements were also made to disease assessment including a change in termination criteria (Section 3.2.2), a more detailed scoring system was employed (Table 3.2.2) and the manual callipers were replaced with spring callipers (Section 3.2.5). The mice generated in this experiment were employed in Chapter 6, study A to investigate cell proliferation.

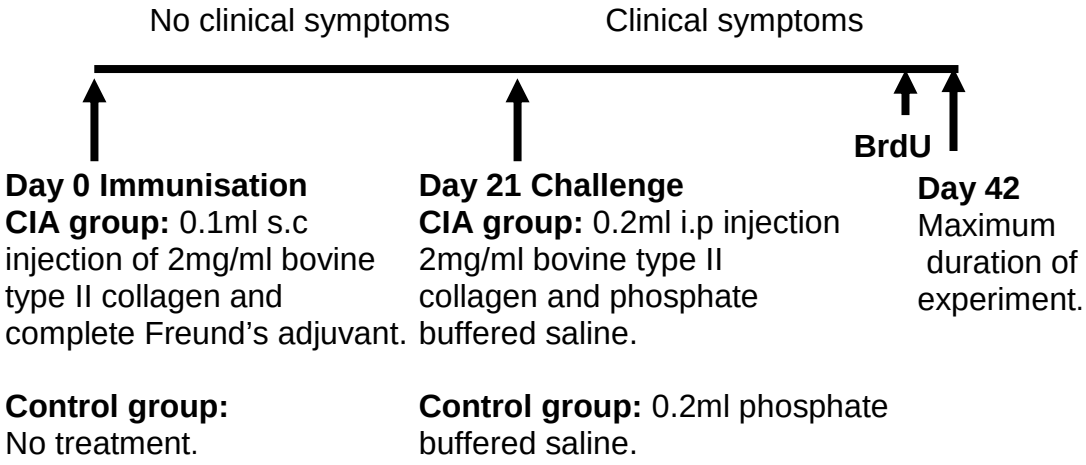

Figure 3.2.1 Schematic of the murine model of CIA.

3.2.2 Termination criteria.

Study 1.

In accordance with the Home Office project licence any mouse with a decrease in body weight of 20% or greater compared to their previous body weight measurement was terminated by a Schedule 1 method. Any mouse with a clinical score of twelve or over was culled (Section 2.1.2).

Study 2.

In accordance with the Home Office project licence animals were assigned a score of ill-health where any mouse with an ill-health score of 7 or greater was killed by a Schedule 1 method (Section 2.1.2).

3.2.3 Clinical score.

In all CIA experiments animals were monitored for clinical signs of disease from day 20 post immunisation, by scoring each of the 4 limbs using a clinical scoring system (Section 2.1.3). The sum score of the four limbs was calculated on each day per animal and the median clinical score for each limb was calculated each day per group of animals. The clinical scoring system used for Study 1 is shown in Table 3.2.1. The clinical scorning system in Table 3.2.2. was used to evaluate Study 2.

Study 1.

Clinical score	Description
0	No disease/ normal.
1	Erythema of hock joint.
2	Erythema from hock to the limb.
3	Erythema and swelling of hock and limb.
4	Loss of function in the limb.

Table 3.2.1 Description of clinical scoring system used in study 1.

Study 2.

Clinical score	Description
0	No disease/ normal.
1	Erythema and mild swelling of hock joint.
2	Erythema and mild swelling from the hock to the metacarpal articulations or metatarsal articulations.
3	Erythema and moderate swelling from the hock to phalangeal articulations.
4	Erythema and severe swelling of the limb.

Table 3.2.2 Description of clinical scoring system used to in study 2.

3.2.4 Disease incidence.

The incidence of disease was calculated as a percentage of all mice which demonstrated clinical symptoms of swelling and erythema.

3.2.5 Calliper measurements.

Study 1.

In the initial CIA model mice were monitored for swelling of the hock using manual callipers which were placed between the hock joint and the paw on each of the 4

limbs per mouse. In the CIA model, from day 20 post immunisation calliper measurements were recorded every second day (Section 2.1.6).

Study 2.

In the next CIA experiment a set of spring callipers were used to record paw thickness. From day 20 post immunisation, calliper measurements were recorded every second day by holding the paw horizontal and placing the two heads of the callipers above and below the paw. The spring callipers were released clamping the paw and applying the same pressure to give a measurement of paw thickness (Section 2.1.6).

3.2.6 Histological assessment of joint pathology.

Study 2.

On day 42 post immunisation, hind limbs were harvested and fixed in neutral-buffered formalin for histological assessment of joint pathology. Both the right and left hind limbs from the control group (n=12) and the CIA group (n=12) were contracted out to the Pathology department to be decalcified, paraffin embedded and cut on a microtome before haematoxylin and eosin staining. One section from each hind limb was examined under a light microscope to determine if cell infiltration was present in either the digits or hock joint.

3.2.7 Statistical analysis.

All CIA immunised animals with a clinical score of 0 were excluded from the CIA group. Data for clinical scores are presented as the median and data for the calliper measurements and body weight are presented as mean ±SEM. Statistical significance was determined using a Mann Whitney test to investigate changes in the hock or paw thickness summary measurements. To examine the correlation between clinical score and calliper measurements a Pearson’s correlation test was used.

Results 3.3

3.3.1 Study 1: Health status.

Visual inspection of the animals in their home cages revealed that both the control group and CIA group remained inquisitive, continued to respond to touch, were not hunched over and maintained a healthy appearance of coat and eyes. Mice were able to move at a rapid pace around the cage and even those with swollen limbs were not impeded. No mice lost more than 20% of their original body weight. There was an increase in body weight over the majority of the experiment which levelled off at approximately day 35 post immunisation. There was no difference in body weight between the control and CIA groups (Figure 3.3.1).

3.3.2 Study 1: Disease features and incidence.

Visual inspection of the individual limbs for the key features of the disease were used to assign a graded objective clinical score (Table 3.2.1). In brief a clinical score of 0 represents a normal limb, in which the joints in the hock and digit are clearly visible. A clinical score of 1 represents swelling of the hock, which then extends into the limb representing a clinical score of 2. By comparison to a clinical score of 3/ 4 represents swelling and erythema of the hock extends into the limb and digits. A clinical score of 4 represents a limb with severe swelling and erythema from the hock which extends into the limb and 4-5 digest leading to loss of function (Figure 3.3.2).

The presence of arthritis was defined as any mouse with a clinical score above 0 in any limb. In this study only 4 mice out of a possible 9 immunised developed clinical symptoms of arthritis representing a disease incidence of 44%, however as 2 mice were culled early the maximum disease incidence at any one time point was 37%.

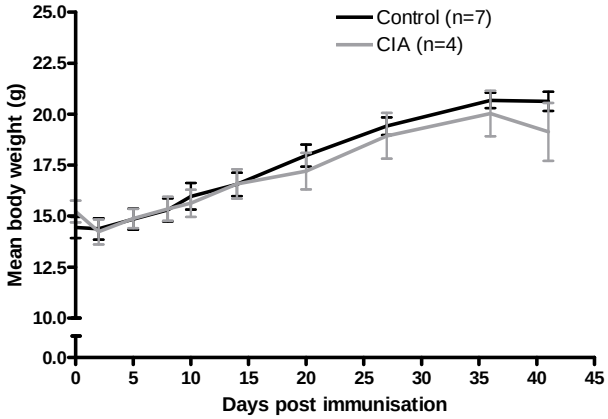

Figure 3.3.1 Study 1: Mean body weight of CIA group and control group.

The control group (n=7) and the CIA group (day 0-21 inclusive n=4; day 22-41 inclusive n=3; and on day 42 n=2) were weighed at least once a week throughout the experiment. The graph above illustrates similar mean body weights of the CIA and the control groups which increased gradually over time. Data are presented mean ± SEM

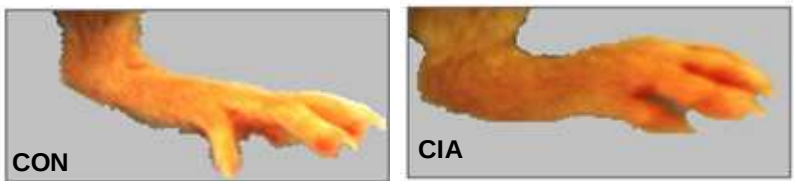

Figure 3.3.2 Representative image of a normal and diseased limb.

In the control limb there is no swelling and erythema and the joints are clearly visible in the digits and at the hock. This animal would score 0 for the limb. In the CIA limb there is erythema and swelling spanning from the hock and into the digits. The joints in the digit and at the hock are no longer clearly defined. This animal would be assigned a clinical score of 4 and would be described as having severe swelling and erythema.

3.3.3 Study 1: Clinical score.

Out of the 4 mice which demonstrated clinical symptoms of swelling and erythema, 3 mice developed clinical symptoms at day 21 post immunisation as predicted in this model. The fourth mouse was assigned a clinical score of 12 prior to day 21 post immunisation and was culled at this time in line with the conditions of the Home Office Licence. No control animals showed any clinical signs of arthritis at all time points examined.

Front limbs appeared to be more severely affected by disease than hind limbs having the higher clinical scores (Figure 3.3.3, A-D). To provide a summary measure of disease severity for each animal the sum of the clinical scores of the 4 limbs was plotted over time and the area under the curve calculated. The CIA group had a wide range of disease severity summary measures (4-124). No control animals showed any signs of swelling and erythema so had a disease severity summary score of 0 at all time point investigated (Figure 3.3.4).

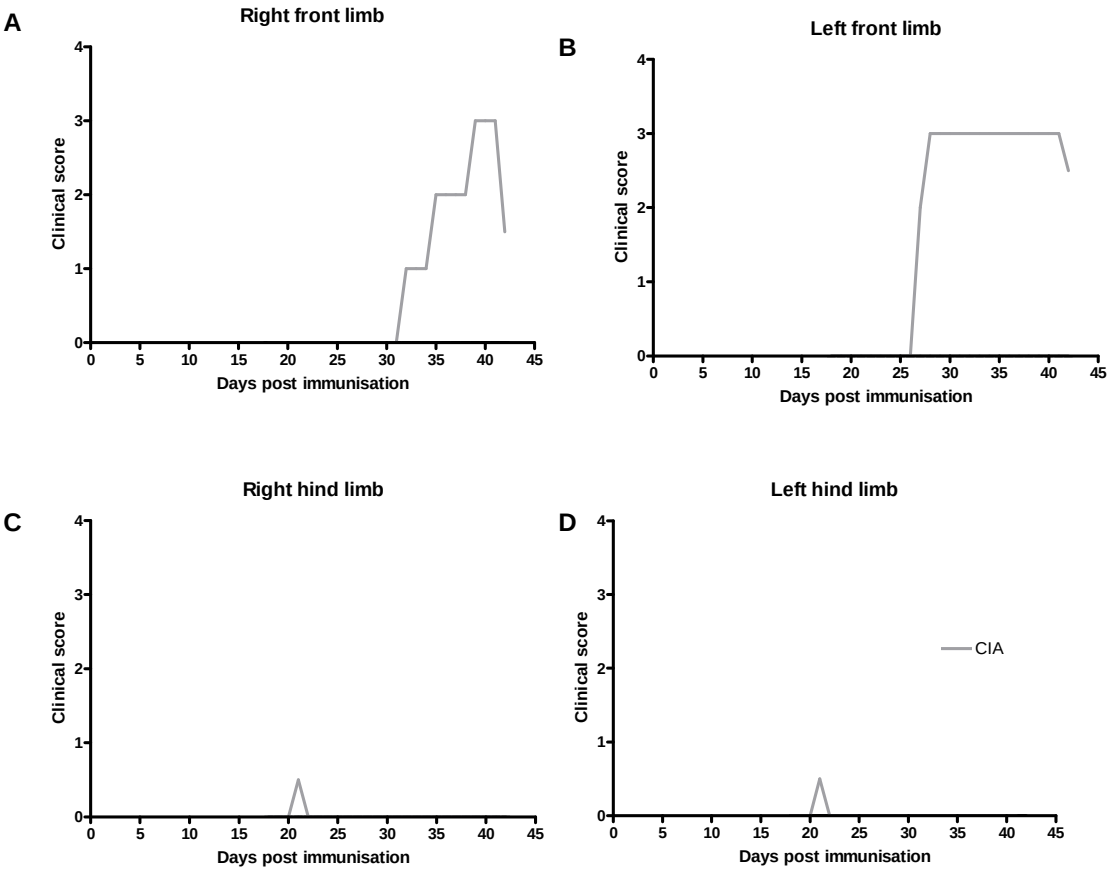

Figure 3.3.3 Study 1: Clinical score.

The graphs present the clinical score in the front and the hind limbs as the median of the CIA group (day 0-21 inclusive n=4; day 22-41 inclusive n=3; and on day 42 n=2). No animals from the control group (n=7) displayed any clinical symptoms at any time point examined

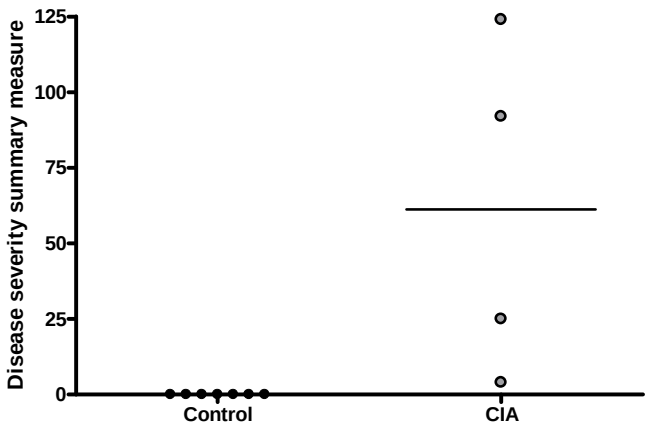

Figure 3.3.4 Study 1: Disease severity summary measures.

The sum clinical scores of the 4 limbs were plotted over time and the area under the curve calculated to give a disease severity summary measure for each animal. In the CIA group (day 0-21 inclusive n=4; day 22-41 inclusive n=3; and on day 42 n=2) there were a range of disease severities whereas the control group (n=7) displayed no clinical symptoms at any time points investigated. Data are presented as the mean.

3.3.4 Study 1: Calliper measurements.

In naïve adult DBA1/A mice a normal hock is approximately 1.8-2.0mm thick. The swelling in the front limbs of the CIA group reached a maximum hock thickness in excess of 2.5mm (Figure 3.3.5 A, B). By comparison the maximum hock thickness in the hind limbs of the CIA group did not exceed 2.5mm (Figure 3.3.5 C, D).

During this study a single mouse was culled at day 21 post immunisation, which resulted in a low hock thickness summary measure. Overall there was no significant difference in the summary measurements of hock thickness in the CIA group by comparison to the control group (Figure 3.3.6).

A correlation between the daily clinical score and calliper measurements of hock thickness showed that as the clinical scores increased so did the hock thickness (Figure 3.3.7).

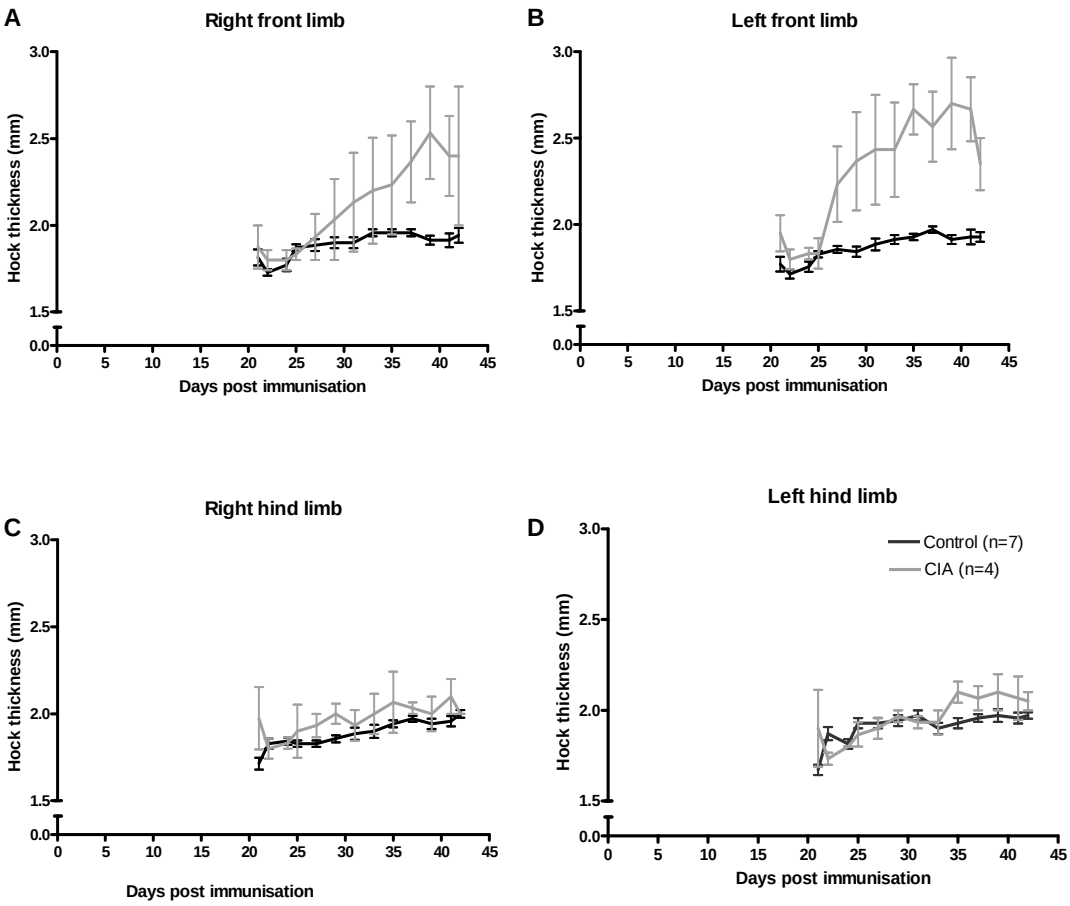

Figure 3.3.5 Study 1: Hock thickness of the individual limbs.

The graphs above illustrate mean hock thickness of front and hind limbs in the control group (n=7) and the CIA group (day 0-21 inclusive n=4; day 22-41 inclusive n=3; and on day 42 n=2). Data are presented mean ± SEM.

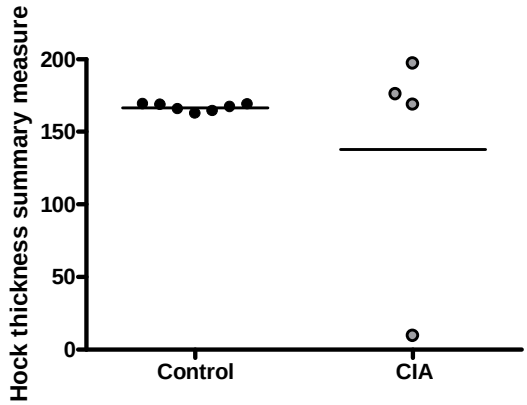

Figure 3.3.6 Study 1: Hock thickness summary measure.

The sum hock thicknesses of the individual limbs were plotted over time and the area under the curve calculated to give a summary measure of hock thickness. The graph above depicts no significant difference in the hock thickness summary measure of the CIA group (day 0-21 inclusive n=4; day 22-41 inclusive n=3; and on day 42 n=2) in comparison to the control group (n=7). Statistical significance was determined using a Mann Whitney test and the data are presented as the mean (*p<0.05).

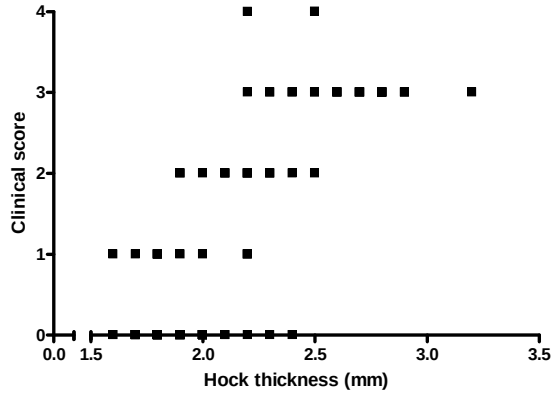

Figure 3.3.7 Study 1: Relationship between clinical score and hock thickness.

Clinical scores were paired with calliper measurements of hock thickness in the same animal at the same time point. There was a significant correlation between the clinical score and the hock thickness (***r=0.8302). Statistical significance was calculated using a Pearson's rank test.

3.3.5 Study 2: Clinical score and disease incidence.

Ten mice out of a possible 12 developed clinical symptoms of erythema and swelling representing a disease incidence of 83%. The CIA group developed clinical symptoms at approximately day 21-28 post immunisation. Front limbs appeared to be more severely affected by disease than hind limbs having the higher clinical scores (Figure 3.3.8). No control animals showed any clinical signs of arthritis at any time point examined.

To provide a summary measure of disease severity for each animal the sum of the clinical scores of the 4 limbs were plotted over time and the area under the curve calculated. The CIA group had a wide range of disease severities summary measures (60-190). No control animals showed any signs of clinical symptoms so had a disease severity summary measure of 0 at all time points investigated (Figure 3.3.9).

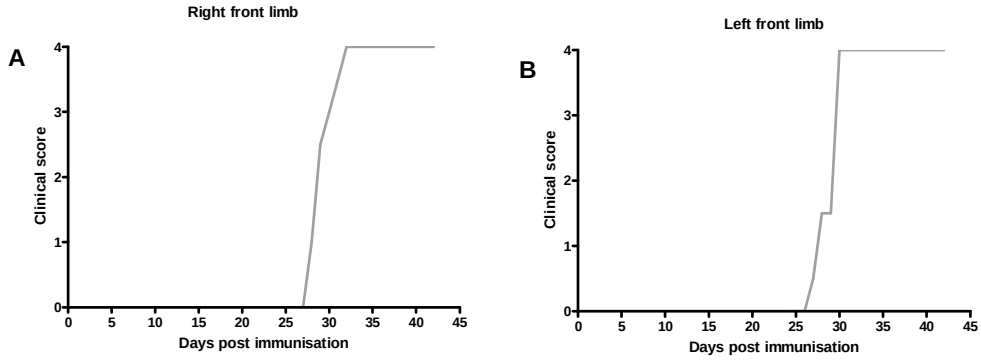

Figure 3.3.8 Study 2: Clinical score.

From day 20 post immunisation, each limb was monitored for clinical symptoms of arthritis and assigned a daily clinical score ranging between 0-4. The graphs present the clinical score in the front and the hind limbs as the median of the CIA group (n=10). The hind limbs had a median clinical score of 0 at all time points examined. No animals from the control group (n=12) displayed any clinical symptoms at any time point investigated.

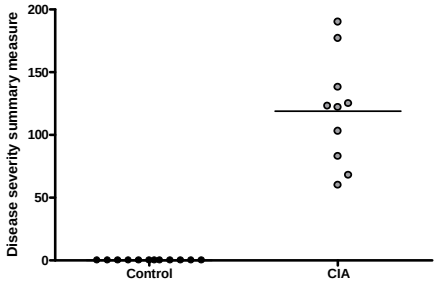

Figure 3.3.9 Study 2: Disease severity summary measure in the CIA group and control group.

The sum clinical scores of the 4 limbs were plotted over time and the area under the curve calculated to give a disease severity summary measure for each animal. Data are

3.3.6 Study 2: Calliper measurements of paw thickness.

To quantify the extent of limb swelling, from day 20 post immunisation spring calliper measurements of paw thickness were made every second day. Normal paws are approximately 1.8-2.0mm thick in naïve adult DBA1/A mice. The swelling in the front limbs and hind limbs of the CIA group reached a maximum paw thickness of 3.1mm, however overall the swelling in the front limbs was greater by comparison to the hind limbs (Figure 3.3.10).

To provide a summary measure of paw thickness for the duration of the experiment for each animal in both the control and CIA group, the sum paw thickness of the 4 limbs was plotted over time and the area under the curve calculated. Overall there was a significant increase in the paw thickness summary measure in the CIA group compared to the control group (***$p<0.001$; Figure 3.3.11).

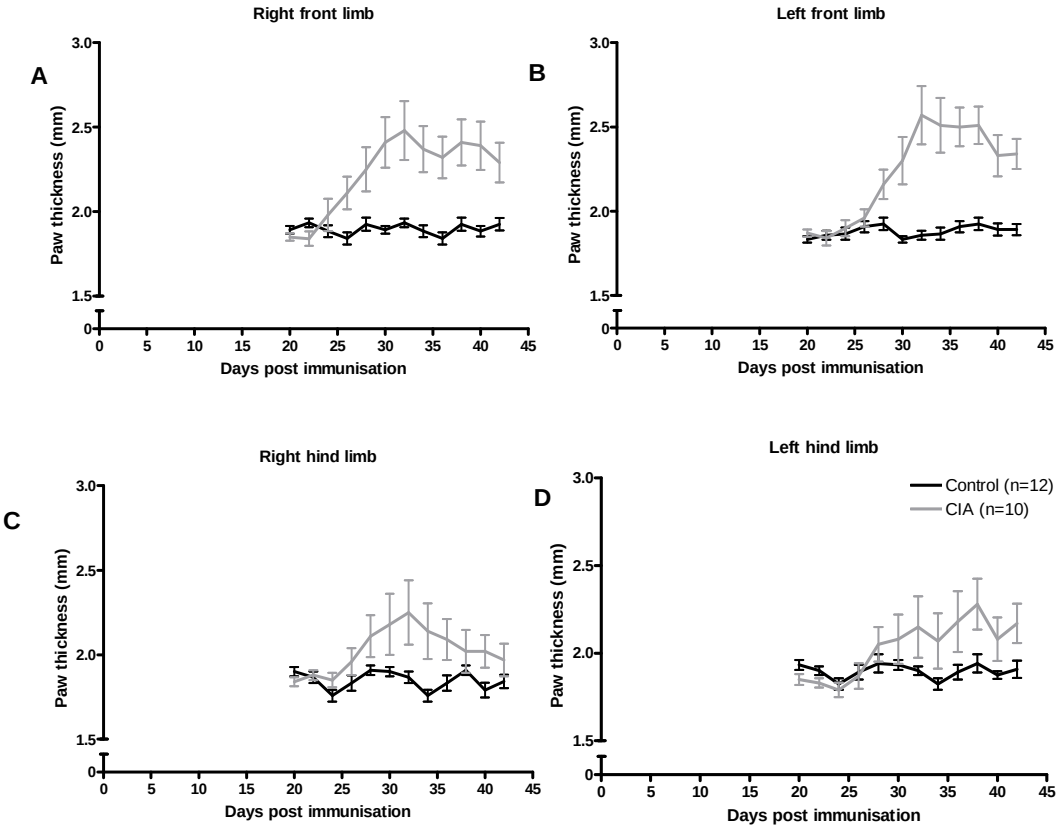

Figure 3.3.10 Study 2: Paw thickness.

The graphs above depict the mean paw thickness in the front and hind limbs of the control group (n=12) and the CIA group (n=10). Data are presented as mean ±SEM.

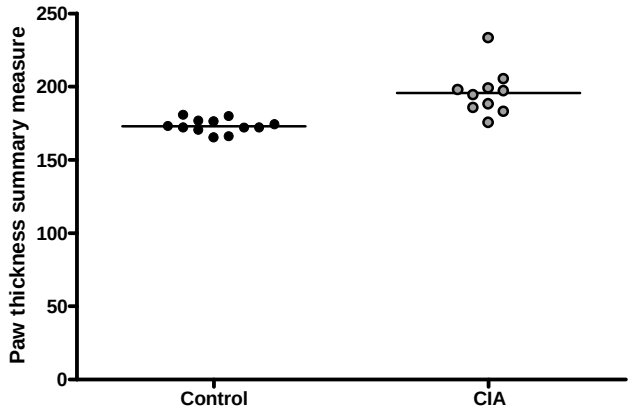

Figure 3.3.11 Study 2: Paw thickness summary measure.

The sum paw thickness of the individual limbs per animal were plotted over time and the area under the curve calculated to give a summary measure of paw thickness. The graph above depict a significant difference in the summary measure of paw thickness in the CIA group (n=10) compared to the control group (n=12). Statistical significance was determined using a Mann Whitney test (***p< 0.001).

3.3.7 Study 2 Histological assessment of joint pathology.

In addition to the clinical score another way to evaluate the murine CIA model is by histological examination of the joint. The characteristic features of this model are infiltration of inflammatory cells such as, monocytes, macrophage, basophils, eosinophils or neutrophils in the bone marrow (BM) and synovial tissue (ST). Synovial hyperplasia (SH) occurs when macrophage proliferate. Not observed in the image is development of the pannus over the cartilage (C) which leads to destruction of the cartilage and eventual erosion of the joint (Rowley et al., 2008). We were able to replicate the infiltration of inflammatory cells previously reported in the literature in response to immune activation (Courtenay et al., 1980; Wu et al., 2007).

I examined one stained section from both hind limbs from each mouse by light microscope to determine if inflammatory cell infiltration of the joint were present or absent. All control mice had the appearance of healthy joints and no obvious inflammatory cell infiltration (Figure 3.3.12, A). However, in the right hind limb of the CIA group out of the 4 limbs that displayed clinical symptoms only 3 limbs displayed inflammatory cell infiltration. In the left hind limb 3 mice displayed clinical symptoms of arthritis and all of which displayed corresponding inflammatory cell infiltration (Figure 3.3.12, B).

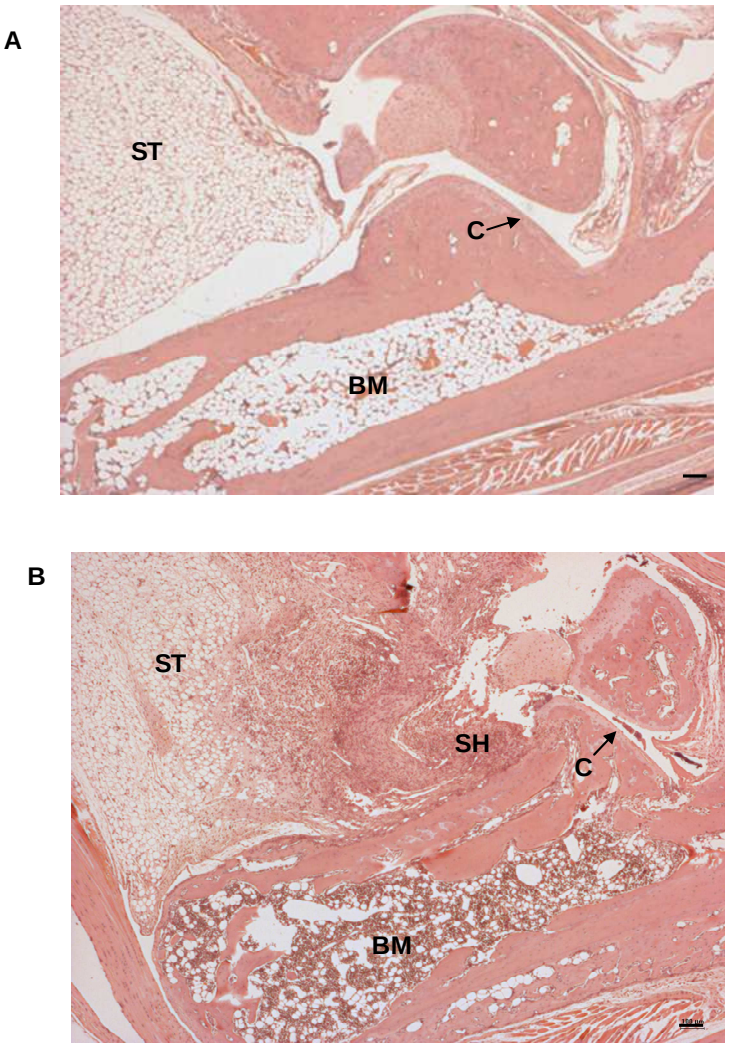

Figure 3.3.12 Study 2: Histological joint sections.

At day 42 post immunisation, hind limbs were processed and stained with haematoxylin and eosin. Section A is representative of the control group (n=12) with no inflammatory cell infiltration. Section B is representative of the CIA group (n=12) with synovial hyperplasia (SH) and inflammatory cell infiltration, which can be seen in the bone marrow (BM) and synovial tissue (ST).
(cartilage(C)) Scale bar = 100 µM

3.4 Discussion.

The murine model of CIA was first reported by Courtenay et al., 1980 and since then it has become the gold standard model for investigating the pathological mechanisms involved in arthritis and to investigate novel therapeutic targets. The present study was undertaken to establish the murine model of CIA for the first time within our research group. To achieve this I used a method that has been previously used for the induction of CIA in DBA/1 mice. To illustrate the successful induction of CIA data was gathered the temporal evolution of the disease including, disease incidence, clinical scores and hock/paw thickness. In addition to this I also examined the general health status of the mice. A significant detrimental effect on general health status could impact on the validity of any *in vivo* experiment. The induction of CIA by subcutaneous injection of type II collagen emulsification is technically challenging and ulcerations can occur if the type II collagen emulsification consistency is incorrect or if the injection site is too close to the tail (Brand, 2005). No ulcerations developed in mice exposed to type II collagen emulsification at any time point investigated and overall mice appeared healthy apart from the characteristic features of swelling and erythema of the limbs.

Although in study 1 the incidence of disease within the CIA group was lower than predicted from published studies, the characteristic clinical features of the disease in terms of limb swelling and erythema, observed were similar to those that have been described previously (Brand et al., 2007). In study 1, I examined the temporal progression of the disease in the individual limbs, and found the temporal evolution of the clinical scores and hock thickness were similar to the typical development of clinical symptoms reported in previous studies (Brand et al., 2007; Shibata et al., 2009).

In study 1, the clinical scores and calliper measurements demonstrate erythema and swelling in the front limbs only. CIA mice can develop arthritis in any limb and in any combination of limbs. The temporal evolution of arthritis in individual mice is unique and the reason why arthritic symptoms develop in a limb or limbs is ambiguous. Even although my results illustrate clinical symptoms in the front limbs only in CIA mice, the literature suggests that clinical symptoms are more frequently

observed in the hind limbs (Brand et al., 2007). However in these sets of experiments there was a poor incidence of clinical symptoms making any difference in the location of the appearance of arthritis inconclusive.

In this study the hock thickness summary measurement had one outlier which may account for non significant difference between the control and CIA groups of mice as subsequent studies reported in this thesis of paw thickness found a significant difference between the groups.

I successfully replicated the characteristic clinical features that have previously been described in the murine model of CIA, but had a lower incidence of disease than that reported in the literature. Previous studies have indicated the disease incidence that can be expected in the CIA model. This ranges from 80-100% (Brand et al., 2007; Courtenay et al., 1980; Niedbala et al., 2008; Xu et al., 2008). The lower than expected arthritic incidence in the present study of 25% may be due to a number of factors. It is possible that the type II collagen was denatured during preparation due to lack of experience with the technique. Improvements in the disease incidence in subsequent studies reported in this thesis have led me to believe that the homogeniser was not adequately submerged during the type II collagen emulsification in this current experiment. This resulted in an increase in the length of time required to get the correct consistency, during which the homogenizer produced heat, which may have produced sufficient heat to denature the type II collagen. Improvements in homogenisation technique in study 2 resulted in a decrease in the length of time required to obtain the correct emulsification consistency from an hour to approximately 20 minutes. This was associated with an increased arthritic incidence from 25% found in Study 1 to 83% in study 2. In study 2 the CIA model was further characterised using histological joint sections which illustrated the infiltration of inflammatory cells as previously reported within other research groups (Courtenay et al., 1980).

3.4.1 Conclusion

In study 1, the murine model of CIA produced a lower disease incidence and severity than expected compared to published data. Even although the disease incidence was low the characteristic features of erythema and swelling were observed in the animals demonstrating clinical symptoms. The clinical symptoms followed the typical temporal evolution observed in the literature. To improve the disease incidence technical improvements were made to the preparation of the type II collagen emulsification associated with increased disease incidence in subsequent studies. To characterise the arthritis further histological joint section illustrated the infiltration of inflammatory mediates, providing further evidence of the establishment of the murine model of CIA with in our department. The CIA model was continuously employed throughout this thesis to investigate neurochemical, structural and functional changes.

Chapter 4

Autoradiographic study of serotonin and dopamine transporter in the murine CIA model.

4.1 Introduction.

The immune system is active in depressed patients and evidence for this comes from increased IL-1β, IL-6, IFN-γ and TNF-α mRNA expression in peripheral blood mononuclear cells (Tsao et al., 2006). There is however limited evidence as to how these pro-inflammatory cytokines modulate the monoaminergic neurotransmitter systems in patients which have a co-morbidity between peripheral inflammatory disease and depression. A few *in vitro* studies have investigated the affect of individual cytokines on serotonin transporter (SERT) function. SERT is present on pre-synaptic terminals and is responsible for recycling serotonin back into the nerve terminal, regulating synaptic levels of the transmitter (Rang et al., 2003). Pro-inflammatory cytokines IL-1β (Ramamoorthy et al., 1995; Mossner et al., 1998) and TNF-α (Mossner et al., 1998) have been shown to increase serotonin uptake *in vitro*. This is consistent with a later experiment which demonstrated increased serotonin uptake in response to TNF-α and IL-1β exposure *in vitro* (Zhu et al., 2006). In comparison, the anti-inflammatory cytokine IL-4 has been shown to decrease serotonin uptake *in vitro* (Mossner et al., 2001). Therefore it can be construed that an increase in pro-inflammatory cytokines may increase SERT expression, which decreases serotonin availability through increased serotonin uptake, resulting in depressive symptoms. This has led to the hypothesis that elevated pro-inflammatory cytokines in the murine CIA model of rheumatoid arthritis will result in increased levels of SERT binding.

Although SERT binding was our main focus, dopamine transporter (DAT) binding was also quantified within the CNS of CIA immunised mice with clinical symptoms. DAT is present on pre-synaptic terminals and is responsible for recycling dopamine back into the nerve terminal. Dopaminergic neurotransmission is involved in the regulation of motor control and mood (Rang et al., 2003). However, there is limited evidence pertaining to the relationship between the dopaminergic and immune systems. Previous studies have shown that administration of dopamine receptor agonists enhance immune cell production (Tsao et al., 1997). Further links between

the dopaminergic and immune systems have been illustrated by target deletion of the DAT gene which resulted in reduced production of IFN-γ by immune cells (Kavelaars et al., 2005). The pro-inflammatory cytokine IFN-γ has been shown to be neuroprotective, as when administered prior to methamphetamine, a drug of abuse known to damage striatal dopaminergic neurons, there was less damage to dopaminergic neurons (Hozumi et al., 2008). However, when macrophage cell cultures from DAT gene deficient mice were stimulated with LPS there was enhanced production of pro-inflammatory cytokine, TNF-α and anti-inflammatory cytokine, IL-10 (Kavelaars et al., 2005). The association between the dopaminergic and immune systems has led to the hypothesis that pro-inflammatory cytokines released during the development of the murine CIA model will alter DAT binding in the CNS.

The limited amount of evidence available in the literature regarding the relationship between SERT, DAT and the immune system, which makes the data presented in this chapter extremely novel. As the murine CIA model is used to develop a peripheral immune response with which to investigate changes in the monoaminergic system. To achieve this *in vitro* autoradiography was employed using [^{123}I]-βCIT, a radioligand used in single photon emission computed tomography (SPECT) studies to investigate SERT and DAT binding. [^{123}I]-βCIT was the first ligand to be used to image SERT in depressed patients. Using this method SERT binding was revealed to be reduced in the brainstem of non-medicated patients (Malison et al., 1998). This study also reported no difference in [^{123}I]-βCIT binding of DAT in the striatum.

4.1.1 Aims.

The main aim of this chapter was to map the distribution of both SERT and DAT binding sites in discrete anatomical locations. To achieve this, the radioligand [^{125}I]-βCIT was employed to visualise the distribution of both SERT and DAT binding sites within the same tissue sections. Displacers were then utilised to visualise SERT and DAT binding in adjacent sections. [^{125}I]-βCIT is a non-specific ligand so to fully realise the aim of this chapter highly specific ligands [^{3}H]-citalopram and [^{3}H]-WIN 35,428 were utilised to label SERT and DAT respective

4.2 Methods.

4.2.1 Animals.

Mouse brain sections from the control group and the arthritic CIA group described in Chapter 3 were utilised in the *in vitro* autoradiographic studies described in this chapter (Section 3.3.1-3.3.7). The presence of arthritis was defined as any mouse with a clinical score above 0 in any limb. In this study only 4 mice out of 9 immunised developed clinical symptoms of swelling and erythema. The 4 mice which demonstrated clinical symptoms were termed the CIA group. The control group did not exhibit clinical symptoms of swelling and erythema at any time point examined.

4.2.2 *In vitro* autoradiography.

On day 42 post immunisation, all brains were harvested and frozen in isopentane at -45ºC (section 2.2.2). Coronal sections 20µm thick were cut on a cryostat set at -20ºC, and mounted on poly-L-lysine coated slides and stored at -20ºC prior to use. Slides with tissue sections from the control group (n=6) and the CIA group (n=4) were removed from storage at -20ºC and *in vitro* autoradiography performed to map the distribution of SERT and DAT binding sites within the CNS. Sections were brought to room temperature and pre-incubated in buffer prior to incubation with a radioactive ligand. Binding to both SERT and DAT, defined as total binding, was determined by incubating sections with 50pM [^{125}I]-βCIT alone. Mazindol specifically binds to DAT and was used as a displacer to determine SERT binding (50pM [^{125}I]- βCIT in the presence of 1µM mazindol). Fluoxetine specifically binds to SERT and was used as a displacer to determine DAT binding ([^{125}I]- βCIT in the presence of 50nM fluoxetine). Non-specific binding was determined using 50pM [^{125}I]-βCIT in the presence of 1µM mazindol and 10µM fluoxetine (McGregor et al., 2003).

Due to the non-selective nature of the SPECT radioligand [^{125}I]- βCIT SERT and DAT were also labelled in separate sets of sections from the same animals using the highly specific ligands [^{3}H]-citalopram and [^{3}H]-WIN 35,428, respectively. Non-

specific binding for 2nM [^{3}H]-citalopram was determined in the presence of 20µM fluoxetine (Hebert et al., 2001) and 10nM [^{3}H]-WIN-35,428 in the presence of 30µM nomifensine (Andersen et al., 2005). Following incubation with ligand, sections were washed in buffer and dipped in distilled water. Sections were left to dry overnight and then exposed to film along with a set of pre-calibrated standards for varying periods of time (for full description of methods see section 2.2.3-2.2.4).

4.2.3 Quantification of ligand binding.

The optical densities of the pre-calibrated [^{125}I] or [^{3}H] standards were measured to produce a calibration curve of optical density against radioactivity. The optical densities of discrete anatomical regions were then determined from anonymised autoradiograms. The measuring frame was altered to fit specific anatomical regions and the same region was measured bilaterally in 3 tissue sections from the same animal and the average optical density used for analysis (Section 2.2.5).

4.2.4 Statistical analysis.

Ligand binding is presented as the mean±SEM. Statistical significance was determined using a Mann Whitney Test (*$p < 0.05$, **$p<0.01$) to investigate changes in ligand binding in 12-15 discrete anatomical regions throughout the CNS. The percentage changes was calculated as the difference between the groups divided by the control group and multiplied by 100.

4.3 Results.

4.3.1 [^{125}I]-βCIT labelling of both SERT and DAT.

The distribution of SERT and DAT binding sites are displayed in Figure 4.3.1. Autoradiograms are an example of regions sampled and visually display that binding of [^{125}I]-βCIT in the absence of displacers (total binding) is greater than in the presence of displacers (SERT, DAT and non-specific binding). Minimal non-specific binding of [^{125}I]-βCIT can be visually observed in the majority of regions sampled. A high level of non-specific binding was observed in the caudate putamen (25%), a dopaminergic structure (Figure 4.3.1) in comparison to the non-specific binding in the rest of the brain which was low (average 8%) compared to [^{125}I]-βCIT labelling of SERT and DAT.

Binding of [^{125}I]-βCIT in the absence of displacers represents labelling of both SERT and DAT. [^{125}I]-βCIT labelling in the absence of displacers in all fifteen regions of interest investigated did not differ significantly in the CIA group compared to the control group (Figure 4.3.2).The majority of structures displayed minimal changes in binding in the CIA group. The greatest change in binding was in the nucleus accumbens (41%) which was not significant.

Binding of [^{125}I]-βCIT in the presence of mazindol represents labelling of SERT. Three out of the 15 anatomical locations investigated demonstrated a significant difference in the CIA group in comparison to the control group. There was a significant change in binding in the nucleus accumbens (58%), thalamus (62%) and dentate gyrus (-60%). In all other regions examined the groups did not differ significantly (Figure 4.3.3).

Binding of [^{125}I]-βCIT in the presence of fluoxetine represents labelling of DAT. One out of the 14 anatomical locations investigated, the caudate putamen (95%) demonstrated a significant change in the CIA group in comparison to the control group. In all other regions examined the groups did not differ significantly (Figure 4.3.4).

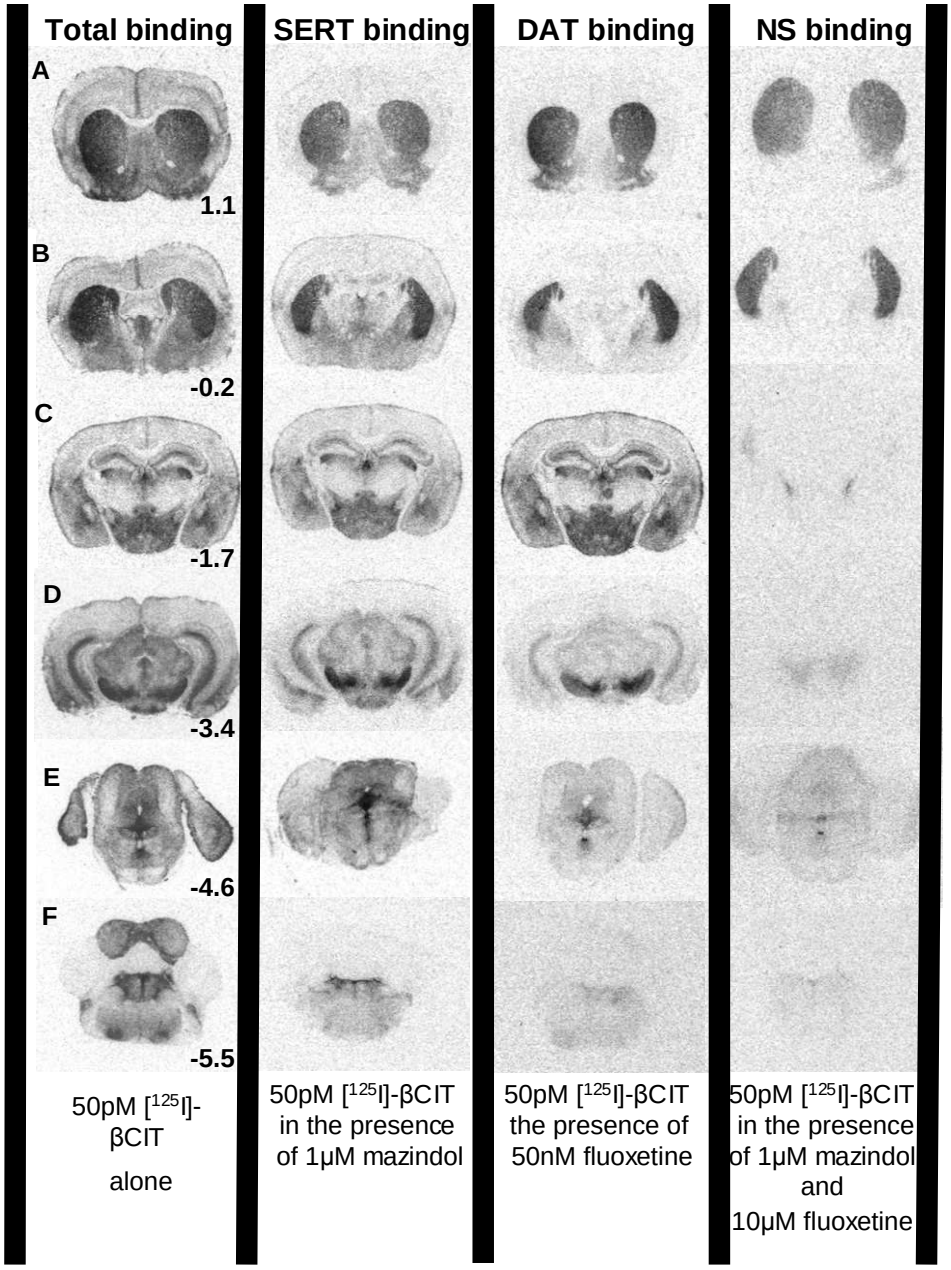

Figure 4.3.1 Autoradiogram of [^{125}I]-βCIT binding *in vitro.*

Representative autoradiograms at different levels (A-F) from bregma 1.1mm to -5.5mm of total [^{125}I]-βCIT binding, serotonin transporter (SERT) binding, dopamine transporter (DAT) binding and non-specific (NS) binding.

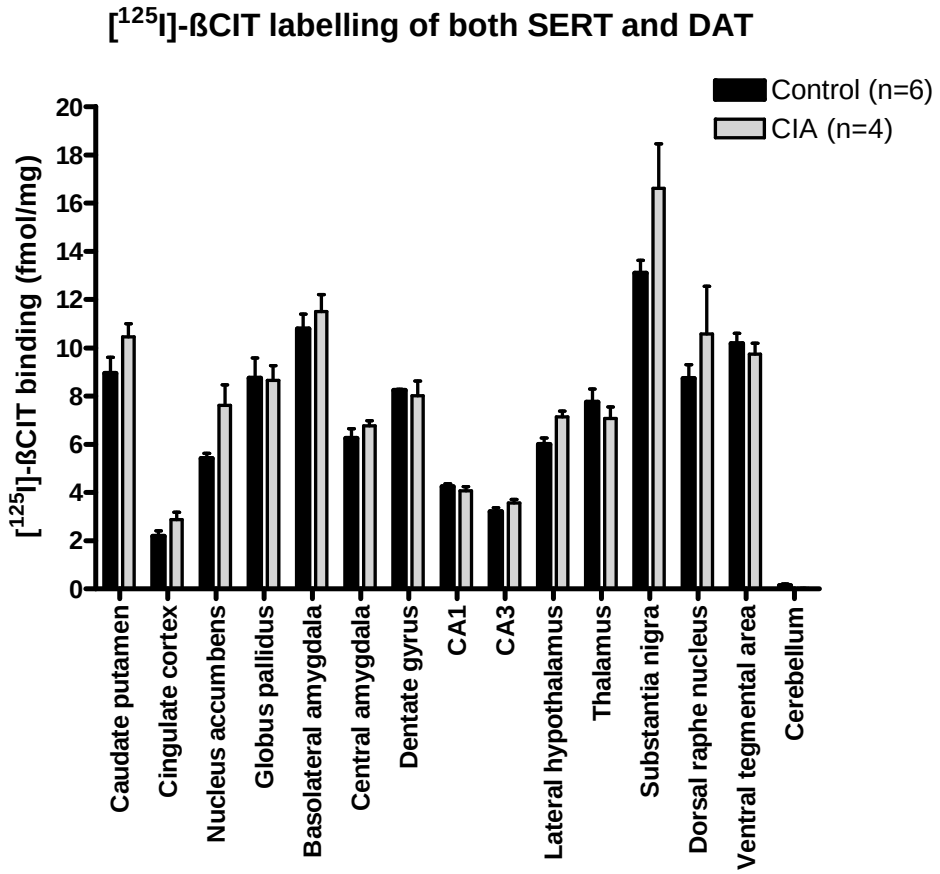

Figure 4.3.2 Total binding: [^{125}I]-βCIT binding in the absence of displacers.

Tissue sections from a CIA group and control group were incubated in the presence of [^{125}I]-βCIT alone. Binding of [^{125}I]-βCIT in the absence of displacers represents labelling of both SERT and DAT (total binding). Minimal differences in total binding between the groups were recorded. Data are presented mean ±SEM and statistical significance was determined using a Mann Whitney Test.

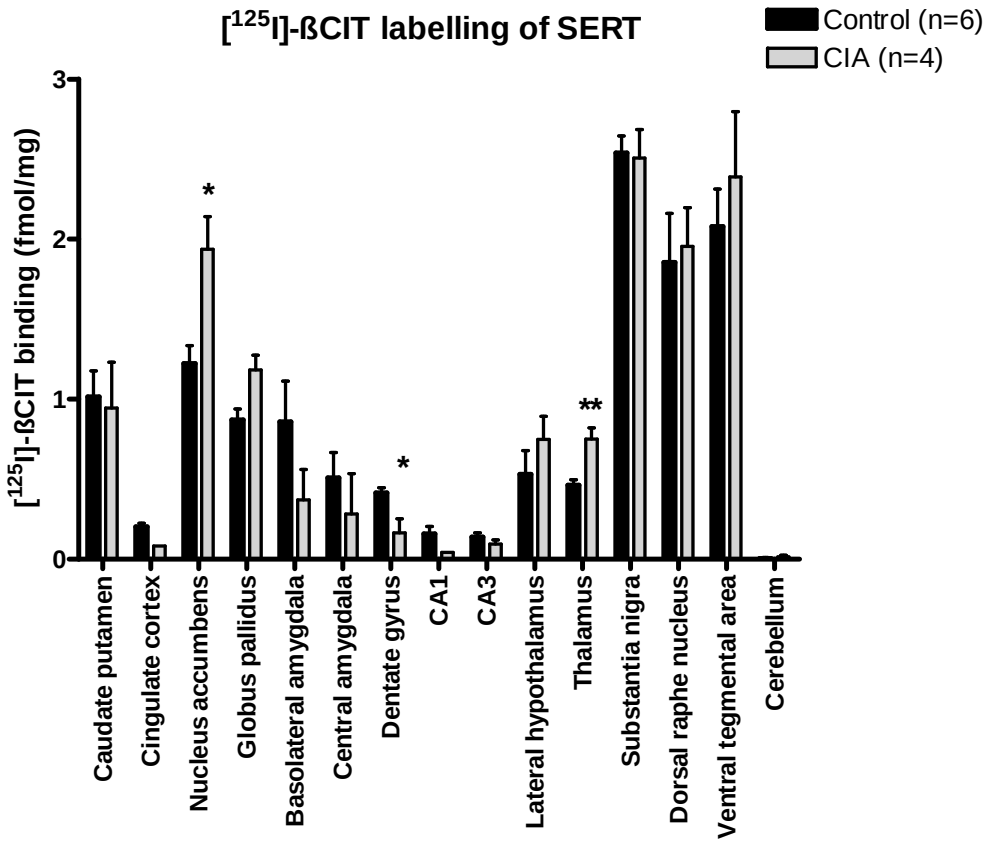

Figure 4.3.3 SERT binding: [^{125}I]-βCIT in the presence of mazindol.

Binding of [^{125}I]-βCIT in the presence of displacer mazindol represents labelling of SERT. In the CIA group binding reached a significant difference in the nucleus accumbens, dentate gyrus and thalamus in comparison to the control group. Data are presented mean±SEM and statistical significance was determined using a Mann Whitney Test (*p< 0.05, **p<0.01).

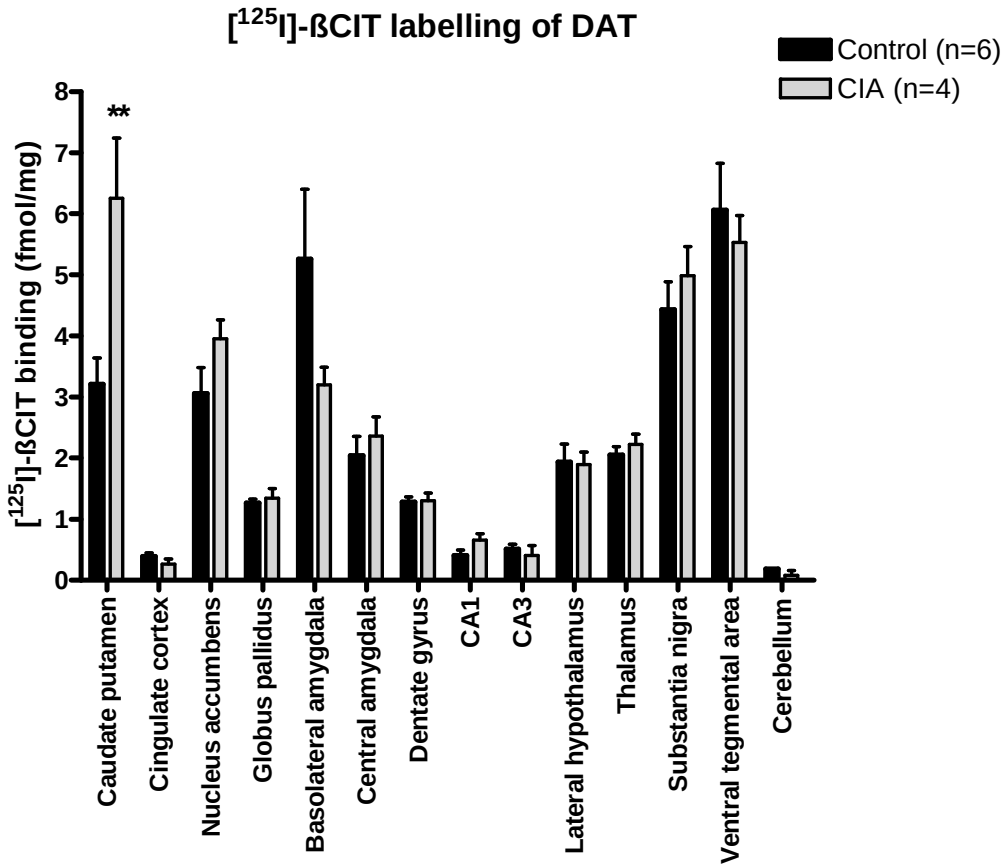

Figure 4.3.4 DAT binding: [^{125}I]-βCIT in the presence of fluoxetine.

Binding of [^{125}I]-βCIT in the presence of displacer fluoxetine represents labelling of DAT. In the CIA group a significant difference in DAT binding was only reached in the caudate putamen in comparison to the control group. Data are presented mean±SEM and statistical significance determined using a Mann Whitney Test (**p<0.01).

4.3.2 [^{3}H]-Citalopram labelling of SERT.

Autoradiographic distribution of SERT binding sites using [^{3}H]-citalopram, are displayed in Figure 4.3.5, illustrating regions of interest and the high level of [^{3}H]-citalopram labelling in the dorsal raphe nucleus and substantia nigra. Autoradiograms of [^{3}H]-citalopram labelling in the presence of displacer fluoxetine are not shown but the non-specific binding was extremely low (average 13 %) in comparison to [^{3}H]-citalopram labelling of SERT in the brain.

[^{3}H]-citalopram labelling of SERT was greatest in the dorsal raphe nucleus which is densely populated with serotonergic neurons that project to the limbic system. However, in all the regions of interest investigated there were minimal differences in SERT binding between the groups (Figure 4.3.6). Two of the structures in the limbic system, the nucleus accumbens (28%) and the thalamus (33%) displayed the greatest percentage change in SERT labelling in the CIA group compared to the control group but this difference did not reach statistical significance.

4.3.3 [^{3}H]-WIN 35,428 labelling of DAT.

Autoradiographic distribution of DAT binding sites using [^{3}H]-WIN 35,428 are displayed in Figure 4.3.7, illustrating regions of interest and the high level of labelling in the caudate putamen in comparison to other structures. [^{3}H]-WIN 35,428 labelling of DAT was low in the majority of the brain including the dorsal hippocampus making it impossible to distinguish between the dentate gyrus, CA1 and CA3 areas. Autoradiograms of [^{3}H]-WIN 35,428 labelling in the presence of displacer nomfensine are not shown but the non-specific binding was high (average 45%) in comparison to [^{3}H]-WIN 35,428 labelling of DAT in the brain. [^{3}H]-WIN 35,428 labelling of DAT was greater in areas with densely populated dopaminergic neurons including the caudate putamen, ventral tegmental area and the substantia nigra. In all regions of interest investigated [^{3}H]-WIN 35,428 labelling of DAT did not differ significantly between the CIA group compared to the control group (Figure 4.3.8).

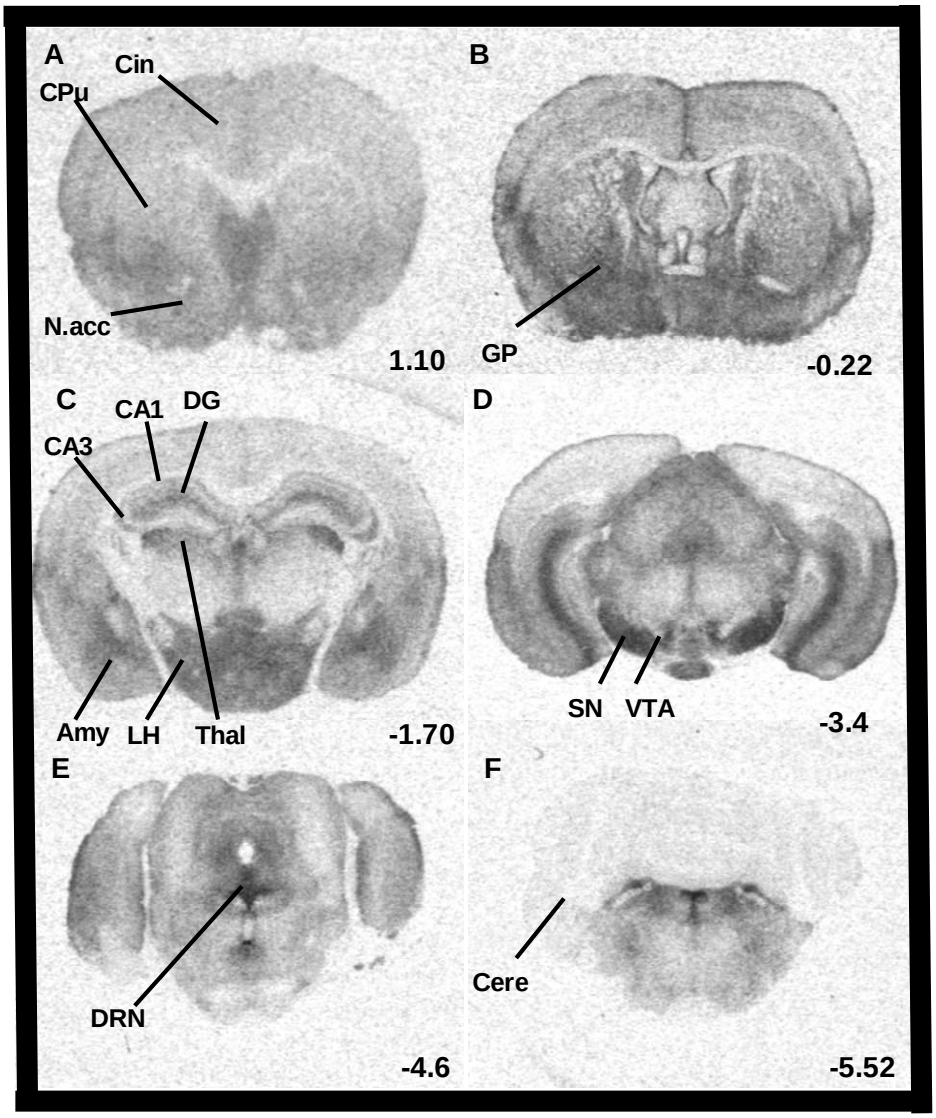

Figure 4.3.5 Representative autoradiogram of [^{3}H]-citalopram binding.

Autoradiograms of mouse brain sections (A-F) extending from bregma 1.1mm to -5.5mm (Franklin K.B.J and Paxinos G., 2007). (A) Illustrates the cingulate cortex (cin), caudate putamen (CPu) and nucleus accumbens (N.acc). (B) Illustrates the globus pallidus (GP). (C) Illustrates the lateral hypothalamus (LH), thalamus (Thal), amygdala (Amy) and dorsal hippocampus including the dentate gyrus (DG), CA1 and CA3 areas. (D) Illustrates the substantia nigra (SN) and ventral tegmental area (VTA). (E,F) illustrates the dorsal raphe nucleus (DRN) and the cerebellum (Cere).

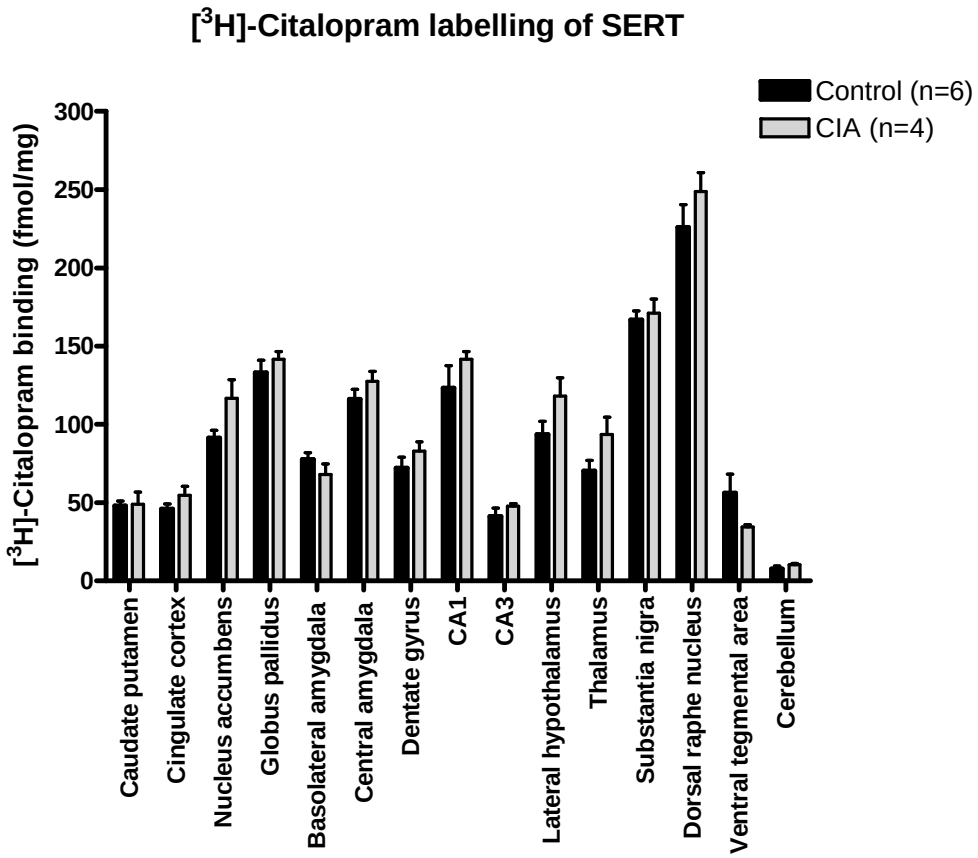

Figure 4.3.6 SERT binding: [^{3}H]-citalopram.

Binding of [^{3}H]-citalopram represents SERT binding. There were minimal differences in SERT binding in all areas of interest investigated in CIA group in comparison to the control group. Data are presented mean±SEM and statistical significance was determined using Mann Whitney Test.

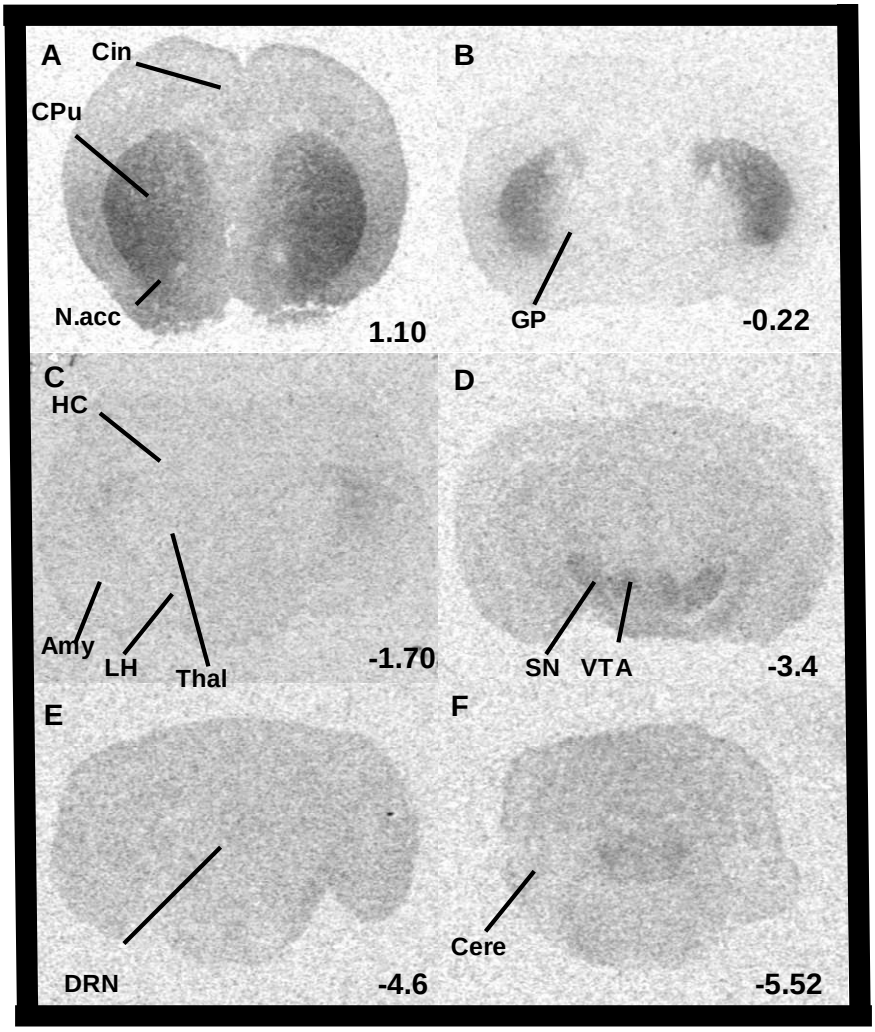

Figure 4.3.7 Representative autoradiogram of [^{3}H]-WIN 35,428 binding.

Autoradiograms of mouse brain sections (A-F) extending from bregma 1.1mm to -5.5mm (Franklin K.B.J and Paxinos G., 2007). (A) Illustrates the cingulate cortex (cin), caudate putamen (CPu) and nucleus accumbens (N.acc). (B) Illustrates the globus pallidus (GP). (C) Illustrates the lateral hypothalamus (LH), thalamus (Thal), amygdala (Amy) and dorsal hippocampus including the dentate gyrus (DG), CA1 and CA3 areas. (D) Illustrates the substantia nigra (SN) and ventral tegmental area (VTA). (E,F) illustrates the dorsal raphe nucleus (DRN) and the cerebellum (Cere).

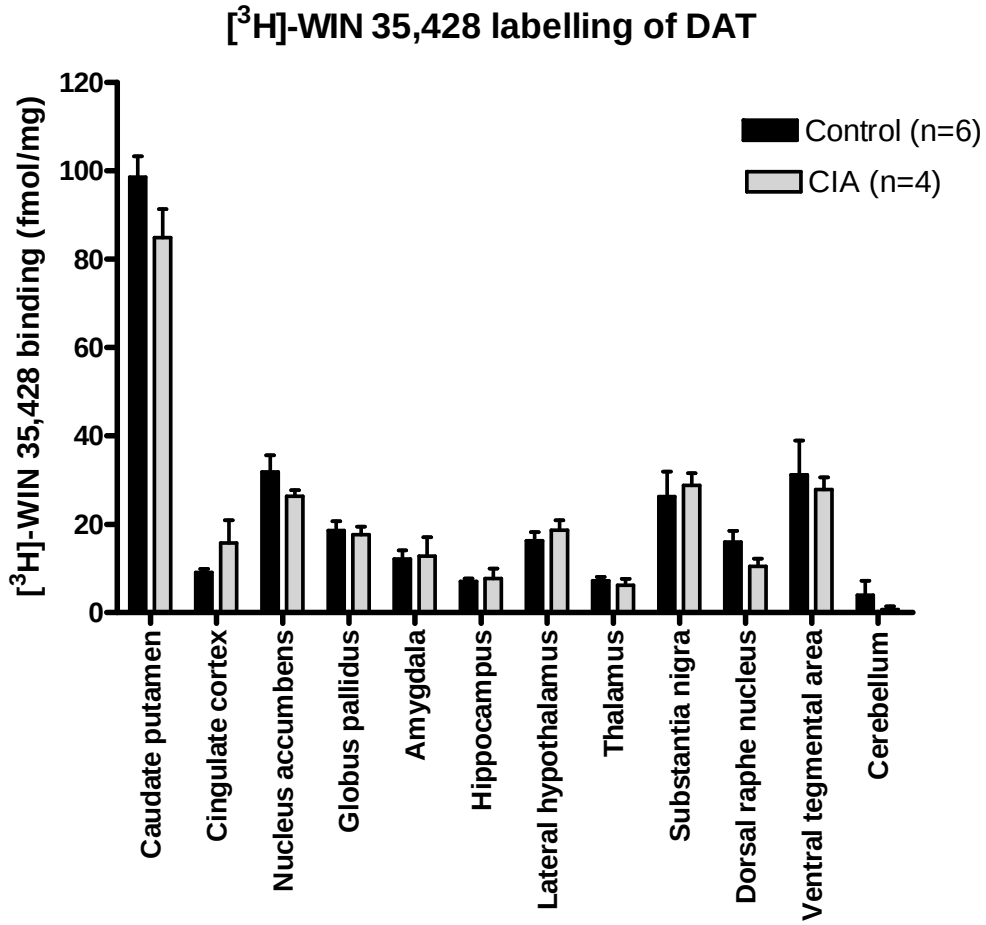

Figure 4.3.8 DAT binding: [^{3}H]-WIN 35,428.

Binding of [^{3}H]-WIN 35,428 represents labelling of DAT. There were minimal differences in DAT binding in all anatomical locations investigated. Data are presented mean±SEM and statistical significance was determined using a Mann Whitney Test.

4.4 Discussion.

To my knowledge this is the first study to investigate binding in discrete brain anatomical locations in the murine CIA model of rheumatoid arthritis. However, there is limited evidence of the effect pro-inflammatory cytokines have on SERT and DAT in this animal model. The primary aim of this chapter was to map the distribution of both SERT and DAT in CIA immunised mice which developed clinical symptoms. Overall the data suggest minimal influence of CIA on SERT and DAT binding. It may have been a combination of factors which led to minimal differences in SERT and DAT binding in the CIA group in comparison to the control group. All the autoradiographic studies described in this chapter were performed on brain sections from a pilot CIA experiment, which was used to establish the CIA model within the department (Chapter 3, study 1). All mice within the CIA group had mild swelling and erythema of the limbs which is described in more detail in the previous chapter (Chapter 3). It is for this reason that there was a low n number in the CIA group (n=4).

The overall hypothesis of this thesis is that there is an association between depression and the peripheral immune response associated with rheumatoid arthritis. The hypothesis tested in this chapter was that there would be increased SERT labelling in response to elevated levels of pro-inflammatory cytokines in the murine CIA model. [^{125}I]-βCIT labelling of SERT reached a significant increase in the nucleus accumbens and thalamus and a significant decrease in the dentate gyrus of the hippocampus in the CIA group compared to the control group (Figure 4.3.3). The nucleus accumbens, thalamus and hippocampus are limbic regions implicated in the symptoms of depression and the increase in SERT binding observed in the nucleus accumbens and thalamus is consistent with previous studies *in vitro* which have shown increased SERT activity in response to pro-inflammatory cytokines (Zhu et al., 2006). The increase in [^{125}I]-βCIT labelling of SERT in the thalamus is also consistent with a SPECT study which used the SERT-specific ligand [^{11}C]-DASB in non-medicated major depressive patients which reported a significant increase in SERT binding in the thalamus (Cannon et al., 2007). However, no statistically significant difference was apparent between the groups using the specific SERT ligand [^{3}H]-citalopram (Figure 4.3.6). This is

consistent with a previous SPECT study in non-medicated majorly depressed patients, using [^{11}C]-DASB which reported no change in SERT binding (Meyer et al., 2004). SPECT studies of SERT binding in non-medicated depressive patient have shown varied results using both βCIT (Malison et al., 1998; Lehto et al., 2006) and [^{11}C]-DASB (Cannon et al., 2007; Meyer et al., 2004). A possible explanation for this is that imaging studies of SERT binding in patients with depressive symptoms usually comprise small sample sizes, patient variation and different antidepressants have varied effects on SERT binding. This adds a level of difficulty interpreting SPECT studies as most depressed patients are medicated and the examples described above of non-medicated patients have been medication free for as little as 2 or 3 weeks (Malison et al., 1998; Newberg et al., 2005), to greater than 3 months (Meyer et al., 2004). This may have an unknown impact on SERT binding as there is limited information about the length of time the patients in these studies were previously on medication and which antidepressants they were prescribed.

Ligands used in SPECT studies give an indication of possible changes in transporter expression within the CNS. On the other hand *in vitro* autoradiography gives a quantitative measure of altered transporter labelling in an animal experiment, in which variability is controlled. However, autoradiographic experiments sample from a number of anatomical regions throughout the brain which can led to false positives. This may be a possible explanation why significant differences in binding were observed in [^{125}I]-βCIT labelling of SERT but not replicated using a second more specific ligand. [^{125}I]-βCIT is a non-specific ligand which binds to SERT, DAT and to a lesser extent noradrenaline, this can be observed in the autoradiograms of non-specific binding (Figure 4.3.1). This has led to the conclusion that peripheral inflammation in the CIA group has minimal effects on SERT expression. A possible explanation for the minimal differences in SERT binding may be the temporal evolution of inflammation in the CIA model. The CIA experiment has a duration of 42 days post immunisation, after which time the disease is still progressing. Therefore it is possible that it may take weeks for peripheral inflammation to alter SERT expression within the CNS in the murine CIA model and termination at day 42 post immunisation may be too early to detect changes.

The second hypothesis to be tested in this chapter was that the peripheral immune response in the CIA model would alter DAT expression. One difference between the experiments was the average non-specific binding, which may be due to the different specifities of the ligands. Overall there was low binding of [^{3}H]-WIN 35,428 in all anatomical locations except for the caudate putamen. Therefore when the non-specific binding was compared to [^{3}H]-WIN 35,428 binding in the brain the average non-specific binding appeared high (average 45%). In comparison, [^{125}I]-βCIT is a non-specific ligand which binds to both SERT and DAT. This may be the reason [^{125}I]-βCIT labelling of DAT was more pronounced throughout the brain compared to [^{3}H]-WIN 35,428 labelling of DAT and when [^{125}I]-βCIT non-specific binding was compared to the [^{125}I]-βCIT labelling of DAT, the non-specific binding calculated as a lower percentage (average 8%).

Nevertheless, there were minimal differences between the experimental groups using [^{3}H]-WIN 35,428 or [^{125}I]-βCIT labelling of DAT. A previous PET study has reported reduced DAT binding in the caudate putamen of patients with depressive symptoms (Meyer et al., 2001). However, there was an increase in [^{125}I]-βCIT labelling of DAT in the caudate putamen of the CIA group compared to the control group (Figure 4.3.4). In this study the mice were not tested for anhedonia, a characteristic feature of depression. It is therefore possible, that there was no decrease in DAT binding as the mice are not experiencing anhedonia and that the observed increase is in response to the induction of CIA. However, the increase in DAT binding was not replicated using the [^{3}H]-WIN 35,428, a specific ligand used to measure DAT binding in adjacent tissue sections (Figure 4.3.8). There are a number of explanations for the differences in binding between the ligands. As mentioned above autoradiographic experiments sample from a number of different regions which can led to a false positive result. The ligands [^{125}I]-βCIT and [^{3}H]-WIN 35,428 have different specificities and affinities for DAT. This can be observed in the autoradiograms, [^{3}H]-WIN 35,428 has a high specificity for DAT and there is low binding in all anatomical locations except for the caudate putamen (Figure 4.3.7). However, in the autoradiograms representing [^{125}I]-βCIT labelling of DAT the structures are more defined (Figure 4.3.1). It has been noted in the literature that the ligands [^{125}I]-βCIT and [^{3}H]-WIN 35,428 may bind to different forms of DAT

resulting in different densities of binding being calculated in different anatomical locations (Coulter et al., 1995). The ligands may bind to different forms of DAT but I believe that it is the lack of specificity of [^{125}I]-βCIT labelling of DAT which is responsible for the observed differences in binding and that [^{3}H]-WIN 35,428 autoradiographic labelling of DAT is more accurate. This has led to the conclusion that the peripheral immune response in CIA immunised mice has a minimal effect on DAT expression.

A subordinate aim of this chapter was to investigate combined SERT and DAT binding within in the same tissue section. In all anatomical locations investigated there were minimal differences in combined SERT and DAT binding between the groups (Figure 4.3.2).

4.4.1 Conclusion.

There were minimal changes in SERT and DAT binding in tissue sections from the CIA group compared to the control group. This suggests that any change in SERT or DAT binding is very subtle or that SERT or DAT expression is unaltered. Overall, this study adds to the limited evidence available in the literature and in the future may aid in understanding the relationship between the immune and monoaminergic systems.

Chapter 5

[^{14}C]-2-deoxyglucose autoradiographic study of local cerebral glucose utilisation in the murine CIA model.

5.1 Introduction.

The [^{14}C]-2-deoxyglucose autoradiographic technique ([^{14}C]-2-DG) is used to investigate functional changes in glucose utilisation in discrete anatomical regions throughout the CNS. In the brain glucose provides energy for different types of cells including glia and neurons and for energy dependent processes including neurotransmitter release, synthesis, re-uptake and to maintain ion gradients. The basic principle underlying [^{14}C]-2-DG is that glucose catabolism under normal physiological conditions is directly related to energy consumption in cerebral tissue.

There is evidence that pro-inflammatory cytokines influence different brain systems, which could led to altered brain function. In the pre-synaptic terminals of neurons, abnormal local cerebral glucose utilisation (LCMRglu) could be the result of altered synthesis, storage or release of neurotransmitters or altered SERT density. Cytokines have been shown to increase serotonin uptake *in vitro* (Ramamoorthy et al., 1995; Mossner et al., 1998). In addition IL-2 and/or IFN-α therapy in cancer patients has been shown to led to the development of depression and decreased plasma levels of tryptophan (Capuron et al., 2002). In depressed patients there is decreased 5-HT$_{1A}$ receptor mRNA expression, in the hippocampus and prefrontal cortex compared to controls (Lopez-Figueroa et al., 2004). Similarly *in vitro* studies investigating the effect of IFN- α on 5-HT$_{1A}$ receptors in cell cultures illustrated a reduction in 5-HT$_{1A}$ receptors, which was reversed by administering fluoxetine or desipramine (Cai et al., 2005). IFN-α is just one of a number of elevated cytokines in the CIA model (Thornton et al., 1999; Mauri et al., 1996). The evidence suggests that cytokines can affect either the pre- or post-synaptic serotonergic system or both.

The previous chapter investigated serotonin transporter density in the murine CIA model. In this chapter mice with CIA were challenged with fenfluramine, an agent

that alters synaptic serotonin levels, in an attempt to reveal any abnormalities in serotonergic function caused by the disease. Fenfluramine is an amphetamine analogue, originally used as an anorexigenic drug (Munro et al., 1966) which has also been used as a pharmacological tool to investigate blunted serotonergic response in patients with mood disorders (Newman et al., 1998). Early studies on the effect of fenfluramine in the brain demonstrated that fenfluramine targeted the serotonergic system to deplete central stores of serotonin (Costa et al., 1971; Tagliamonte et al., 1971). The first study to investigate the mechanism of action of fenfluramine showed a dual mechanism of induced serotonin release from nerve terminals and inhibition of serotonin re-uptake in blood platelets (Buczko et al., 1975). Evidence that fenfluramine inhibits serotonin re-uptake has been further shown by the selective serotonin re-uptake inhibitors, fluoxetine (Sarkissian et al., 1990; Sabol et al., 1992) and the ability of citalopram (Kreiss et al., 1993) to attenuate fenfluramine induced release of serotonin. A possible explanation for this effect is that antidepressants inhibit the uptake of fenfluramine, which competes with serotonin for the serotonin transporter. Once within the nerve terminal there is evidence from studies using tetanus toxin, an exocytosis inhibitor, that suggest fenfluramine induces exocytotic release of serotonin containing vesicles from the nerve terminal (Gobbi et al., 1993).

The [^{14}C]-2-DG technique is a similar technique to positive emission tomography (PET) using ^{18}F-Fludeoxyglucose (^{18}FDG); both techniques measure *in vivo*, LCMRglu in discrete anatomical locations of the nervous system. ^{18}FDG, an analog of glucose is used as a radiotracer in PET brain imaging studies to assess cerebral glucose metabolism (Gallagher et al., 1978). The first study to use PET to investigate fenfluramine challenge in healthy males found an increase in LCMRglu in the prefrontal cortex and a decrease in the occipital-temporal regions compared to placebo in the same subject (Kapur et al., 1994). This study was presented as a short communication, and a couple of years later a more in-depth study also examined the effect of fenfluramine challenge in healthy volunteers resulting in an increase in LCMRglu in the prefrontal cortex and left temporal and parietal cortex (Mann et al., 1996). PET studies have also utilised the fenfluramine challenge to investigate regional abnormalities in the serotonergic system in patients with depressive symptoms. Fenfluramine challenge resulted in a significant increase in

LCMRglu in the prefrontal and frontal cortex in healthy male volunteers compared to medication free male depressed patients (Anderson et al., 2004). This suggests that patients with depression have a blunted response to fenfluramine challenge compared to healthy controls implicating altered brain function in patients with depressive symptoms.

The CIA model is a well established model used to investigate novel anti-cytokine agents to treat inflammation. The hypothesis underlying this thesis is that pro-inflammatory cytokines released by the peripheral immune response influence the brain. The hypothesis of this chapter is that cerebral glucose utilisation is altered in the CIA model. The first objective of this chapter was to use [^{14}C]-2-DG autoradiography to investigate regional cerebral metabolism in CIA mice which developed clinical symptoms. A second objective was to explore the serotonergic system further in CIA mice by employing a fenfluramine challenge to reveal any abnormalities in serotonergic function as detected by [^{14}C]-2-DG autoradiography.

5.1.1 Aims.

1. Measure LCMRglu in CIA group compared to a control group (Study 1)
2. Challenge the serotonergic system with fenfluramine in naïve mice and measure changes in LCMRglu (Study 2).
3. Challenge the serotonergic system with fenfluramine in a CIA group compared to a control group and measure changes in serotonergic transmission (Study 3).

5.2 Methods.

5.2.1 Experimental protocol for semi-quantitative [^{14}C]-2-deoxyglucose autoradiography.

Mice were fasted overnight before receiving an intraperitoneal injection of [^{14}C]-2-DG (5μCi in 0.4mls sterile saline) at a steady rate over 10 seconds. Forty-two and a half minutes after [^{14}C]-2-DG administration, mice were anaesthetised with 4% isofluorane in a mixture of 30% oxygen/70% nitrogen for 2.5 minutes. Exactly 45 minutes after [^{14}C]-2-DG administration mice were decapitated, a terminal blood sample taken by torso inversion and blood immediately centrifuged. The plasma samples were stored in ice until the afternoon, when glucose levels were analysed using a semi-automated glucose oxidase enzyme assay (Glucose analyser 2, Beckman) and plasma [^{14}C] levels were measured using a liquid scintillation counter. After blood collection, brains were rapidly dissected from the skull and frozen in isopentane at -45ºC. Coronal brain sections (20μm thick) were cut on a cryostat at -15 ºC. Three out of every 6 brain sections were collected on coverslips and dried on a hotplate at 60 ºC. The sections were then exposed to x-ray film for 4 days along with a set of pre calibrated [^{14}C]-standards and developed using an x-ray film processor (Sokoloff, 1977).

5.2.2 Study groups.

In study 1, on day 0, a CIA experiment was initiated in a CIA group (n=12) and a control group (n=12), as previously described in Chapter 3. On day 41 or 42 post immunisation the experimental protocol for [^{14}C]-2-DG was performed on controls (n=12) and CIA mice exhibiting clinical symptoms of disease (n=5).

In study 2, naïve Balb/c mice (n=6) were injected intraperitoneally with 10mg/kg fenfluramine 30 minutes prior to [^{14}C]-2-DG. A control group (n=6) received saline 30 minutes prior to [^{14}C]-2-DG.

In study 3, on day 0, a CIA experiment was initiated in a CIA group (n=12) and a control group (n=12). On day 41/42 post immunisation the control group (n=12),

and CIA mice exhibiting clinical symptoms of disease (n=7) were injected intraperitoneally with 10mg/kg fenfluramine 30 minutes prior to the [^{14}C]-2-DG technique (Figure 5.2.1). During study 3, one mouse was terminated on day 0 post immunisation due to an injury unrelated to the induction of CIA.

Study 1: CIA group compared to a control group.

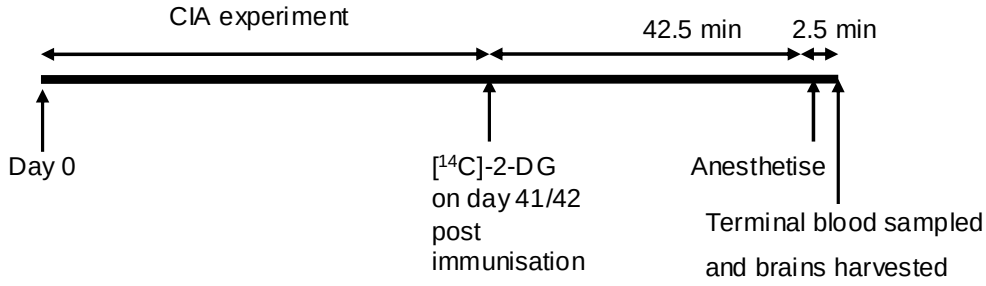

Study 2: Fenfluramine challenge in naïve mice.

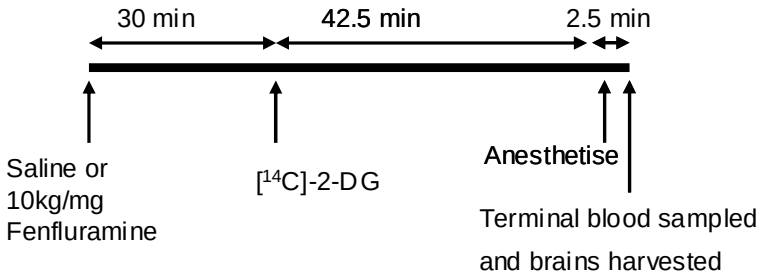

Study 3: Fenfluramine challenge in a CIA group compared to a control group.

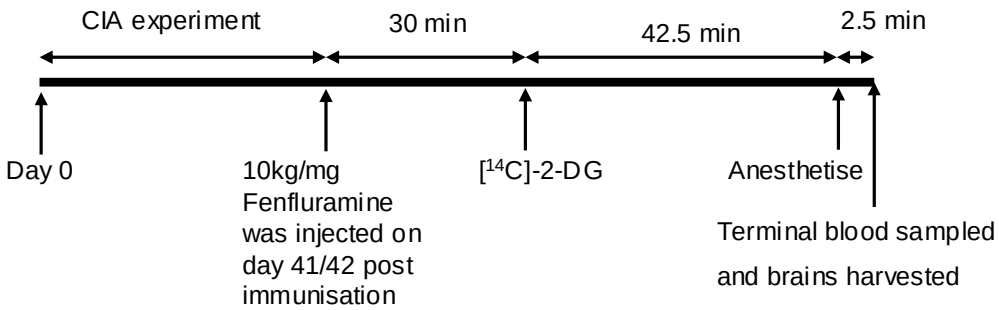

Figure 5.2.1 Schematic of [^{14}C]-2-DG experiments.

5.2.3 Calculation of iLCMRglu.

Optical density measurements were made by placing a measuring frame over 33/34 discrete anatomical regions on anonymised autoradiographic images. The size of the measuring frame was adjusted depending on the region of interest and the average optical density of 3 non-overlapping frames in each region of interest in both hemispheres was obtained. The index of LCMRglu (iLCMRglu) was calculated according to the methods in chapter 2, Section 2.3.2. The equation used for this calculation is displayed below:

$$\textbf{iLCMRglu} = \left(\frac{C_i^*(T)}{\text{mean}(C_p^*/C_p)_{\text{control group}}} \right)$$

Figure 5.2.2 Equation used to calculate iLCMRglu.

C_i*(T) represents the total ^{14}C tissue concentration in a region of interest. **C_p** and **C_p*** represents the glucose concentration and [^{14}C]-2-deoxyglucose concentration in the arterial plasma respectively.

5.2.4 Statistical analysis.

The disease severity summary measure and paw thickness summary measure data are presented as the mean. Statistical significance was determined using a Mann Whitney test to determine differences between the groups in the summary measurements of paw thickness.

Plasma glucose, plasma [^{14}C] and plasma glucose/ plasma [^{14}C] ratio data for the 3 studies was analysed using 2-way ANOVA with Bonferroni correction. iLCMRglu data are presented as mean+SEM and statistical significance was determined using a Students unpaired t-test. The percentage difference for each animal within a group was added together and divided by the number of regions of interest to provide an average percentage difference. In study 1, autoradiograms from one

control animal were excluded from analysis as the autoradiographic images were not sharp enough for analysis, resulting in n=11.

5.3 Results.

5.3.1 Disease features and incidence in the CIA model.

Study 1.

Five mice out of the 12 immunised with CIA developed clinical symptoms of arthritis representing a disease incidence of 42%. No control animal displayed any sign of limb swelling and erythema at any time point investigated. The severity of disease differed between animals resulting in a range of disease severities. The swelling in the front and hind limbs of the CIA group reached a maximum paw thickness of 2.7mm. There was a significant increase in the summary measure of paw thickness in the CIA group compared to the control group. These data show that the mice used in study 1, had clinical symptoms of CIA and that there was a statistically significant difference in paw swelling in the disease group compared to the control group (Figure 5.3.1).

Study 3.

Seven mice out of 12 immunised developed clinical symptoms of swelling and erythema. One mouse was culled on day 0 post immunisation due to injury unrelated to CIA immunisation. Therefore, the 7 mice with clinical symptoms represent a disease incidence of 64%. No control animals exhibited clinical symptoms of swelling or erythema. The graphs show that the CIA group used in study 3, displayed clinical symptoms and that the swelling of the paws reached a statistical significant difference in the CIA group compared to the control group (Figure 5.3.2).

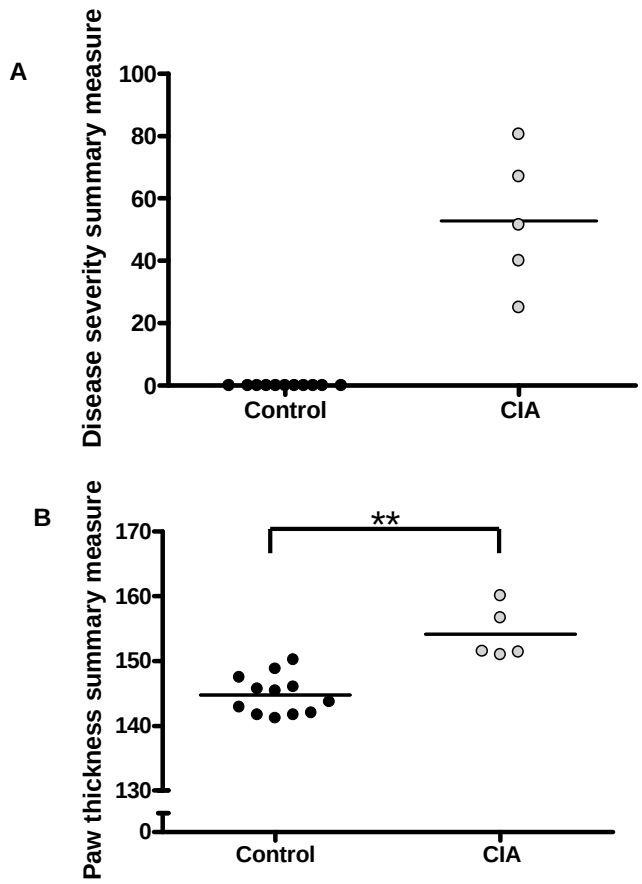

Figure 5.3.1 Study1: Summary measures depicting the disease in the CIA group compared to the control group.

The sum clinical score and the paw thickness were plotted over time and the area under the curve calculated to give a summary measure of disease severity and a summary measure of paw thickness in each animal. A) The disease severity varied between animals in the CIA group. No animal in the control group showed any signs of clinical symptoms. B) The graph above depicts a significant difference in the summary measure of paw thickness in the CIA group compared to the control group. Horizontal bar represents the mean. Statistical significance was determined using a Mann Whitney test (**p< 0.01).

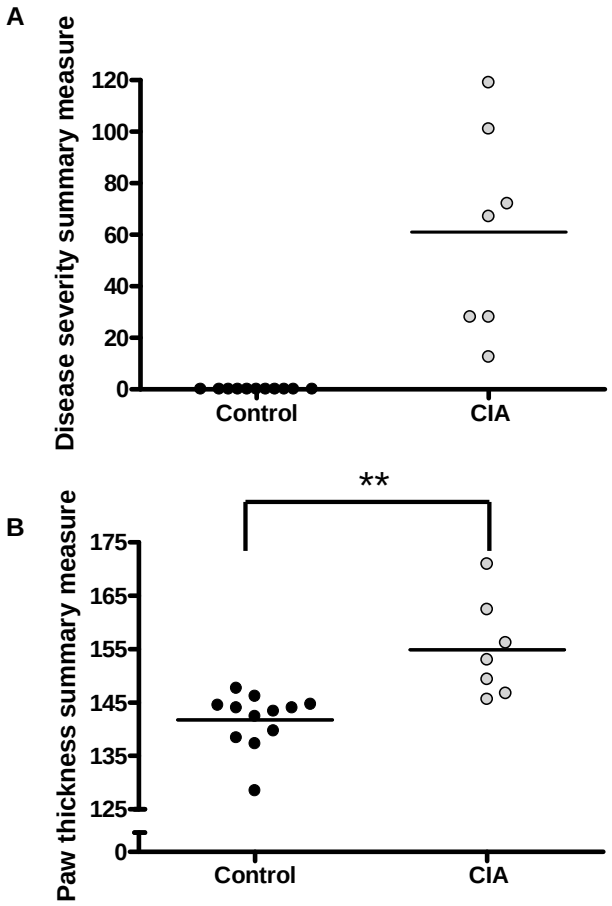

Figure 5.3.2 Study 3: Summary measures depicting the disease in the CIA group compared to the control group.

The sum clinical scores and the paw thickness were plotted over time and the area under the curve calculated to give a summary measure of disease severity and a summary measure of paw thickness in each animal. A) The disease severity varied between animals in the CIA group. No animal in the control group showed any signs of clinical symptoms. B) The graph above depicts a significant difference in the summary measure of paw thickness in the CIA group compared to the control group. Horizontal bar represents the mean. Statistical significance was determined using a Mann Whitney test (**p< 0.01).

5.3.2 Terminal plasma glucose and ^{14}C concentrations.

Both the blood plasma glucose and [^{14}C] were similar between the groups and within the same range as those previously reported in the literature (Dawson et al., 2009). Therefore, neither CIA nor fenfluramine challenge appears to affect the plasma glucose or plasma [^{14}C] alone. In comparison, when CIA and fenfluramine were combined (study 3) there was a significant difference in the blood plasma [^{14}C] compared to the control group in study 1. However, the significant difference in [^{14}C] in study 3 did not influence the blood plasma glucose and [^{14}C] ratio, which is used to calculate the iLCMRglu.

	Study 1		**Study 2**		**Study 3**	
	Control	**CIA**	**Control**	**FEN**	**Control FEN**	**CIA FEN**
Plasma Glucose ($\mu mol \cdot ml^{-1}$)	6.8 ± 0.22	7.0 ± 0.43	7.1 ± 0.56	6.7 ± 0.36	6.5 ± 0.38	6.6 ± 0.20
Plasma [^{14}C] ($nCi \cdot ml^{-1}$)	126.1 ± 8.92	117.6 ± 5.33	115.6 ± 19.49	125.2 ± 14.76	117.7 ± 5.09	106.9* ± 4.33
Plasma Glucose/Plasma [^{14}C] ($nCi \cdot \mu mol^{-1}$)	18.5 ± 1.45	17.59 ± 1.45	16 ± 2.97	18.95 ± 2.47	18.75 ± 0.95	16.64 ± 0.58

Table 5.3.1 Plasma glucose and ^{14}C.

Plasma glucose and ^{14}C values used to calculate iLCMRglu for the individual experiments (FEN= fenfluramine). There was a significant difference in plasma [^{14}C] in the CIA FEN group in study 3 in comparison to the control group in study 1. Data are presented mean ± SEM and were analysed using 2 way ANOVA with Bonferroni correction ($p<0.05$).

5.3.3 Study 1: iLCMRglu in the CIA group compared to the control group.

iLCMRglu did not differ significantly between the CIA and control groups in any of the 34 anatomical locations investigated (Figure 5.3.3). The trend indicated minimal changes in iLCMRglu (average -2%) between the control and CIA groups. This trend was also observed within the dorsal raphe nucleus (Figure 5.3.8), which is densely populated with serotonergic neurons, where there was no difference (0%) in iLCMRglu between the groups.

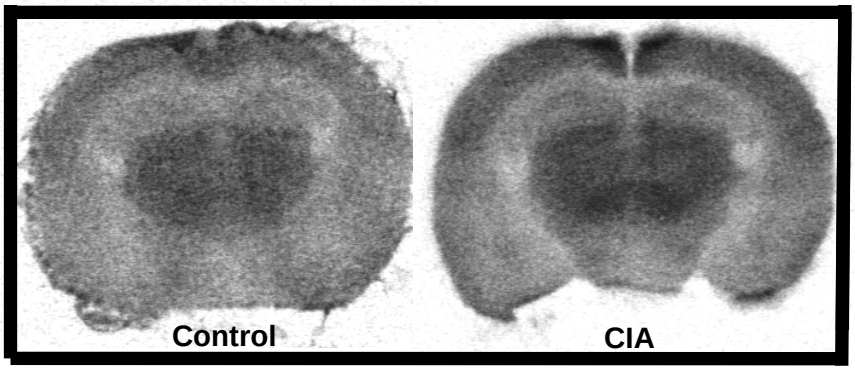

Figure 5.3.3 Representative autoradiographic images of [^{14}C] at bregma -1.7mm in the tissue of a control and a CIA animal (Franklin K.B.J and Paxinos G., 2007).

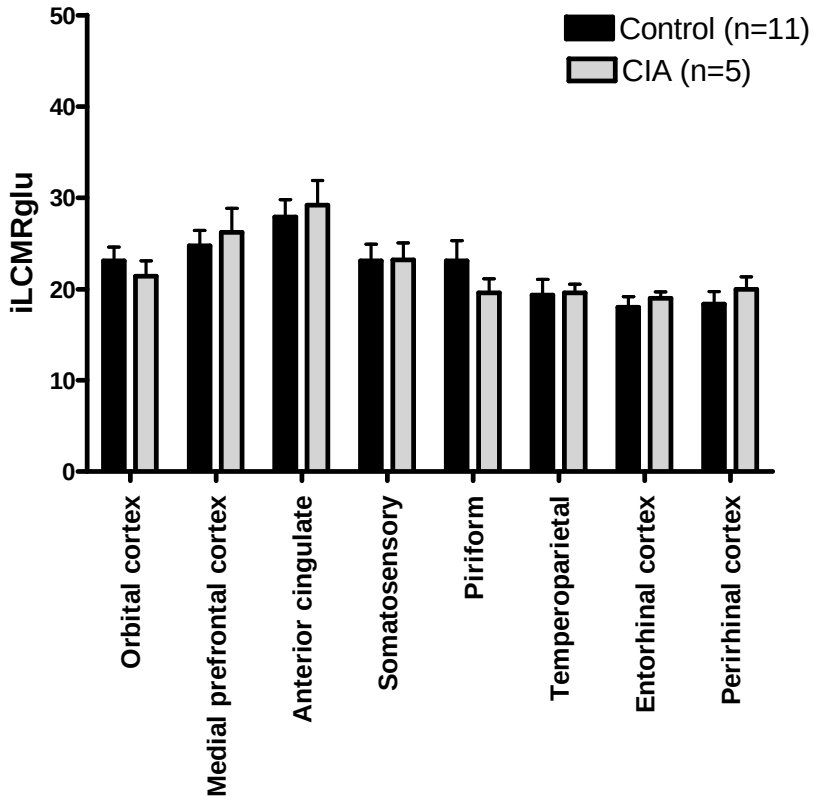

Figure 5.3.4 iLCMRglu in cortical regions of the CIA group compared to the control group.

[^{14}C]-2-DG was performed on a CIA group and control group on day 41/42 post immunisation. The CIA group was defined as any mouse with a clinical score greater than 0 in any limb. The graph depicts iLCMRglu in cortical regions of the control and CIA groups. There were minimal differences in iLCMRglu in all cortical regions examined. Data are presented as mean+SEM and statistical significance was determined using a Students unpaired t-test.

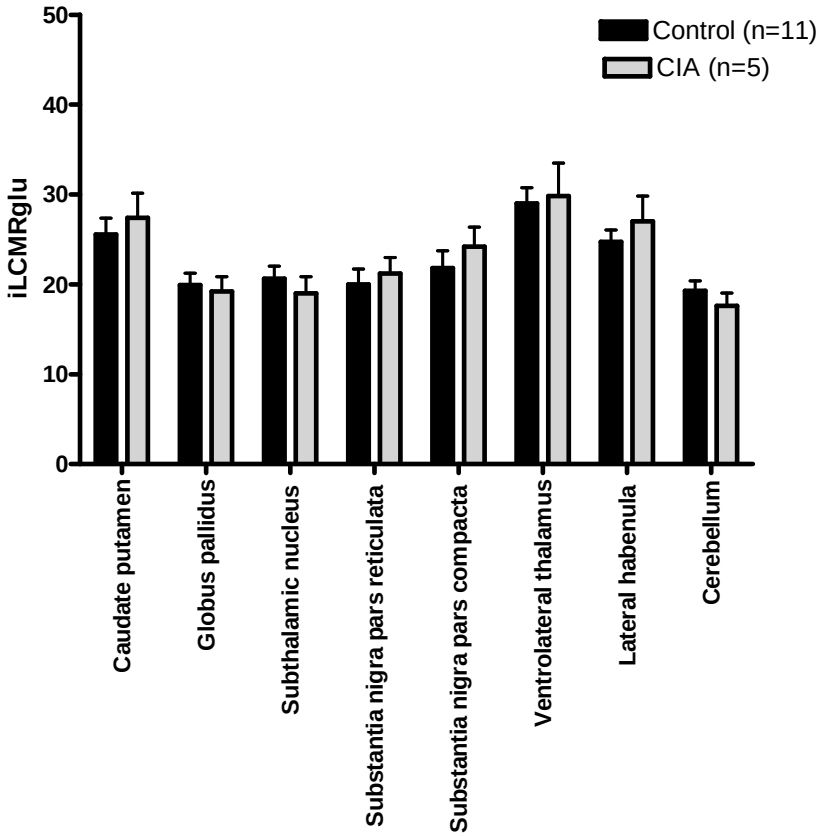

Figure 5.3.5 iLCMRglu in motor regions of the CIA group compared to the control group.

[^{14}C]-2-DG was performed on a CIA group and control group on day 41/42 post immunisation. The CIA group was defined as any mouse with a clinical score greater than 0 in any limb. The graph depicts iLCMRglu in motor regions of the control and CIA groups. There were minimal differences in iLCMRglu in all motor regions examined. Data are presented as mean+SEM and statistical significance was determined using a Students unpaired t-test.

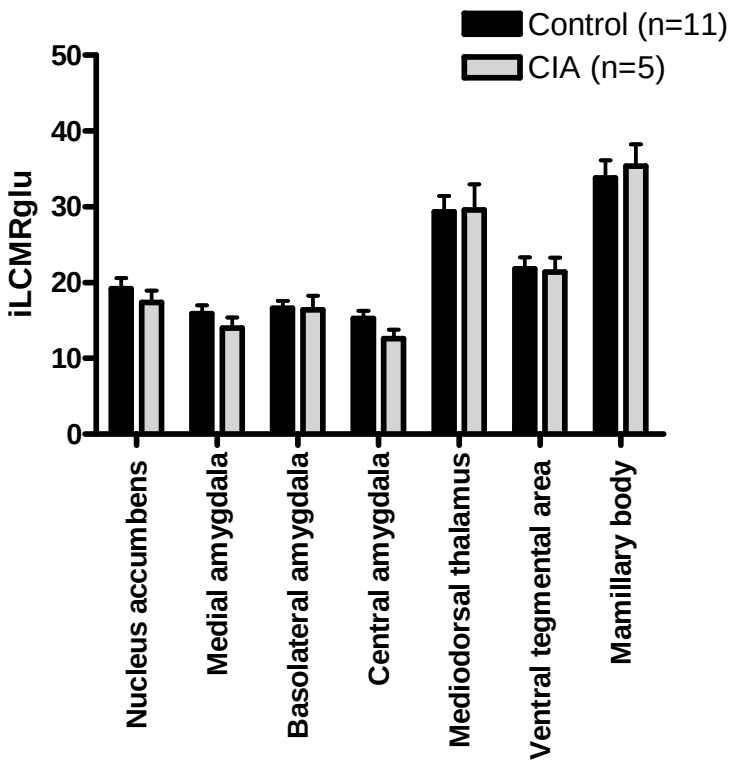

Figure 5.3.6 iLCMRglu in limbic regions of the CIA group compared to the control group.

[^{14}C]-2-DG was performed on a CIA group and control group on day 41/42 post immunisation. The CIA group was defined as any mouse with a clinical score greater than 0 in any limb. The graph depicts iLCMRglu in limbic regions of the control and CIA groups. There were minimal differences in iLCMRglu in all limbic regions examined. Data are presented as mean+SEM and statistical significance was determined using a Students unpaired t-test.

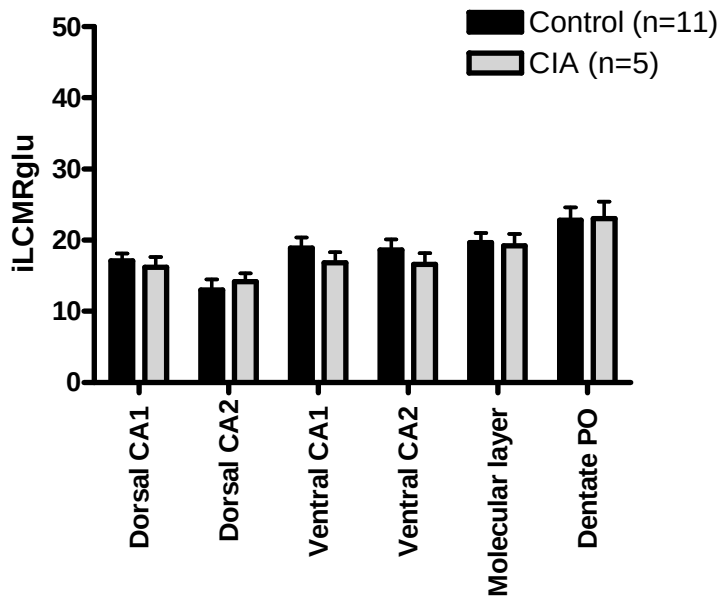

Figure 5.3.7 iLCMRglu in hippocampal regions of the CIA group compared to the control group.

[^{14}C]-2-DG was performed on a CIA group and control group on day 41/42 post immunisation. The CIA group was defined as any mouse with a clinical score greater than 0 in any limb. The graph depicts iLCMRglu in hippocampal regions of the control and CIA groups. There were minimal differences in iLCMRglu in all hippocampal regions investigated. Data are presented as mean+SEM and statistical significance was determined using a Students unpaired t-test.

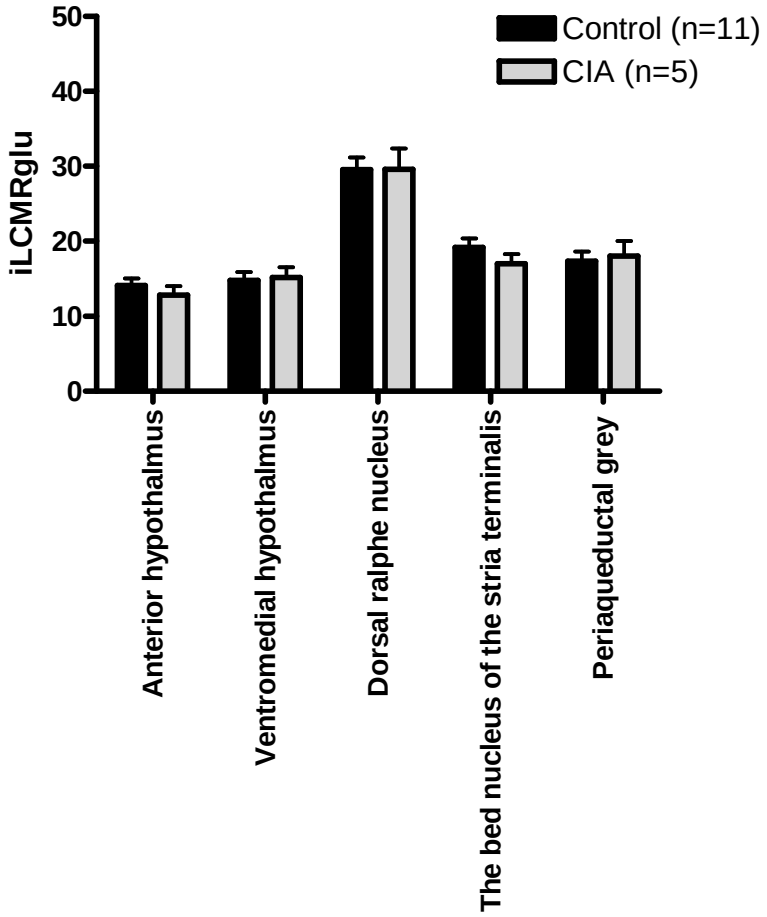

Figure 5.3.8 iLCMRglu in other regions of the CIA group compared to the control group.

[^{14}C]-2-DG was performed on a CIA group and control group on day 41/42 post immunisation. The CIA group was defined as any mouse with a clinical score greater than 0 in any limb. The graph depicts iLCMRglu in other brain regions in the control and CIA groups. There were minimal differences in iLCMRglu in all other brain regions investigated. Data are presented as mean+SEM and statistical significance was determined using a Students unpaired t-test.

5.3.4 Study 2: LCMRglu after fenfluramine challenge in naïve mice.

Fenfluramine challenge in naïve mice resulted in iLCMRglu in 24 out of the 33 brain region of interest examined being significantly different compared to controls. Lower glucose utilisation after fenfluramine challenge is illustrated by the lighter autoradiograms in comparison to the control group (Figure 5.3.9). The average difference between the control and CIA group was -26%, the greatest significant percentage difference was in the ventrolateral thalamus (Figure 5.3.11), where after fenfluramine challenge there was a 36% reduction in iLCMRglu compared to the control group. A significant difference was also reached in the dorsal raphe nucleus (Figure 5.3.14). The dorsal raphe nucleus is densely populated with serotonergic neurons which project to cortex, hippocampus, hypothalamus and limbic system (Rang et al., 2003). Overall fenfluramine challenge appears to have a global effect on the brain decreasing iLCMRglu in all hippocampal regions examined and the majority of cortical, motor and limbic regions examined.

The majority of areas did not display statistically significant reductions still showed minimal changes in iLCMRglu. The anterior hypothalamus and ventromedial hypothalamus displayed a 5% and 9% change in iLCMRglu between the groups, respectively (Figure 5.3.14). Another region where a significant difference was not reached was the periaqueductal grey (Figure 5.3.14) which is involved in the reward pathway and in afferent and efferent pain pathways (Borsook et al., 2007).

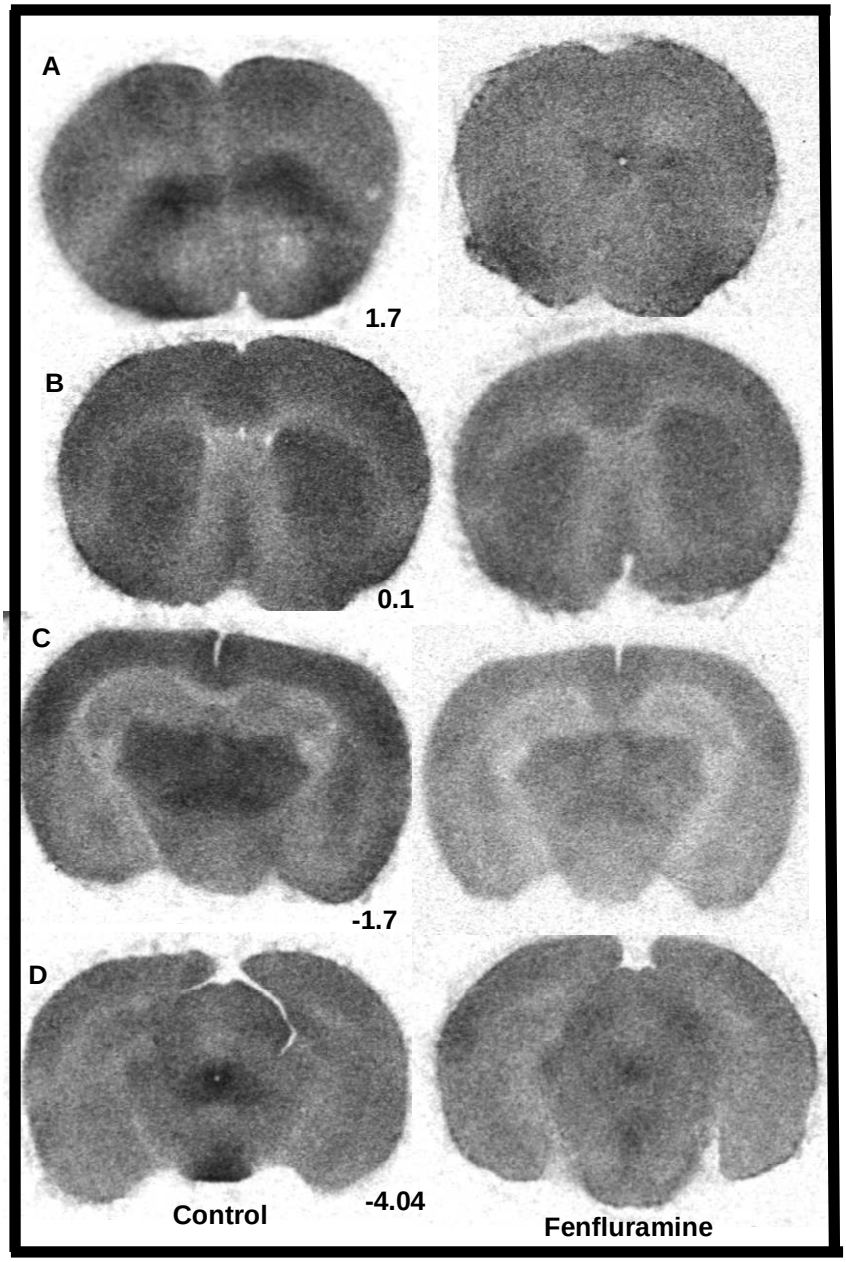

Figure 5.3.9 Autoradiograms illustrating the effect of fenfluramine challenge.

Representative autoradiograms at different levels (A-D) from bregma 1.7mm to -4.04mm of glucose utilisation in a control group and fenfluramine group (Franklin K.B.J and Paxinos G., 2007).

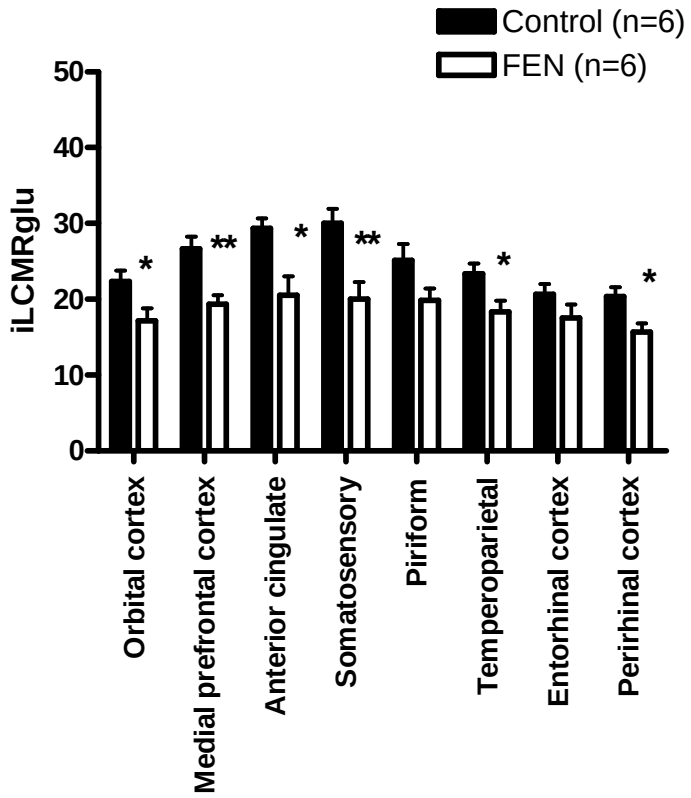

Figure 5.3.10 iLCMRglu in cortical regions of the fenfluramine treated group compared to the control group.

The graph depicts iLCMRglu in cortical regions of fenfluramine treated (10mg/kg) naïve mice in comparison to a saline treated controls. There were differences in iLCMRglu in the majority of cortical regions examined that reached statistical significance in the orbital cortex, medial prefrontal cortex, anterior cingulate, somatosensory, temperoparietal and perirhinal cortex. Data are presented as mean+SEM and statistical significance was determined using a Students unpaired t-test (* $p < 0.05$, ** $p < 0.01$).

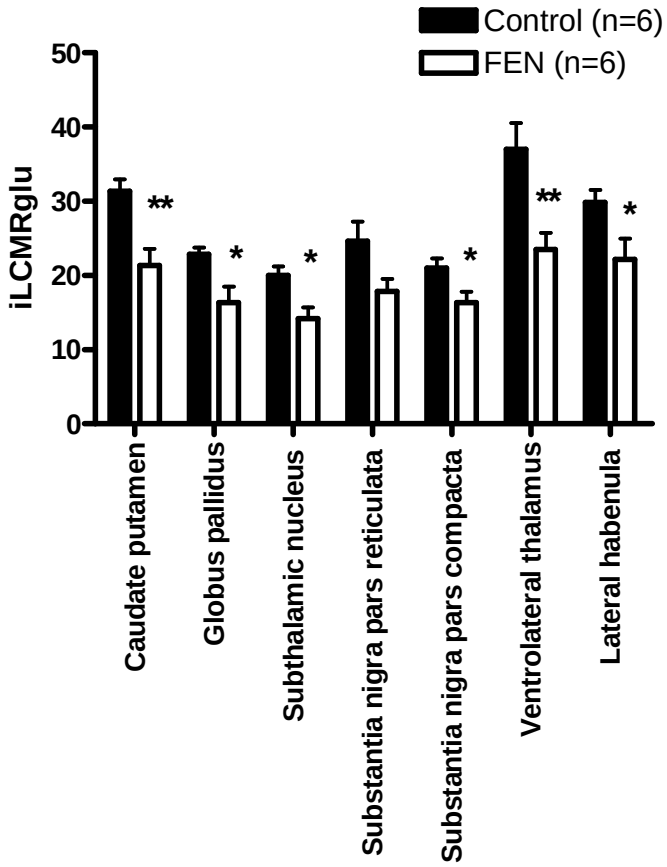

Figure 5.3.11 iLCMRglu in motor regions of the fenfluramine treated group compared to the control group.

The graph depicts iLCMRglu in motor regions of fenfluramine treated (10mg/kg) naïve mice in comparison to a saline treated controls. The difference in iLCMRglu reached statistical significance in the majority of motor regions examined, these included the caudate putamen, globus pallidus, subthalamic nucleus, sunstantia nigra par compacta, ventrolateral thalumus and lateral habenula. Data are presented as mean+SEM and statistical significance was determined using a Students unpaired t-test (* $p< 0.05$, ** $p< 0.01$).

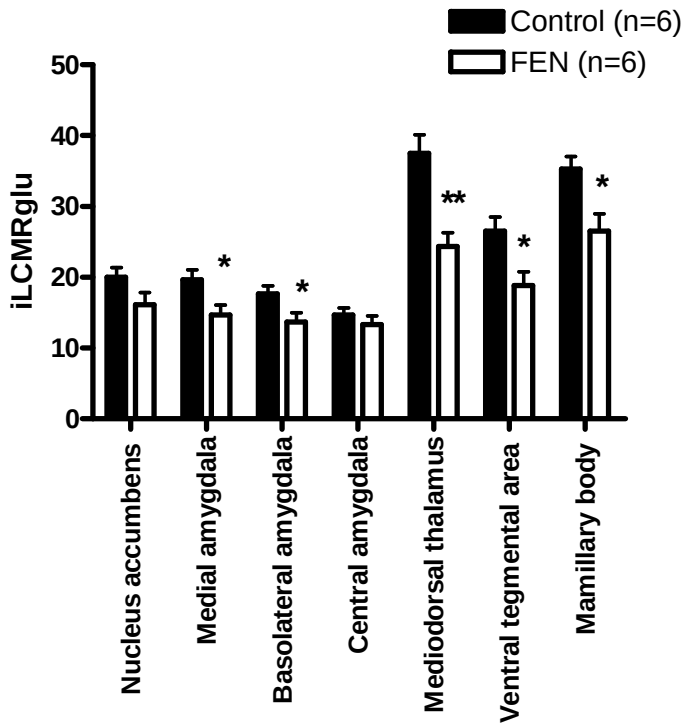

Figure 5.3.12 iLCMRglu in limbic regions in the fenfluramine treated group compared to the control group.

The graph depicts iLCMRglu in limbic regions of fenfluramine treated (10mg/kg) naïve mice in comparison to saline treated control group. There were differences in iLCMRglu in all limbic regions examined that reached statistical significance in the medial amygdala, basolateral amygdala, medialdorsal thalamus, ventral tegmental area and mammillary body. Data are presented as mean+SEM and statistical significance was determined using a Students unpaired t-test (* $p < 0.05$, ** $p < 0.01$).

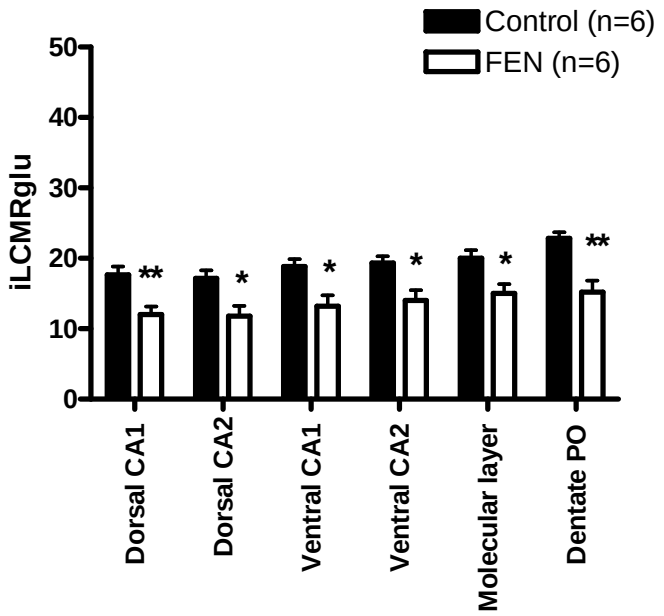

Figure 5.3.13 iLCMRglu in hippocampal regions in the fenfluramine treated group compared to the control group.

The graph depicts iLCMRglu in hippocampal regions of fenfluramine treated (10mg/kg) naïve mice in comparison to a saline treated controls. The difference in iLCMRglu reached significance in all hippocampal regions examined, these included the dorsal CA1, dorsal CA2, ventral CA1, ventral CA2, molecular layer and dentate PO. Data are presented as mean+SEM and statistical significance was determined using a Students unpaired t-test (*$p<0.05$, **$p< 0.01$).

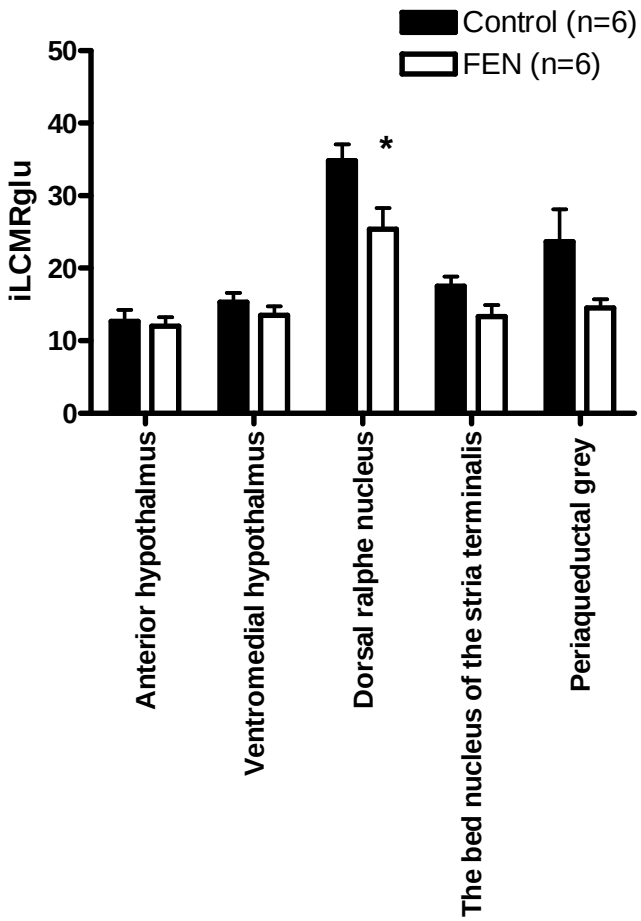

Figure 5.3.14 iLCMRglu in other regions of the fenfluramine treated group compared to the control group.

The graph depicts iLCMRglu in other regions of fenfluramine treated (10mg/kg) naïve mice in comparison to a saline treated controls. There were minimal differences in iLCMRglu in the hypothalamus and the bed nucleus of the stria terminalis. iLCMRglu reached a significance difference in the dorsal raphe nucleus. Data are presented as mean+SEM and statistical significance was determined using a Students unpaired t-test (* $p < 0.05$).

5.3.5 Study 3: The effect of fenfluramine challenge on iLCMRglu in the CIA group compared to the control group.

Fenfluramine challenge in the CIA group resulted in only 2 out of the 34 regions of interest examined being significantly different from fenfluramine challenged controls. The orbital cortex (-41%, Figure 5.3.16) and the molecular layer (-26%, Figure 5.3.19) of the hippocampus were the only regions where a significant difference in iLCMRglu was demonstrated. In the majority of regions of interest investigated there was a trend for serotonergic transmission to be lower in the CIA group in comparison to the control group which were not significant. The average percentage change in iLCMRglu was -14%, but overall there were minimal differences between the groups after fenfluramine challenge. This could be visually observed in the autoradiograms, where the darker the structure the greater the glucose utilisation (Figure 5.3.15)

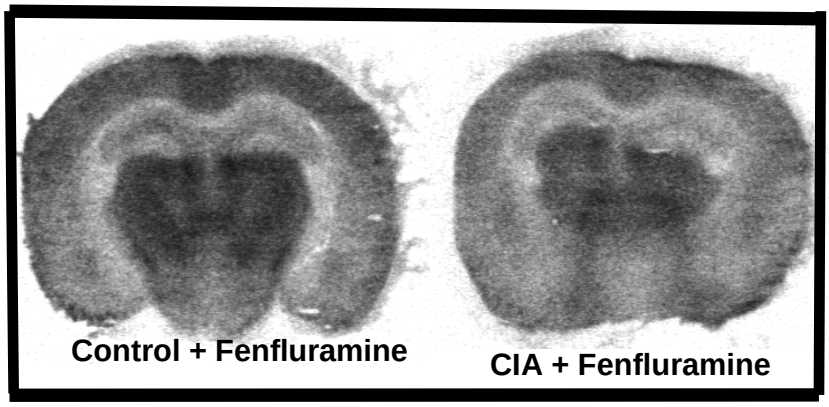

Figure 5.3.15 The effect of fenfluramine challenge on tissue [^{14}C] in the control group and CIA group at bregma -1.7mm (Franklin K.B.J and Paxinos G., 2007).

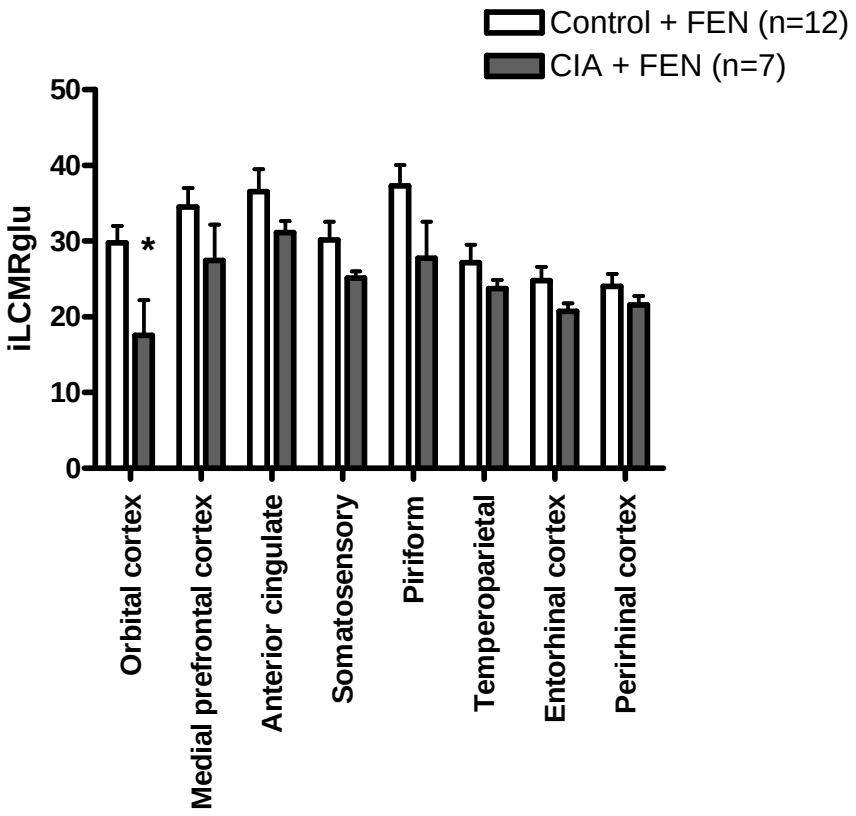

Figure 5.3.16 The effect of fenfluramine challange on iLCMRglu in cortical regions of the CIA group compared to the control group.

The CIA group was defined as CIA immunised mice, which demonstrated clinical symptoms. Both the control group and the CIA group were challenged with fenfluramine (10mg/kg), 41/42 days post immunisation. The graph depicts iLCMRglu in cortical regions of the control and CIA groups. iLCMRglu reached a significance difference between the groups in the orbital cortex. However, in all other cortical regions examined there were minimal differences in iLCMRglu in the CIA group compared to the control group. Data are presented as mean+SEM and statistical significance was determined using a Students unpaired t-test (*$p<0.05$).

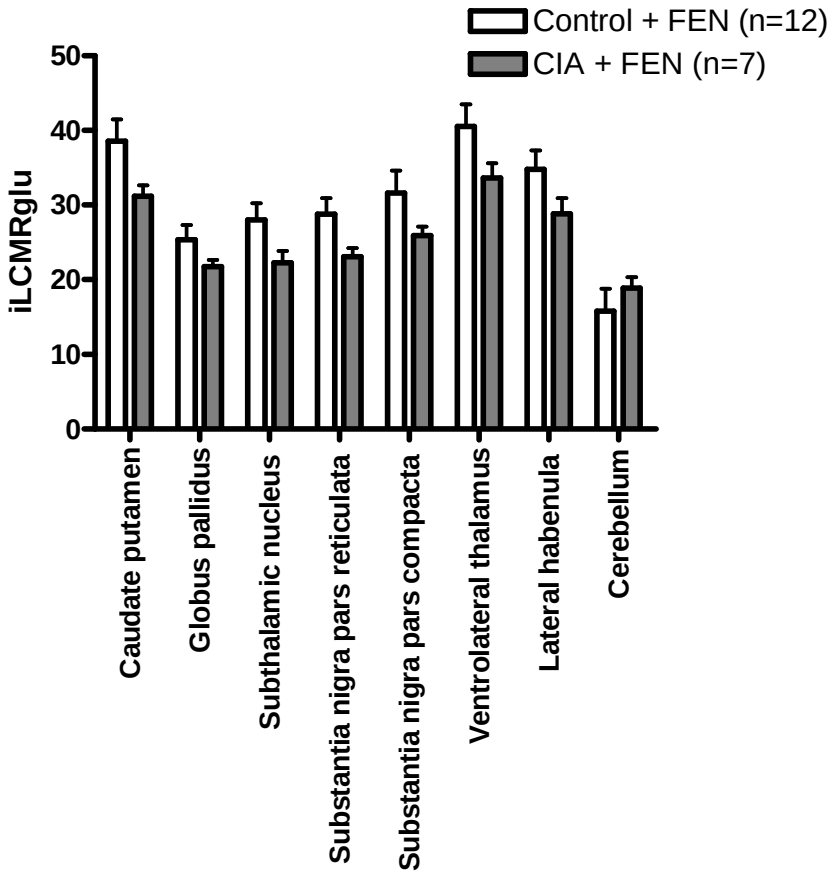

Figure 5.3.17 The effect of fenfluramine challenge on iLCMRglu in motor regions of the CIA group compared to the control group.

The CIA group was defined as CIA immunised mice, which demonstrated clinical symptoms of swelling and erythema. Both the control group and the CIA group were challenged with fenfluramine (10mg/kg), 41/42 days post immunisation. The graph depicts iLCMRglu in the motor regions of the control and CIA groups. There were minimal differences in iLCMRglu in the CIA group compared to the control group in all motor regions examined. Data are presented as mean+SEM and statistical significance was determined using a Students unpaired t-test.

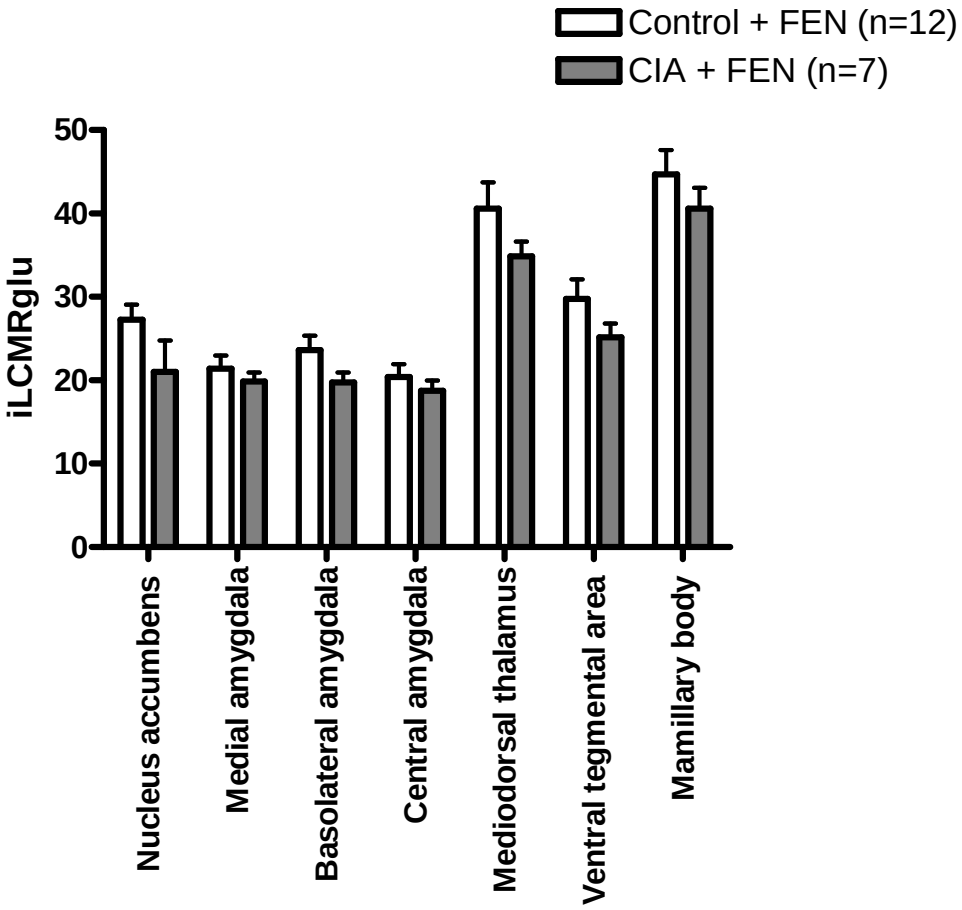

Figure 5.3.18 The effect of fenfluramine challenge on iLCMRglu in limbic regions of the CIA group compared to the control group.

The CIA group was defined as CIA immunised mice, which demonstrated clinical symptoms. Both the control group and the CIA group were challenged with fenfluramine (10mg/kg), 41/42 days post immunisation. The graph depicts iLCMRglu in limbic regions of the control and CIA groups. There were minimal differences in iLCMRglu in the CIA group compared to the control group in all limbic regions examined. Data are presented as mean +SEM and statistical significance was determined using a Students unpaired t-test.

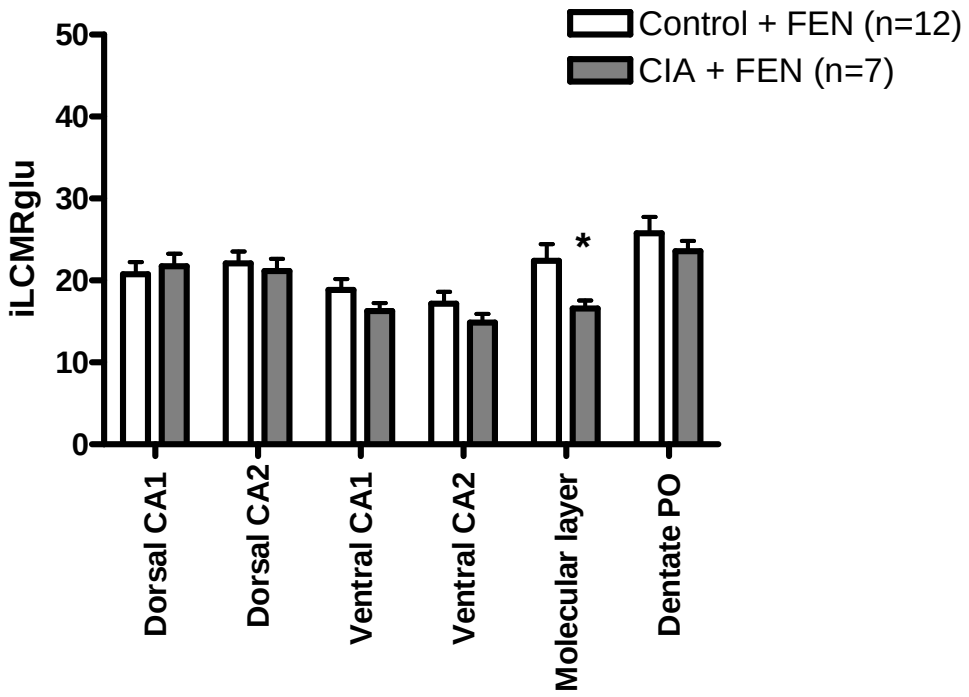

Figure 5.3.19 The effect of fenfluramine challenge on iLCMRglu in hippocampal regions of the CIA group compared to the control group.

The CIA group was defined as CIA immunised mice, which demonstrated clinical symptoms. Both the control group and the CIA group were challenged with fenfluramine (10mg/kg), 41/42 days post immunisation. The graph depicts iLCMRglu in hippocampal regions of the control and CIA groups. iLCMRglu reached a significance difference in the molecular layer of the hippocampus. However, in all other hippocampal regions examined there were minimal differences in iLCMRglu between the groups. Data are presented as mean+SEM and statistical significance was determined using a Students unpaired t-test (*$p<0.05$).

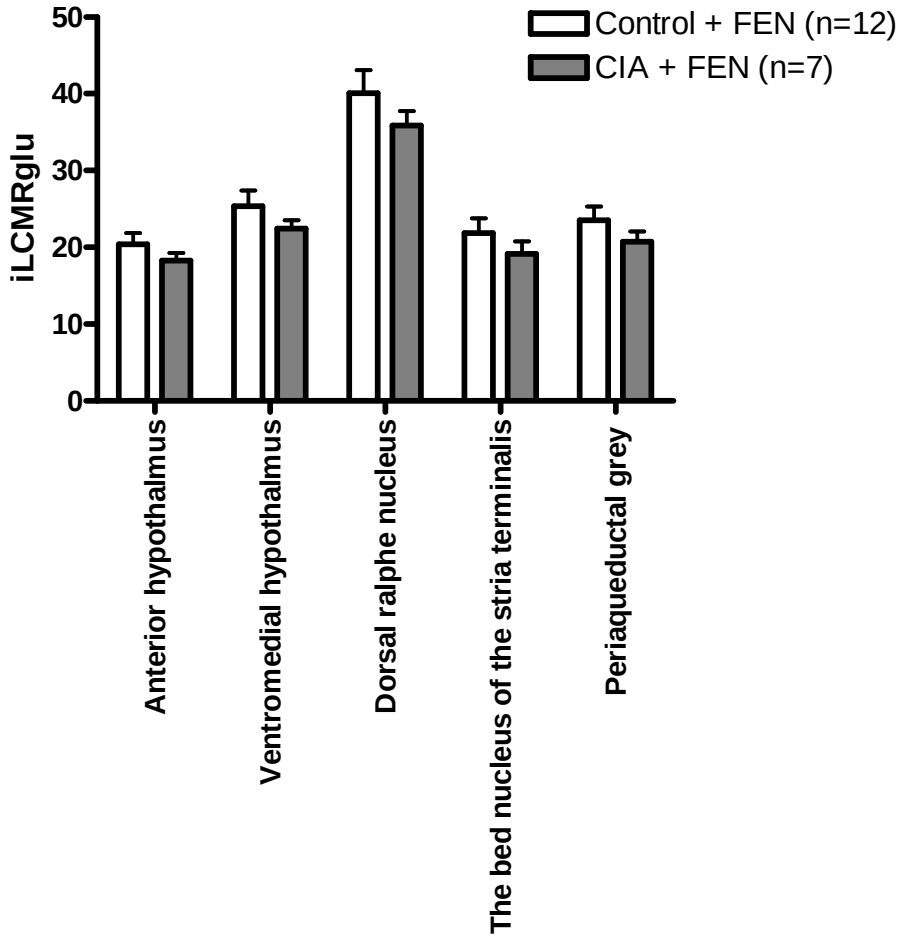

Figure 5.3.20 The effect of fenfluramine challenge on iLCMRglu in other regions of the CIA group compared to control group.

The CIA group was defined as CIA immunised mice, which demonstrated clinical symptoms of swelling and erythema. Both the control group and the CIA group were challenged with fenfluramine (10mg/kg), 41/42 days post immunisation. The graph depicts iLCMRglu in other brain regions of the control and CIA groups and in all other regions examined there were minimal differences in iLCMRglu between the groups. Data are presented as mean+SEM and statistical significance was determined using a Students unpaired t-test (* $p < 0.05$).

5.4 Discussion.

The focus of this thesis is the hypothesis that there is altered brain function in CIA immunised mice with proven clinical symptoms. This chapter used the [^{14}C]-2-DG autoradiographic technique and a challenge to the serotonergic system to identify any abnormal brain function within the CIA model from regional glucose utilisation values.

To the author's knowledge, there have been no previous attempts to investigate altered cerebral metabolic function in the CIA model. The [^{14}C]-2-DG autoradiographic technique has however previously been utilised to investigate altered cerebral metabolic function during the temporal evolution in the rat adjuvant monoarthritic model to investigate brain function related to pain (Neto et al., 1999). This study reported increased metabolic function in the thalamic, cortical and limbic regions at day 2 and 14 but not day 4, suggesting metabolic function varies during the temporal evolution of the model (Neto et al., 1999). There was no difference in glucose utilisation in the CIA model after a chronic inflammatory response on day 42 post immunisation, a similar time point to day 14 in the adjuvant monoarthritic model. Both models have a similar period of clinical symptoms. However, the CIA model is very different from the adjuvant monoarthritic model. The CIA model has a greater severity than the adjuvant monoarthritic model as multiple joints and limbs develop clinical symptoms of disease in the CIA model in comparison to a single joint in the left limb of the adjuvant monoarthritic model. Since the CIA model has greater severity it would be expected that the CIA model would also have altered cerebral glucose utilisation in the thalamus, cortical and limbic regions associated with pain, but this was not the case. Both studies used complete Freunds's adjuvant which was administered via different routes. In the CIA model mice were immunised with a subcutaneous injection of type II collagen in complete Freund's adjuvant emulsification. In comparison in the adjuvant monoarthritic model, complete Freund's adjuvant was injected into the left tibiotarsal joint. The diverse immunisation techniques and the dissimilar degrees of severities between the models may have influence metabolic function differently. The temporal evolution of the models also differs and may account for the difference in cerebral metabolic function as the glucose metabolism was shown to vary during the temporal

evolution of the adjuvant monoarthritic model (Neto et al., 1999). This suggests that there may be also be altered metabolic function in the CIA model at a different time points. This is consistent with recent reports which suggest the BBB integrity varies during the temporal evolution of CIA (Nishioku et al., 2010b).

Although there were no abnormalities in glucose utilisation in the CIA group this does not necessarily, mean that neuronal pathways are not compromised by the disease. The previous chapter (chapter 4) investigated altered serotonin transporter density and discussed the influence of pro-inflammatory cytokines on the serotonergic system. To assess altered serotonergic function, fenfluramine challenge was applied to drive serotonergic transmission. Study 2, characterised the iLCMRglu response to fenfluramine challenge and verified the dose in naïve mice. The results illustrated reduced iLCMRglu in a number of regions throughout the brain including cortical, motor, hippocampal and a few limbic regions. This was as expected because fenfluramie has driven the serotonergic system depleting serotonergic stores, so that 30 minutes later when 2-DG is administered, the brain has still not recovered resulting in reduced cerebral glucose utilisation. Serotonergic neuronal pathways originate from the raphe nucleus which displayed a significant reduction in cerebral glucose utilisation and is known to project to limbic and hippocampal regions which are involved in emotional and cognitive behaviour (Jacobs and Azmitia, 1992). Therefore the reduction in cerebral glucose response is consistent with the literature describing serotonergic pathways. From the data in study 2, it was concluded that 10mg/kg fenfluramine was a suitable dose of fenfluramine to drive the serotonergic system.

In study 3, both groups were administered a fenfluramine challenge, examining altered serotonergic transmission in the murine CIA model, in comparison to the previous study which examined iLCMRglu response in the CIA model *per se*. The results demonstrated a significant difference in serotonergic transmission in the orbital cortex and the molecular layer of the hippocampus, structures which are known to be implicated in the pathology of depression and pain. Evidence for the involvement of the orbital cortex in the development of depression comes from reduced orbital cortex volume (Drevets et al., 2008) and increased cerebral blood flow in the orbital cortex of major depressive patients (Price et al., 1996). The

hippocampus is known to be involved in the modulation of emotional behaviour and there is evidence of reduced hippocampal volume in people suffering from depression which is intensified with repeated episodes and duration (Sheline et al., 1996; Sheline et al., 2003). The orbital cortex and hippocampus are also involved in the neuro-circuitry of pain. The orbital cortex, thalamus and periaqueductal grey are involved in the pathway believed to modulate pain (Tang et al., 2009). The hippocampus is also believed to be involved in aversive behaviour associated with pain. The difference in serotonergic transmission observed in the hippocampus and orbital cortex correspond to the altered glucose response observed in the rat adjuvant monoarthritic model, which the author attributed to pain. To discount this future studies are required which employ a non-anti-inflammatory pain killer, to inhibit pain but not the immune response to determine if altered brain function is attributed to pain or the inflammation.

In study 3 glucose utilisation was greater than was expected when compared to the previous studies. There were a number of differences between study 3 and the previous studies which may account for the observed difference in iLCMRglu. Although there were similar plasma glucose levels between all the studies. There was significantly lower plasma [^{14}C] in the CIA FEN group in study 3 compared to the control group in study 1. This however did not appear to affect the plasma glucose/ plasma [^{14}C] ratios as there was no significant difference between all the studies (Table 5.3.1). The [^{14}C]-2-DG technique is a very sensitive method of investigating altered brain function which relies heavily on normal glucose levels. Glucose levels may become altered if an animal is stressed. However, if the animal was stressed or if it was given a higher dose of [^{14}C]-2-DG this would be apparent in the plasma profiles. Furthermore, a new bottle of [^{14}C]-2-DG was used in the final study with a specific activity of 57.7 mCi/mmol compared to the bottle of [^{14}C]-2-DG used in study 1 and study 2 which has a specific activity of 50.0 mCi/mmol. Other members of the department who performed experiments with both bottles of [^{14}C]-2-DG reported no differences between studies. The greatest unknown was the fact in study 3 both groups received a fenfluramine challenge and investigated serotonergic function compared to the previous studies which investigated glucose response. Both the control group and the CIA group were administered fenfluramine. This fact possibly combined with the differences in plasma glucose

and plasma [^{14}C] may have resulted in the increased glucose utilisation observed in the final study. All the studies were performed on separate days and may have been exposed to different variables. In hind sight if I were to repeat these study I would perform a single experiment with 4 groups; control, control with fenfluramine challenge, CIA and CIA with fenfluramine challenge in the hope of identifying compromised brain function in the CIA model.

5.4.1 Conclusion.

In the CIA mice there was no significant change in glucose response and minimal differences in serotonergic transmission. This still does not mean that CIA has no effect on brain function. In the future the experiment needs to be repeated as a single experiment with 4 experimental groups. It will also be important to consider the CIA model and identify the time points with increased likelihood of altered cerebral metabolic function.

Chapter 6

Cell proliferation and cell survival in the hippocampus of the murine CIA model.

6.1 Introduction.

Stem cells proliferate into neural progenitor cells which have the ability to differentiate into new neurones, astrocytes or oligodendrocytes (Gage et al., 1998). Neurogenesis occurs throughout adult life within the subventricular zone and the subgranular zone of the dentate gyrus only. Stem cells born in the subgranular zone of the dentate gyrus differentiate and migrate to the cellular level of the dentate gyrus where they mature into new neurons (Elder et al., 2006). Mature neurons have been shown to integrate into the existing neuronal circuitry to both receive synaptic input (Van Praag et al., 2002) and transmit neuronal output to postsynaptic targets (Toni et al., 2008). The functional implications and importance of neurogenesis within the subventricular zone and the subgranular zone are unknown.

There is some evidence to suggest that reduced neurogenesis in the subgranular zone of the hippocampus is linked to deficits in learning and memory (Zhao et al., 2008). Magnetic resonance imaging (MRI) has provided evidence of reduced hippocampal volume in people suffering from depression (Frodl et al., 2002; Bremner et al., 2000; Sheline et al., 1996). Investigation of the functional implications of altered hippocampal morphology using MRI found an association between reduced hippocampal volume and deficits in executive memory (Frodl et al., 2006). The reduction in hippocampal volume observed in depressive patients may be associated with reduced neurogenesis as, a MRI study on hippocampal volume in untreated depressed patients has suggested antidepressant treatment may be beneficial and protect the hippocampus (Sheline et al., 2003). Complementary rodent studies have shown chronic antidepressant treatment may increase hippocampal neurogenesis (Santarelli et al., 2003).

LPS induced systemic inflammation reduces cell proliferation and microglia cells are found in close proximity to proliferating cells in the subgranular zone (Ekdahl et al., 2003). LPS induced inflammation has been shown to be dependent on the activation of microglia as treatment with minocycline, inhibits microglia activation and restores neurogenesis (Ekdahl et al., 2003). Pro-inflammatory cytokine are secreted from microglia in response to trauma and infection and LPS treated microglia cell cultures showed upregulation of IL-6, and TNF-α mRNA expression (Kim and de Vellis, 2005) which have been shown to reduce neurogenesis. Transgenic mice expressing IL-6 demonstrated reduced neurogenesis (Vallieres et al., 2002). Similarly exposure to IL-6 (Monje et al., 2003) and TNF-α (Ben Hur et al., 2003; Monje et al., 2003) significantly reduced neurogenesis *in vitro*. Blockade of IL-6 restores neurogenesis suggesting IL-6 is an important mediator in reducing neurogenesis. IL-6 has also been implicated in reduced cell survival (Monje et al., 2003). Deletion of the TNFα-R1 resulted in increased neurogenesis which suggests TNF-α mediates its effect through the TNFα-R1 to reduce neurogenesis (Iosif et al., 2006). Exposure of TNF-α to a hippocampus-derived progenitor cell line also decreases cell survival (Cacci et al., 2005). Exposure to IL-1β or IFN-γ showed no change in neurogenesis (Monje et al., 2003), however other research groups have shown IFN-γ reduces cell proliferation and increases apoptosis (Ben Hur et al., 2003).

In the CIA model immunisation with type II collagen and complete Freund's adjuvant stimulates the recruitment of neutrophils and macrophages which secrete pro-inflammatory cytokines IL-6, TNF-α and IL-1β (Cho et al., 2007). T-cells are important in the induction of arthritis (Ranges et al., 1985) and are observed in the lymph nodes from week three onwards in the CIA model (Cho et al., 2007). The CIA model is a T helper 1 (T_H1) and T_H17 cell mediated disorder. T_H1 cells are activated by IL-12 and express IFN-γ and IL-2, whereas T_H17 cell are activated by IFN-γ, IL-6, TNF-α, IL-1 and IL-17 and express IL-6, TNF-α, IL-1 and IL-17. The secretion of the cytokine IFN-γ by T_H1 leads to negative regulation of T_H17 in comparison to the secretion of cytokines IL-6, TNF-α, IL-1 and IL-17 by T_H17 which led to positive regulation of T_H17 cells (Furuzawa-Carballeda et al., 2007). IL-17 has been linked with the severity of the inflammation, as mice over expressing IL-17 have increased inflammation and joint destruction and blocking IL-17 inhibits the

induction of CIA (Lubberts et al., 2005). Evidence from IL-6 knockout mice illustrate the importance of IL-6 in the induction of CIA as the induction of arthritis was inhibited in IL-6 knockout mice and restored by administration of IL-6 (Alonzi et al., 1998). Cytokines vary throughout the temporal evolution of the CIA model TNF- α and IL-6 are plentiful after the onset of clinical symptoms in comparison to IFN-γ which was scarcely expressed in the synovial tissue (Mussener et al., 1997)

The hypothesis underlying this thesis is that pro-inflammatory cytokines released in the periphery alter the CNS resulting in the development of depression. The hypothesis underlying this study is that during the inflammatory response in the CIA model pro-inflammatory cytokines IL-6 and TNF-α are released by microglia resulting in reduced neurogenesis in the subgranular zone of the hippocampus.

6.1.1 Aims.

The main aim was to investigate cell proliferation in the subgranular zone of the hippocampus at varying stages of disease progression in the murine CIA model. To achieve this, 5' –bromo-2'-deoxyuridine (BrdU), a marker of cell proliferation was injected intraperitoneally into CIA immunised mice at three different time points, to investigate:

1. Establish the BrdU protocol (Study A).
2. Cell proliferation before the onset of clinical symptoms (Study 1).
3. Cell survival during the development of clinical symptoms (Study 2).
4. Cell proliferation after the development of clinical symptoms (Study 3).

6.2 Methods.

6.2.1 Induction of CIA.

On day 0, male DBA/1 mice aged 7-8 weeks (13-15g, Harlan) were anaesthetised with 4% isofluorane in a mixture of 30% oxygen /70% nitrogen and the fur at the base of the tail shaved. Under anaesthetia the CIA group (n=10 or 12) were injected subcutaneously with 0.1ml of collagen emulsification at 2 sites just above the base of the tail, of 0.05ml each. The collagen emulsification was made up of equal volumes of bovine type II collagen and complete Freund's adjuvant. At this time point the control group (n=10/12) received no treatment. On day 21 post immunisation, the CIA group were injected intraperitoneally with 0.2ml bovine type II collagen 2mg/ml in an equal volume of sterile phosphate buffered saline. At this time point the control group received an intraperitoneal injection of 0.2ml sterile phosphate buffered saline. On day 42 post immunisation, brains were harvested (Section 2.1.1). Immunohistochemistry was performed on any mouse which had a clinical score greater than 0 in at least 1 limb. In study 1 and 2 one mouse was excluded from the immunohistochemistry experiments due to inaccurate cryostat cutting.

6.2.2 Termination criteria.

In accordance with the Home Office project licence animals were assigned a score of ill-health. Any mouse with an ill-health score of 7 or greater was killed by a Schedule 1 method on ethical grounds (Section 2.1.2).

6.2.3 Assessment of the disease.

Each limb was assigned a daily clinical score describing the extent of the swelling and erythema in the limb. A score of 0 represents no sign of swelling and erythema, a score of 2 or 3 represents mild swelling and erythema and a clinical score of 4 represents severe swelling and erythema and usually results in the loss of function of the limb (Section 2.1.3). A mouse was defined as having clinical symptoms of arthritis if it was assigned a clinical score greater than 0 in any limb. The incidence

of disease was calculated as the percentage of immunised mice which demonstrated clinical symptoms. To measure paw thickness the paw was held horizontal and the two heads of the spring callipers were placed above and below the paw clamping it in place (Section 2.1.6).

6.2.4 Experimental design.

From the schematic of the CIA model it can be observed that the experiment has a duration of 42 days, on day 0 mice were immunised by an initial subcutaneous injection of type II collagen emulsification. On day 21 post immunisation, mice were challenged with type II collagen mixed with phosphate buffered saline. On days 41 post immunisation mice were injected intraperitoneally with BrdU (150mg/kg). Finally on day 42 post immunisation mice were culled and the brains harvested (Figure 6.2.1).

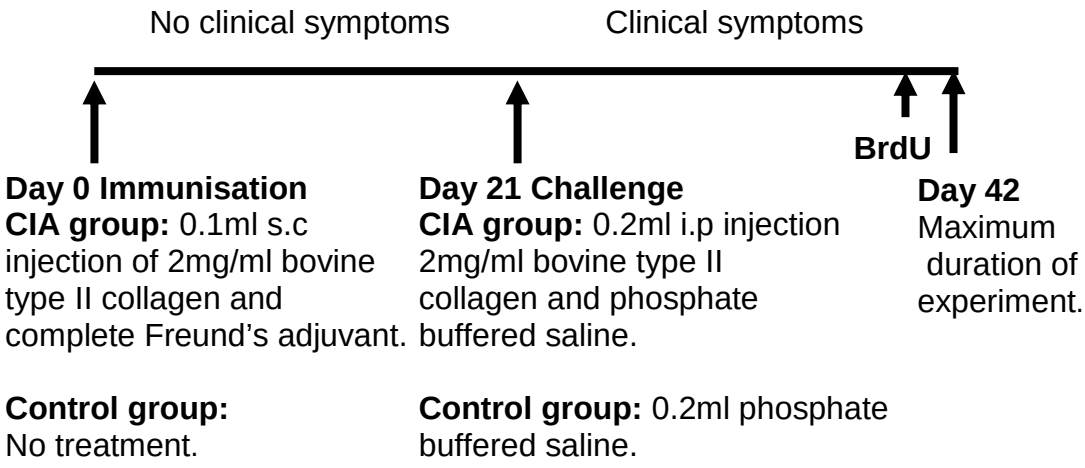

Figure 6.2.1 Study A: Experimental design of a preliminarily cell proliferation study.

From the schematic of the CIA experiment it can be observed that the experiment has duration of 6 days, on day 0 mice were immunised by an initial subcutaneous injection of type II collagen emulsification. Both the CIA (n=10) and control (n=10) groups were injected intraperitoneally with BrdU (100mg/kg) twice daily on days 1-5 inclusive. Mice were culled on day 6 and the brains harvested (Figure 6.2.2).

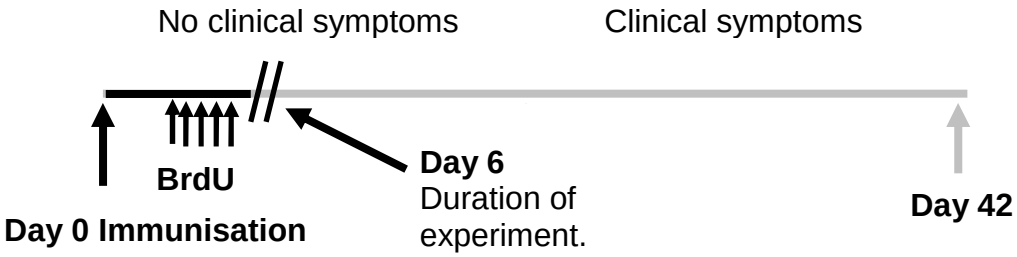

CIA group: 0.1ml s.c injection of 2mg/ml bovine type II collagen and complete Freund's adjuvant.

Control group: No treatment.

Figure 6.2.2 Study 1: Experimental design of the cell proliferation study before the onset of clinical symptoms.

From the schematic of the CIA model it can be observed that the experiment has a duration of 42 days, on day 0 mice were immunised by an initial subcutaneous injection of type II collagen emulsification. On days 18-20 post immunisation mice were injected intraperitoneally twice daily with BrdU (100mg/kg). The CIA experiment then continued and the mice were challenged with type II collagen mixed with phosphate buffered saline on day 21 post immunisation. Then on day 42 post immunisation, mice were culled and brains harvested. This would have given enough time for BrdU positive cells to either differentiate or undergo apoptosis, allowing cell survival to be investigated (Figure 6.2.3).

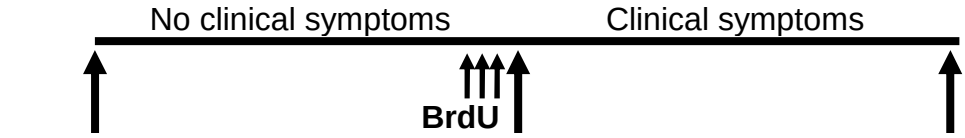

CIA group: 0.1ml s.c injection of 2mg/ml bovine type II collagen and complete Freund's adjuvant.

Control group: No treatment.

CIA group: 0.2ml i.p injection 2mg/ml bovine type II collagen and phosphate buffered saline.

Control group: 0.2ml phosphate buffered saline.

Figure 6.2.3 Study 2: Experimental design of the cell survival study during the development of and clinical symptoms.

From the schematic of the CIA model it can be observed that the experiment has a duration of 42 days, on day 0 mice were immunised by an initial subcutaneous injection of type II collagen emulsification. On day 21 post immunisation, mice were challenged with type II collagen mixed with phosphate buffered saline. On days 39-41 post immunisation mice were injected intraperitoneally twice daily with BrdU (100mg/kg). Finally on day 42 post immunisation mice were culled and the brains harvested (Figure 6.2.4).

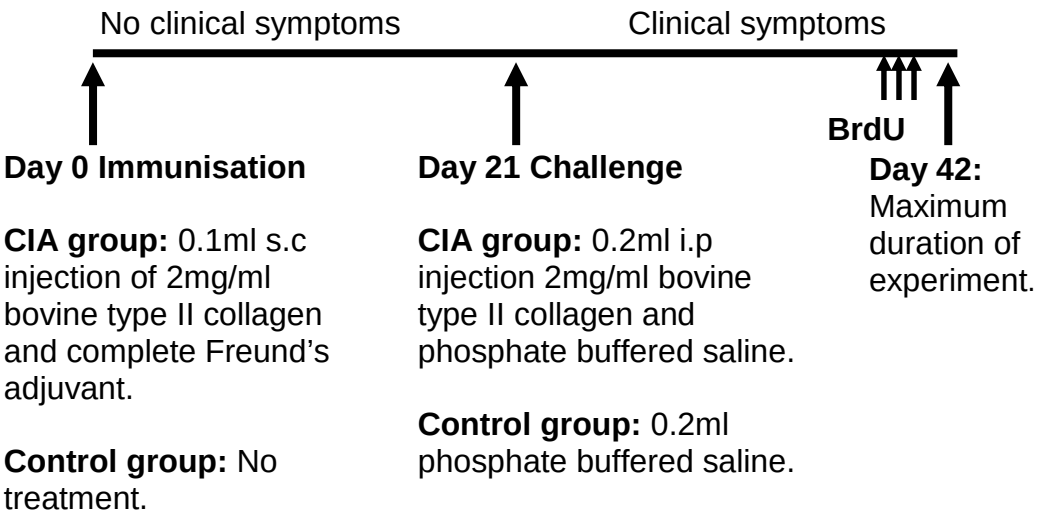

Figure 6.2.4 Study 3: Experimental design of the cell proliferation study after the development of clinical symptoms.

6.2.5 Experimental protocol for BrdU immunohistochemistry.

Sections were placed in a container of sodium citrate buffer (pH6) in a water bath preheated at 98ºC for 40 minutes. Still in the sodium citrate, sections were then placed in a sink of cold water for 20-30 minutes. Once cooled the endogenous peroxidise activity was quenched with 3% hydrogen peroxide in phosphate buffered saline for 10 minutes. Sections were then incubated in 0.025% trypsin solution for 10 minutes. BrdU is incorporated into proliferating cells during mitosis, in order for the BrdU antibody to gain access to the labelled cells DNA was denatured with 2M HCl at 37 ºC for 30 minutes. Non-specific binding sites were blocked for 60 minutes using a blocking solution of 1% normal rabbit serum in phosphate buffered saline and 0.3% triton X-100. Sections were incubated in primary antibody Rat anti-BrdU (1:200, Serotec) and blocking solution at 4ºC overnight. Sections were then incubated in secondary antibody biotinylated rabbit anti-rat (1:200, Vector

Laboratories) in blocking solution for 60 minutes. This was followed by incubation in ABC (Vector Laboratories) for 60 minutes and visualization with DAB (Vector Laboratories). Between each step in the experiment sections were rinsed in two 5 minute phosphate buffered saline washes on a shaker. The only exception was between the non-specific block and the primary antibody incubation where there was no rinse step. Finally sections were rinsed in distilled water for 30 minutes and counterstained with haematoxylin prior to mounting with a cover slip using DPX (Section 2.4.3).

6.2.6 Quantification of BrdU positive cells.

Prior to quantification BrdU sections were anonymised. BrdU positive cells in the subgranular zone, granule cell layer and hilus were counted in every 6^{th} section through the hippocampus using a light microscopy (x400). The total number of BrdU positive cells in each anatomical area was estimated by multiplying the number of cells in each section by 6. A BrdU positive cell was counted as being in the subgranular zone if the distance was less then one cell away or touching the granule cell layer. A BrdU positive cell was classed as being in the granule cell layer if it was within the granule cell layer and a BrdU positive cell was classed as being in the hilus if the distance was more then one cell away from the granule cell layer (Section 2.4.4).

6.2.7 Statistical analysis.

The disease severity summary measure and paw thickness summary measure data are presented as the mean. Statistical significance was determined using a Mann Whitney test to investigate changes in the paw thickness summary measurements between groups. Statistical significance was determined using a Students unpaired t-test to investigate changes in the estimated number of BrdU positive cells in the subgranular zone, granule cell layer or hilus between the groups. To examine the correlation between the disease severity summary measure and the number of BrdU positive cells in the subgranular zone a Spearman rank test was used.

6.3 Results.

6.3.1 Disease incidence and clinical score.

Study A.

Ten mice out of a possible 12 developed clinical symptoms of erythema and swelling representing a disease incidence of 83%. Further details of CIA model used in this study are located in chapter 3 Section 3.3.5-3.3.6.

Study 1.

Both the CIA and control groups displayed no clinical symptoms of erythema or swelling at any time point investigated.

Study 2.

In the cell survival study, 11 mice out of the12 immunised developed clinical symptoms of arthritis representing a disease incidence of 92%. In the CIA group swelling and erythema of the limbs developed between days 21-35 post immunisation. Front limbs appeared to be more severely affected by disease than hind limbs having the higher clinical scores over a longer period of the experiment. No control animal displayed any sign of limb swelling and erythema at any time point investigated.

To provide a summary measure of disease severity for each animal, the sum clinical scores of the 4 limbs were plotted over time and the area under the curve calculated. The severity of disease described by the clinical score differed between animals resulting in a range of disease severities (Figure 6.3.1, A).

Paws are approximately 1.8-2.0mm thick in naïve adult DBA1/A mice. The swelling in the front and hind limbs of the CIA group reached a maximum paw thickness of 3.0mm, however overall the swelling was greater in the front limbs by comparison to the hind limbs. Overall there was a significant increase in the summary measure of paw thickness in the CIA group compared to the control group (***$p<0.001$; Figure 6.3.1, B).

Study 3.

Nine mice out the 10 immunised developed clinical symptoms of arthritis representing a disease incidence of 90%. The CIA group began to develop clinical signs of arthritis at approximately day 23-30 post immunisation. The right front limb appeared to be more severely affected by disease than the rest of the limbs having the higher clinical scores over a longer period of the experiment. No control animals showed any clinical signs of arthritis at any time point examined.

Disease affected each animal to different extents. To provide a summary measure of disease severity for each animal the sum of the clinical scores of the 4 limbs were plotted over time and the area under the curve calculated. The severity of the disease varied in the CIA group. No control animals showed any signs of clinical symptoms so had a disease severity of 0 at all time points investigated (Figure 6.3.2, A).

The swelling in the front and hind limbs of the CIA group reached a maximum paw thickness of 3.0mm. Even although the right hind limb reached a maximum paw thickness of 3.0mm, the majority of right hind limb calliper measurements did not exceed a maximum paw thickness of 2.4mm.

In order to demonstrate the swelling in the CIA group compared to the control group the sum paw thickness of the 4 limbs were plotted over time and the area under the curve calculated to give a summary measure of paw thickness. Overall there was a significant increase in the summary measure of paw thickness in the CIA group compared to the control group (Figure 6.3.2, B).

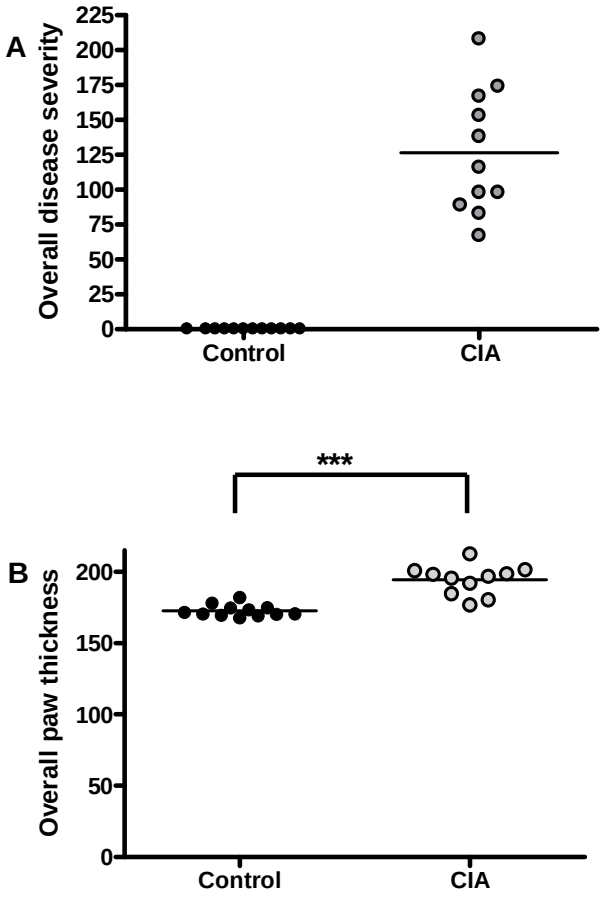

Figure 6.3.1 Study 2: Summary measures depicting the disease in the CIA group compared to the control group.

The sum clinical score and the paw thickness were plotted over time and the area under the curve calculated to give a summary measure of disease severity and a summary measure of paw thickness in each animal in study 2. A) The disease severity varied between animals in the CIA group. No animal in the control group showed any signs of clinical symptoms. B) The graph above depicts a significant difference in the summary measure of paw thickness in the CIA group compared to the control group. Horizontal bar represents the mean. Statistical significance was determined using a Mann Whitney test (***p< 0.001).

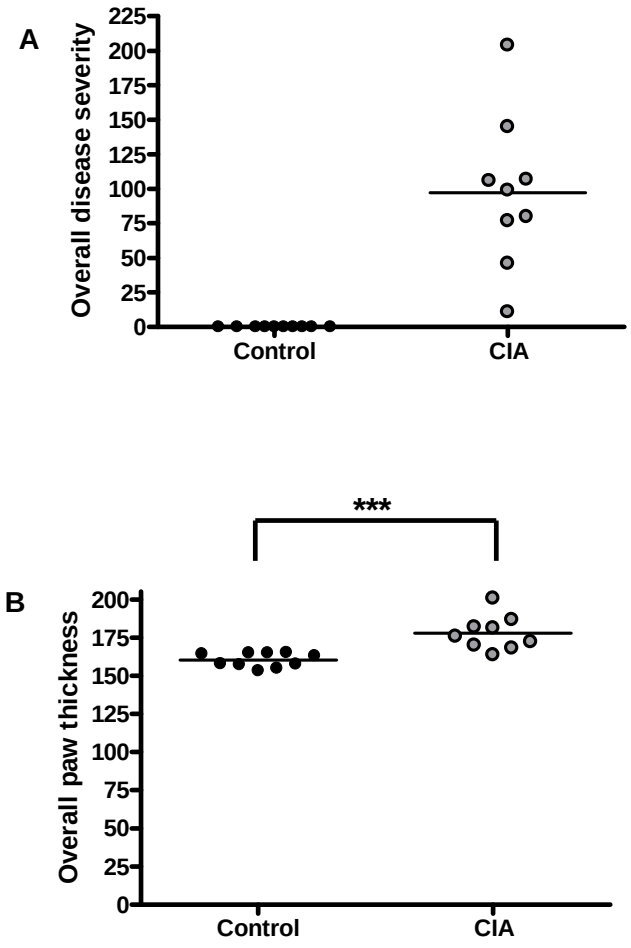

Figure 6.3.2 Study 3: Summary measures depicting the disease in the CIA group compared to the control group.

The sum clinical score and the paw thickness were plotted over time and the area under the curve calculated to give a summary measure of disease severity and a summary measure of paw thickness in each animal in study 3 (A) The disease severity varied between animals in the CIA group. No animal in the control group showed any signs of clinical symptoms. B) The graph above depicts a significant difference in the summary measure of paw thickness in the CIA group compared to the control group. Horizontal bar represents the mean. Statistical significance was determined using a Mann Whitney test (***p< 0.001).

6.3.2 Cell proliferation and cell survival.

BrdU cells were quantified in the subgranular zone, granule cell layer and hilus of the hippocampus in the control and CIA group. A BrdU positive cell was counted as being in the subgranular zone if the distance was less than one cell away or touching the granule cell layer. A BrdU positive cell was classed as being in the granule cell layer if it was within the granule cell layer and a BrdU positive cell was classed as being in the hilus if the distance was greater than one cell from the granule cell layer (Section 2.4.4). BrdU positive cells are predominantly located in the subventricular zone, in contrast cell proliferation occurs throughout the embryonic brain (Figure 6.3.3).

Study A.

On day 42 post immunisation, BrdU positive cell were quantified in the subgranular zone, granule cell layer and hilus of the control and CIA groups. The estimated number of BrdU positive cells was higher in the subgranular zone in comparison to the granule cell layer and hilus. In all anatomical locations examined, no significant difference was found in the number of BrdU positive cells in the CIA group compared to the control group (Figure 6.3.4).

Study 1.

The number of BrdU positive cells was higher in the subgranular zone in comparison to the granule cell layer and the hilus. Within the subgranular zone there was a decrease in the number of BrdU positive cells in the CIA group compared to the control group, however this did not reach statistical significance (Figure 6.3.5 A). In the granule cell layer and hilus there was no significant difference between BrdU positive cells in the CIA group compared to the control group (Figure 6.3.5 B, C).

Study 2.

At day 42 post immunisation there were similar numbers of BrdU positive cells in the subgranular zone, granule cell layer and hilus. There was also no significant difference in the number of BrdU positive cells in the CIA group compared to the control group in all anatomical locations investigated (Figure 6.3.6, A-C).

Study 3.

There was a lower number of proliferating cells within the granule cell layer and hilus by comparison to the subgranular zone. There was no significant difference between the number of proliferating cells in the CIA group compared to the control group in the granule cell layer and the hilus (Figure 6.3.7, B, C). In the subgranular zone however, there was a significant increase in the number of proliferation cells in the CIA group compared to the control group (Figure 6.3.7,A).

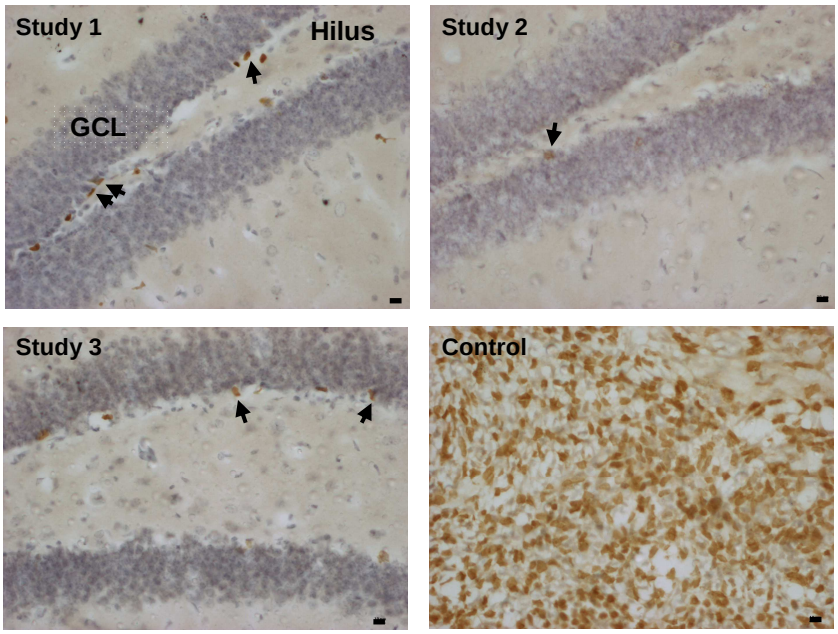

Figure 6.3.3 Representative BrdU immunostained sections.

BrdU positive cells in the subgranular zone (SGZ), granule cell layer (GCL) and hilus were counted using light microscopy (x400). Arrow indicate BrdU positive staining in the SGZ. There is substantial BrdU staining in an embryonic brain and was used as a positive control. Scale bar =10μm.

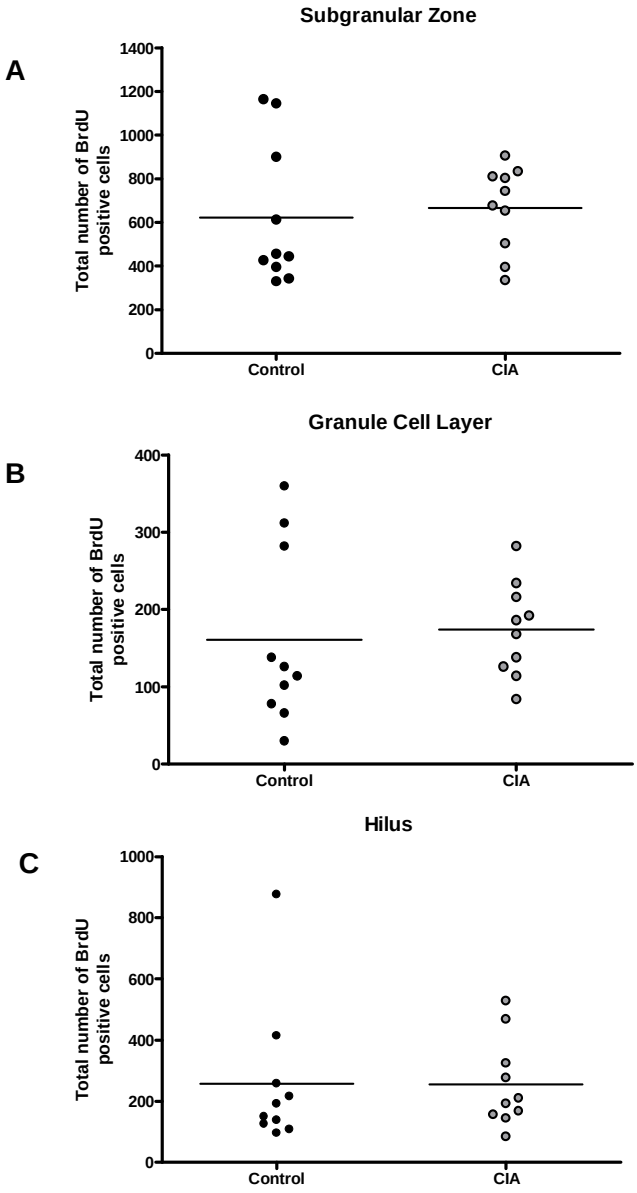

Figure 6.3.4 Study A: Cell proliferation.

On day 41 post immunisation, mice were injected intraperitoneally with 150mg/kg BrdU. On day 42 post immunisation, mice were culled and the brains harvested, stained for BrdU and BrdU positive staining quantified. Quantification of cell proliferation in the subgranular zone, granule cell layer and hilus revealed no significant difference between BrdU positive cells in the CIA group (n=10) compared to the control group (n=10). Statistical difference was assessed using a Student's unpaired t-test.

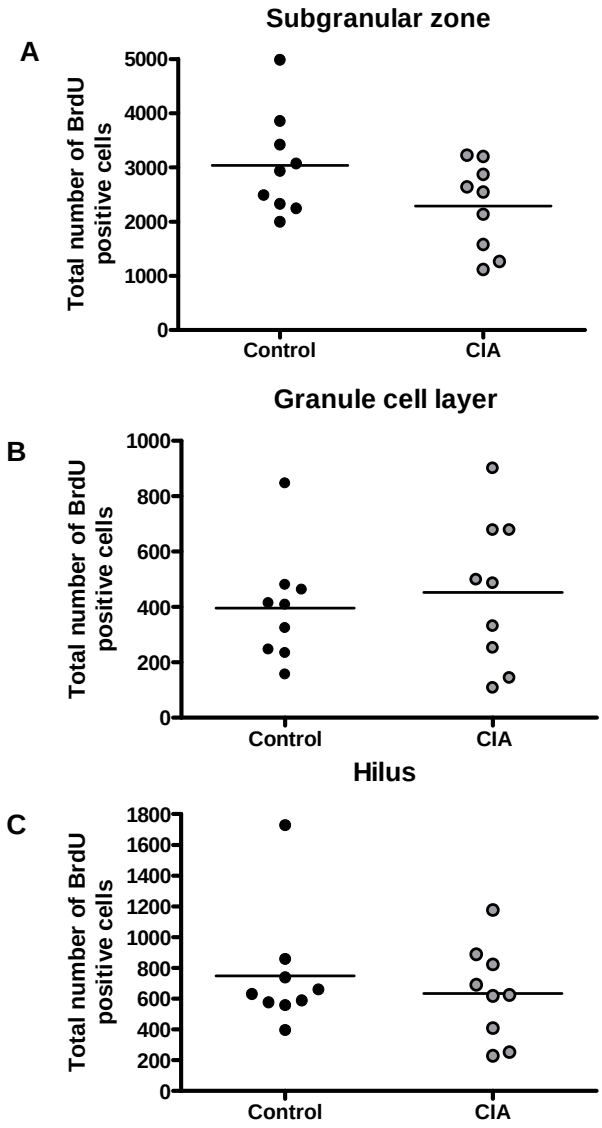

Figure 6.3.5 Study 1: Cell proliferation.

Mice were injected intraperitoneally with 100mg/kg BrdU twice daily on days 1-5 inclusive. On day 6 post immunisation the mice were culled and the brains harvested, stained for BrdU and BrdU positive staining quantified in the subgranular zone, granule cell layer and hilus.There was no significant difference between BrdU positive cells in the CIA group compared to the control group in any anatomical location investigated. Horizontal bars represent the mean. Statistical significance was assessed using a Student's unpaired t-test.

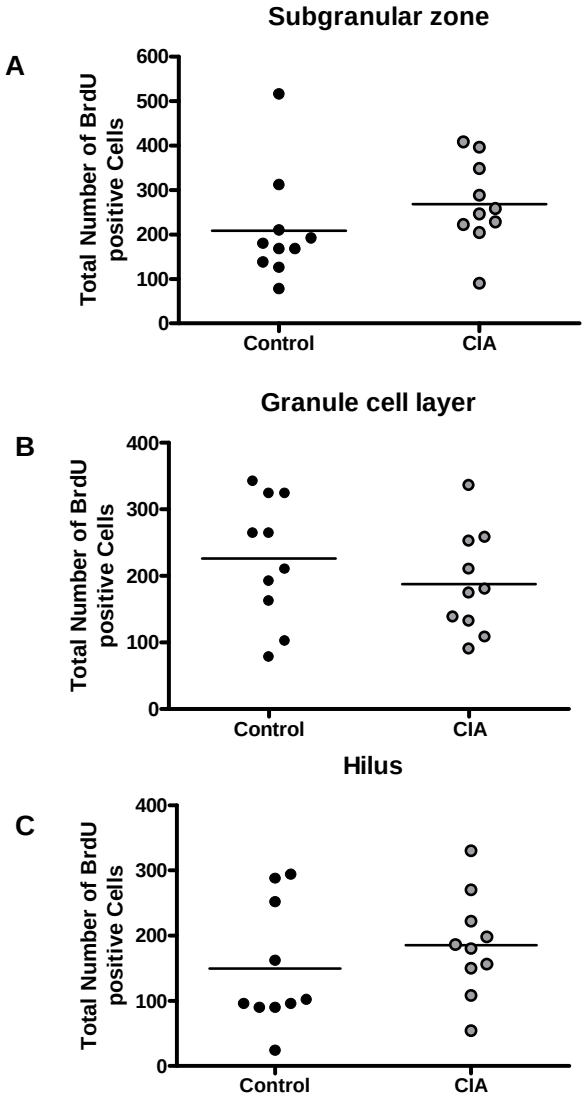

Figure 6.3.6 Study 2: Cell Survival.

Mice were injected intraperitoneally twice daily with 100mg/kg BrdU on days 18-20 inclusive. They were culled on day 42 post immunisation and the brains harvested, stained for BrdU and positive staining quantified. Quantification of BrdU positive cell survival in the subgranular zone and surrounding granule cell layer and hilus revealed that there was no significant difference between BrdU positive cells in the CIA group compared to the control group in any anatomical location investigated. Horizontal bar represents the mean. Statistical difference was assessed using a Student's unpaired t-test.

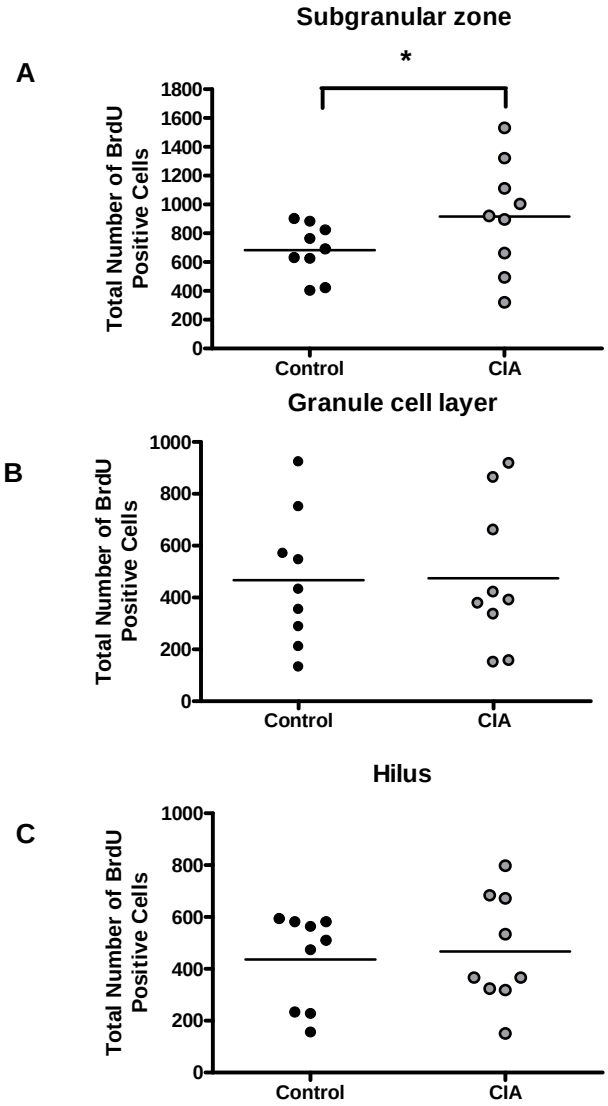

Figure 6.3.7 Study 3: Cell proliferation.

Mice were injected intrapertaneally twice daily with 100mg/kg BrdU on days 39-41 inclusive. They were culled on day 42 post immunisation and the brains harvested, stained for BrdU and BrdU positive staining quantified. Quantification of cell proliferation in the subgranular zone and surrounding granule cell layer and hilus revealed that there was a significant increase in BrdU mice compared to controls. In the granule cell layer and hilus there was no significant difference between BrdU positive cells in CIA mice compared to controls. Statistical difference was assessed using a Student's unpaired t-test (*$p<0.05$).

6.3.3 Relationship between disease severity and cell survival and proliferation.

Study 2.

Disease severity varied between animals in the CIA group. To investigate the impact varying disease severities has on cell proliferation, the summary measurement of disease severity was compared with the estimated number of BrdU cells in the subgranular zone in the same animal. The results show no association between clinical score and number of BrdU positive cells (Figure 6.3.8 A).

Study 3.

There was a range of disease severity summary measures (Figure 6.3.2, A) which may account for the variation in BrdU labelled cells in the subgranular zone between animals (Figure 6.3.8, A). To investigate this association the summary measurement of disease severity was compared with the total number of BrdU cells in the subgranular zone in the same animal. When plotted the data showed that as disease severity increased so did the total number of BrdU positive cells (Figure 6.3.8, B).

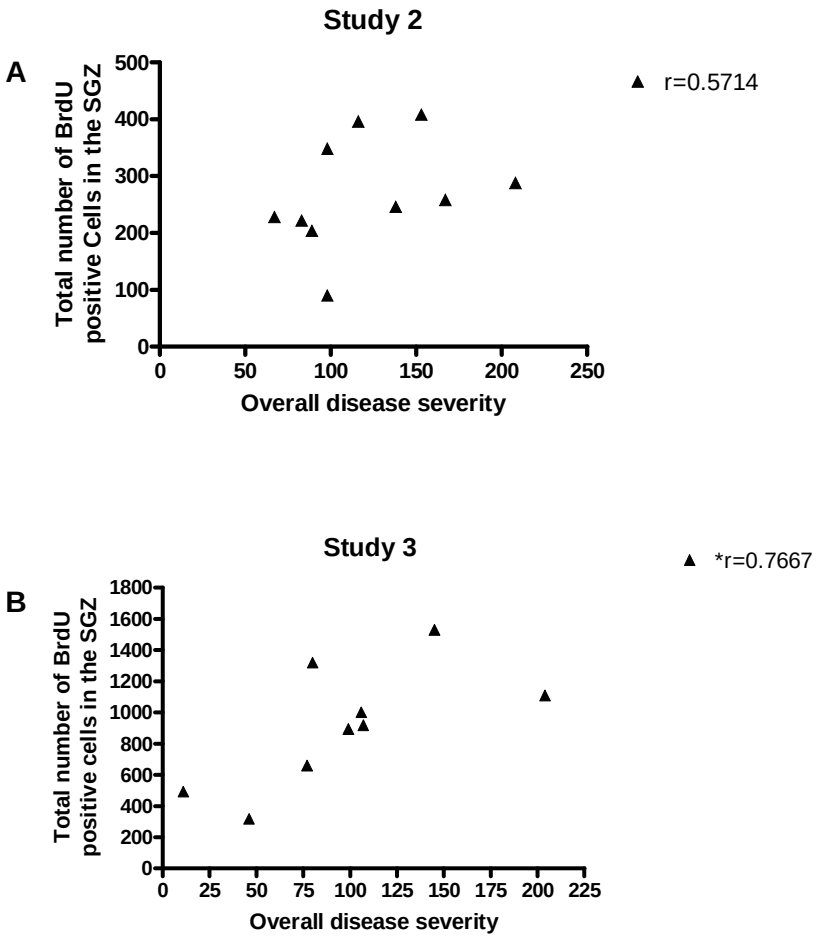

Figure 6.3.8 Relationship between disease severity and cell survival and proliferation.

The summary measurement of disease severity was compared with the total number of BrdU cells in the subgranular zone (SGZ) from the same animal. A) There was no significant correlation (r=0.5714) between clinical score and BrdU positive cells in study 2. B) The results show a significant correlation (r=0.7667) between clinical score and BrdU positive cells in study 3. Statistical significance was calculated using a Spearman rank test.

6.4 Discussion.

Overall the data reported in this chapter show no significant reduction in cell proliferation as described in the hypothesis. There was a negligible reduction in cell proliferation before the onset of clinical symptoms (study 1), however this was not statistically significant. After the development of clinical symptoms there was a significant increase in cell proliferation (study 3). The significant increase in cell proliferation was not reproducible (study A) and the total number of proliferating cells varied per animal.

In study A no significant difference was found in the number of proliferating cells in the subgranular zone, granule cell layer or hilus of the CIA group compared to the control group. Even although there was no significant difference in the number of proliferating cells in the subgranular zone in the CIA group compared to the control group, we were able to reproduce the BrdU staining previously described in the literature (Wojtowicz and Kee, 2006). BrdU staining occurs throughout the entire brain. To illustrate the higher level of BrdU positive staining in the subgranular zone the surrounding granule cell layer and hilus were also quantified. There are a number of possible explanations why no significant difference was observed between the CIA group and the control group. This was the first time I had prepared sucrose brains and the brain tissue immunostained was of poor quality with a high level of crystal artefact. As the tissue was damaged it was difficult to count the BrdU positive staining. Therefore in subsequent studies the brains were left in sucrose for a longer period of time. Another possible reason that no significant change was observed in the number of BrdU positive cells was that there may have not been enough proliferating cells labelled with BrdU. Therefore in the subsequent cell proliferation studies the number of BrdU injections were increased. These methological problems may also account for the differences observed between study A and study 3 as these studies have the same timeline.

To better understand cell proliferation during the temporal development of the CIA model, cell proliferation was investigated at two distinct time points. The first of these was before the onset of clinical symptoms. On day 0 of the murine CIA model, naïve mice were infected with the pathogen complete Freund’s adjuvant

which rapidly activated the innate immune response. Complete Freund's adjuvant is an endotoxin similar to LPS which activates the immune response and is implicated in reduced neurogenesis (Monje et al., 2003; Ekdahl et al., 2003). IL-6 is important in the induction of CIA and has been shown to reduce neurogenesis (Alonzi et al., 1998). We found no significant reduction in cell proliferation within the subgranular zone (Figure 6.3.5). The second time point investigated was after the development of clinical symptoms. By day 42 post immunisation, in the CIA experiment mice have experienced chronic clinical symptoms of rheumatoid arthritis. In this study there was a significant increase in cell proliferation (Figure 6.3.7). This was not the result we had anticipated as the literature has shown that pro-inflammatory cytokine decrease cell proliferation (Monje et al., 2003; Vallieres et al., 2002; Iosif et al., 2006)

The significant increase in cell proliferation after chronic inflammation is consistent with previous studies which have found an increase in neurogenesis in neurodegenerative disorders including Alzheimer's disease (Jin et al., 2004), Parkinson's disease (Shan et al., 2006) and Piron's disease (Steele et al., 2006). A recent publication by Wolf *etal*., 2009 found a significant increase in BrdU labelled cells expressing doublecortin, a marker of immature neurons at day 7 in the adjuvant induced arthritic (AIA) model of rheumatoid arthritis. The main difference between the AIA and the CIA models of rheumatoid arthritis is the temporal evolution. The AIA arthritic model develops between day 1-3 which is described as the acute phase and continued between day 4-21 which is described as the chronic phase. Day 7 in the AIA model is equivalent to day 28 post immunisation in the CIA model. Cell proliferation in CIA model was not investigated at day 28 post immunisation, in this study as it is likely at this time point that the clinical symptoms have just developed and are still continuing to develop. Increased cell proliferation in the CIA model at day 42 post immunisation, however, was not reported in the AIA model at the equivalent time point (Wolf et al., 2009b). Difference in sex, age and n numbers are possible explanations for the difference in proliferating cells between the models. Another important point to note is in the CIA model multiple joints in multiple limbs display clinical signs of disease compared to the AIA model which is limited to the antigen injected joint (Brand, 2005). There was also a substantial difference in BrdU administration, a single intraperitoneal injection of

50mg/kg BrdU was administered in the AIA model compared to twice daily injections of 100mg/kg BrdU over three days in the CIA model. Thus labelling a greater number of BrdU positive cells, which may account for the significant difference observed at day 42 post immunisation in the CIA model. Aside from all these difference in both the AIA and the CIA model there was a significant increase in cell proliferation, which correlated with the clinical symptoms of disease.

Increased $CD4^+$ T-cells in the murine CIA model may stimulate the increase in cell proliferation found in the CIA experiment. A recent publication illustrated that T-cell knockout mice had reduced neurogenesis in the dentate gyrus implicating T-cells involvement in neurogenesis (Wolf et al., 2009b). There is also a reduction in T-cell response in depressed patients (Irwin and Miller, 2007). If T-cells are indeed neuroprotective this may implicate reduced T-cells as a possible mechanism for reduced neurogenesis in depressed patients. T-cells can cross the BBB via the choroid plexus (Engelhardt and Ransohoff, 2005). This makes them possible candidates for translating the peripheral immune response to the CNS. Further investigation is required to determine the full mechanism which may involve the expression of cytokines from T-cells. T-cell derived IFN-γ has also been shown to promote microglia-induced inflammation and impair cell renewal (Butovsky et al., 2006). Therefore it may depend, on the immune homeostasis in the CIA model whether the immune system will have a neuroprotective or detrimental effect.

The increase in cell proliferation observed in our study may not be new neurons but other proliferating cells. Different markers are required to investigate the increase in cell proliferation further to determine the cell phenotype which may be stem cells, new neurons, microglia, oligodendrocytes or astrocytes. There is evidence to suggest that cytokine influence cell proliferation and create a bias towards a particular phenotype. For example IL-4 is believed to promote the differentiation of proliferated cells towards an oligodendritic phenotype, IFN-γ towards a neuronal phenotype (Butovsky et al., 2006) and IL-6 towards an astrocytic phenotype (Nakanishi et al., 2007). These are just three known examples of cytokines which may promote differentiation to a specific phenotype. There are an array of cytokines released during the temporal evolution of the CIA model which may also create a

bias towards a particular phenotype. Therefore further investigation is required to phenotype the newly differentiated cells.

It is also important to note the limitations of BrdU as a marker. Firstly BrdU is a toxin. Secondly, BrdU is a marker of DNA synthesis therefore there may also be some cells labelled during DNA repair, (Selden et al., 1993). Thirdly, labelling does not label all proliferating cells within the CNS it only provides a snap shot as it has a short bioavailability of approximately 2 hours (Taupin, 2007). Finally BrdU labelling is diluted with each subsequent cell division. This is not as important in the cell proliferation studies but is important to consider in the cell survival study.

Cell survival was investigated during the onset of clinical symptoms. There was no significant effect of disease progression on cell survival. However there was a similar number of proliferating cells in the subgranular zone compared to the granule cell layer and hilus (Figure 6.3.6). This is a different trend then that observed in the other studies in this chapter where there was a greater number of proliferating cells in the subgranular zone by comparison to the granule cell layer and hilus. There are a number of possible explanations for this, the increased number of proliferating cells observed in the subgranular zone in the other studies may be new cells with a neuronal phenotype, which do not mature into new neurons but undergo apoptosis. Therefore it is possible that 21 days after BrdU administration the subgranular zone had a similar number of BrdU positive cells compared to the granule cell layer and the hilus as a number of BrdU labelled cells within the subgranular zone had undergone apoptosis. This is consistent with previously published data investigating cell survival which found that after a 4 week period only 43% of BrdU labelled cells survived (Van Praag et al., 1999). Alternatively BrdU is a marker of proliferating cells and can only provide information on the time point it was administered. BrdU was administered prior to day 21 post immunisation. Therefore there may have been a decreased immune response and hence similar levels of proliferating cells in the subgranular zone, granule cell layer and hilus at this particular time point.

6.4.1 Conclusion.

No significant reduction in cell proliferation was observed in the subgranular zone of the CIA group compared to the control group at any time point examined. However, the data implicated an increase in cell proliferation after development of clinical symptoms. Further characterisation of cytokines, microglia and T-cells released in the CNS during the temporal evolution of the CIA model is required to determine potential mechanisms of action.

Chapter 7

General discussion.

7.1 Discussion.

7.1.1 Reproducibility of the CIA model.

One of the main focuses of this thesis has been the effect of CIA on the brain however, it is important to note the variability between CIA experiments. Summary measures of the clinical score were used to give an indication of the varying temporal evolution of disease over the duration of the experiment. The summary measure takes into account the variables of time, clinical score and the number of limbs displaying clinical symptoms. This is important as CIA mice can develop arthritis in any limb and in any combination of limbs over varying periods of time. Therefore the temporal evolution of arthritis in individual mice is unique and the reason why arthritic symptoms develop in a limb or limbs is ambiguous.

Chapter	**3**		**5**		**6**	
Study	1	2	1	3	2	3
n=	4	10	5	7	11	9
Mean summary measure of disease severity	62	119	53	61	127	97

Table 7.1.1 Mean summary measure of disease severity.

The results in Table 7.1.1 show the variability between the CIA groups and highlight that each CIA group produces a unique set of results which are not reproducible between groups. In the future to counteract the variability in the CIA model it may be necessary to increase the n number in the CIA group to determine any effect of CIA on the brain.

7.1.2 CIA has minimal influence on the brain.

The CIA model is a well established model of rheumatoid arthritis used to investigate novel anti-inflammatory agents. However, at the start of this thesis there was no information to our knowledge that characterised changes in the CNS in the model. Due to the novelty of this project we began by identifying key characteristics of depression and examined potential markers of these in the CIA model. Both altered serotonergic system function and hippocampal atrophy are implicated in the pathology of depression. It is believed that pro-inflammatory cytokines IL-1β, IFN-γ, and TNF-α drive IDO activity in activated microglia to metabolise tryptophan to the neurotoxic metabolites 3-hydroxy kynurenine and quinolinic acid (Miura et al., 2008). Thus, depriving the serotonin pathway of tryptophan could possibly result in reduced cell proliferation. My results showed minimal differences in both serotonin transporter levels and hippocampal cell proliferation between CIA immunised mice with proven clinical symptoms compared to controls. Since the serotonergic system appears to be unaltered and there was no reduction in cell proliferation it is possible that IDO activity was not being driven by cytokines and thus not metabolising tryptophan to its neurotoxic metabolites. In addition to the lack of changes in either serotonin transporters or cell proliferation there was also no significant difference in cerebral glucose metabolism between CIA immunised mice with proven clinical symptoms and controls. Altogether the results in the thesis suggest that CIA has minimal influence on the brain, at least on the systems I investigated.

The reduced integrity of the BBB in the CIA model (Nishioku et al., 2010b) increases the likelihood that cytokines released during the peripheral inflammatory response can enter the brain by passive diffusion. Similar to the CIA model, LPS has also been shown to decrease the integrity of the BBB (Nishioku et al., 2010a) and studies investigating cytokine levels in mice challenged with LPS have demonstrated a significant increase in IL-1β, IL-6 or TNF-α expression in the hippocampus, hypothalamus and brainstem (Datta and Opp, 2008). As the permeability of the BBB appears to vary during the temporal development of the CIA model, in the future it would be beneficial to profile the pro-inflammatory cytokine response in the CNS at various time points during development of the

disease. If pro-inflammatory cytokines are not increased within the brain then cytokine-induced mechanisms would not alter brain function in the CIA model.

7.1.3 Compensatory or beneficial mechanisms in the CIA model.

The innovative nature of the project also posed the problem of identifying the time point in the temporal evolution of the CIA model at which the peripheral immune system was most likely to have caused alterations in the brain. Cell proliferation was examined before the development of clinical symptoms and no significant difference was observed. However, there was a significant increase in cell proliferation after the development of clinical symptoms in CIA mice in comparison to controls. The significant increase in cell proliferation after the development of clinical symptoms further supports the interpretation that cytokines are not driving IDO to metabolise tryptophan to its neurotoxic components and that levels of pro-inflammatory cytokines in the brain were not increased. An increase in cell proliferation raises the possibility of compensatory or protective mechanisms. Studies of other rodent models of rheumatoid arthritis have reported protective mechanisms within the brain. Antagonism of the glucocorticoid receptor in the rat streptococcal cell wall model of arthritis increased the severity of arthritic clinical symptoms and it was suggested that corticosterone is beneficial and suppresses arthritic clinical symptoms (Sternberg et al., 1989). A recent study in the adjuvant induced arthritic model illustrated a corticosterone peak which paralleled the increase in neurogenesis. The same group also demonstrated *in vitro* that high levels of corticosterone decreased neurogenesis while lower levels similar to those found in the adjuvant induced arthritic model, increased neurogenesis (Wolf et al., 2009b). In addition, reduced cell survival has been reported in adrenalectomized rats which was attenuated by administration of corticosterone (Sloviter et al., 1989). The studies in the rodent rheumatoid arthritis models suggest possible compensatory mechanisms and there is evidence to suggest a beneficial effect of glucocorticoids. However, increased cell proliferation has been reported in adrenalectomized rats suggesting that normal levels of corticosterone negatively regulate cell proliferation in the rat dentate gyrus (Gould et al., 1992). It is therefore possible that glucocorticoids are both beneficial and detrimental depending on the level of glucocorticoids and the mechanism whereby the HPA-axis is activated. T-

cells may also increase cell proliferation, as T-cell knockout mice were found to have reduced neurogenesis in the dentate gyrus (Wolf et al., 2009a). It is therefore possible that the innate immune system is detrimental to cell proliferation and the adaptive immune system compensates by increasing cell proliferation. If there are compensatory or beneficial mechanisms occurring in the CIA model this suggests that the model does not represent a model of depression.

7.1.4 The CIA model as a model of depression.

There is currently no information which indicates the utility of the CIA model as a model for investigating mechanisms pertinent to depression. There are a number of studies where LPS is administered *in vivo* to investigate the effect of systemic inflammation on rodent behaviour. A characteristic response of LPS treatment is anhedonia and this model has frequently been used to investigate the association between depression and the immune response (Frenois et al., 2007; Yirmiya, 1996). However, one limitation of LPS-induced anhedonia is that it is coupled with sickness behaviour. The CIA model would have a number of benefits over the LPS model as it is chronic and the experimenter can measure the response to peripheral inflammation without the secondary response of sickness behaviour. However, further research is required to determine wither or not the CIA model is a suitable model to investigate the association between peripheral inflammation and depression. There are well established criteria that need to be met before a model is considered an animal model of depression (Willner and Mitchell, 2002). The studies presented in this thesis begin to address the dimension of construct validity, that is the examination of similar neurochemical processes. However, for the CIA model to be considered a valid model of depression it would also have to demonstrate two further dimensions. These are predictive validity; the model responds to antidepressant treatment and face validity; the model has a similar symptom profile (Willner and Mitchell, 2002). The CIA model is believed to mimic the human form of rheumatoid arthritis as in both patients and mice with CIA an autoimmune response develops against type II collagen (Kim et al., 1999; Londei et al., 1989). In addition there are specific major histocompatibility complex class II antigens associated with the development of the disease (Wooley et al., 1981; Rosloniec et al., 1998; Rosloniec et al., 1997) . However, it is unknown if the CIA

model has any face validity for depressive symptoms. Previously it has been shown that hypothalamic IL-1β concentration negatively correlates with sucrose consumption after chronic mild stress in rats (Grippo et al., 2005). Mice find sucrose a rewarding substance and if there is reduced consumption of sucrose it shows the mouse no longer derives pleasure from a rewarding substance suggesting anhedonia. In the future it would be beneficial to employ the saccharine consumption test to investigate anhedonia in the CIA model. If it was confirmed that the CIA model has face validity and the neurochemical changes have been fully characterised, it may then be worthwhile to examine the predictive validity of the model using antidepressant treatment.

7.2 Future work.

The aim of this thesis was to examine the brain in a murine CIA model as a means to investigate possible neurochemical, functional and structural links between rheumatoid arthritis and depression. The results suggest that the CIA model may not be a suitable model to investigate rheumatoid arthritis associated depression. There were a number of limitations in this study and unanswered questions. The most pertinent unanswered question was if CIA immunised mice display symptoms of anhedonia. The best test of anhedonia in the CIA model would be the saccharine solution test as other tests involve movement and it would not be possible to dissociate the effect of swollen limbs from anhedonia. This test was considered but was not performed due to time constraints but if this work were to be continued by another researcher I believe the saccharine test as a test of anhedonia should be their top priority.

The second major limitation of this thesis was the fact the immune response in the brain was not characterised. Our hypothesis was that inflammatory response in the periphery alters the brain. In reflection I feel I focused too much on the cytokine theory of depression. I believe we should have considered the immune system as a whole and cytokines are just a small part of the bigger picture. Nevertheless, it would have been benefical to characterise cytokine expression in the brain. Debbie Paterson a B.Sc. Med Sci student performed a pilot study to investigate pro-inflammatory cytokine expression within the whole brain, cortex, hippocampus and

cerebellum of CIA mice using Enzyme Linked ImmunoSorbent Assay and Multiplex Bead Immunoassay. The study failed to find a significant difference in IL-1β, IL-6 or TNF-α expression in the CIA group compared to the control group (data not published), although this may be attributed to the small sample sizes or the sensitivity of the detection method. This has led me to question whether the murine CIA model was the best model and in retrospective would a rat CIA model have been more appropriate. A rat CIA model would provide larger sample sizes to investigate cytokine expression in discrete brain regions such as the hippocampus and if successful, could be used to characterise the brain cytokine profile during the temporal evolution of the model.

I also feel I concentrated too much on the serotonergic system and should have also taken the time to investigate the hypothalamic-pituitary-adrenal axis (HPA-axis). The HPA-axis is associated with both depression and stress and therefore may more likely be altered in the CIA model. Finally in the distant future once the CIA model has been fully characterised it will then be necessary to dissociate the influence of the immune response to any possible change in the brain due to pain.

7.3 Conclusion

By further understanding animal models of disease they may in the future aid in the identification of target brain regions which, can be used to examine the therapeutic benefit of anti-inflammatory agents to treatment inflammation associated depression.

Reference List

aan het,R.M., Mathew,S.J., and Charney,D.S. (2009). Neurobiological mechanisms in major depressive disorder. CMAJ. *180*, 305-313.

Alexander,S.P., Mathie,A., and Peters,J.A. (2008). Guide to Receptors and Channels (GRAC), 3rd edition. Br. J. Pharmacol. *153 Suppl 2*, S1-209.

Alonzi,T., Fattori,E., Lazzaro,D., Costa,P., Probert,L., Kollias,G., De Benedetti,F., Poli,V., and Ciliberto,G. (1998). Interleukin 6 is required for the development of collagen-induced arthritis. J. Exp. Med. *187*, 461-468.

Andersen,M.L., Papale,L.A., Hipolide,D.C., Nobrega,J.N., and Tufik,S. (2005). Involvement of dopamine receptors in cocaine-induced genital reflexes after paradoxical sleep deprivation. Behav. Brain Res. *160*, 44-50.

Anderson,A.D., Oquendo,M.A., Parsey,R.V., Milak,M.S., Campbell,C., and Mann,J.J. (2004). Regional brain responses to serotonin in major depressive disorder. J. Affect. Disord. *82*, 411-417.

Annon. (1969). Mental problems in rheumatoid arthritis. Br. Med. J. *4*, 319.

Asquith,D.L., Miller,A.M., Hueber,A.J., McKinnon,H.J., Sattar,N., Graham,G.J., and McInnes,I.B. (2009a). Liver X receptor agonism promotes articular inflammation in murine collagen-induced arthritis. Arthritis Rheum. *60*, 2655-2665.

Asquith,D.L., Miller,A.M., McInnes,I.B., and Liew,F.Y. (2009b). Animal models of rheumatoid arthritis. Eur. J. Immunol. *39*, 2040-2044.

Aune,T.M., Golden,H.W., and McGrath,K.M. (1994). Inhibitors of serotonin synthesis and antagonists of serotonin 1A receptors inhibit T lymphocyte function in vitro and cell-mediated immunity in vivo. J. Immunol. *153*, 489-498.

Baldessarini,R.J. (1989). Current status of antidepressants: clinical pharmacology and therapy. J. Clin. Psychiatry *50*, 117-126.

Baldwin,R.M., Zea-Ponce,Y., Zoghbi,S.S., Laurelle,M., al Tikriti,M.S., Sybirska,E.H., Malison,R.T., Neumeyer,J.L., Milius,R.A., Wang,S., and . (1993). Evaluation of the monoamine uptake site ligand [123I]methyl 3 beta-(4-iodophenyl)-tropane-2 beta-carboxylate ([123I]beta-CIT) in non-human primates: pharmacokinetics, biodistribution and SPECT brain imaging coregistered with MRI. Nucl. Med. Biol. *20*, 597-606.

Banda,N.K., Levitt,B., Wood,A.K., Takahashi,K., Stahl,G.L., Holers,V.M., and Arend,W.P. (2009). Complement activation pathways in murine immune complex-induced arthritis and in C3a and C5a generation in vitro. Clin. Exp. Immunol.

Banks,W.A., Kastin,A.J., and Gutierrez,E.G. (1994). Penetration of interleukin-6 across the murine blood-brain barrier. Neurosci. Lett. *179*, 53-56.

Barrientos,R.M., Sprunger,D.B., Campeau,S., Higgins,E.A., Watkins,L.R., Rudy,J.W., and Maier,S.F. (2003). Brain-derived neurotrophic factor mRNA downregulation produced by social isolation is blocked by intrahippocampal interleukin-1 receptor antagonist. Neuroscience *121*, 847-853.

Baumeister,A.A., Hawkins,M.F., and Uzelac,S.M. (2003). The myth of reserpine-induced depression: role in the historical development of the monoamine hypothesis. J. Hist Neurosci. *12*, 207-220.

Ben Hur,T., Ben Menachem,O., Furer,V., Einstein,O., Mizrachi-Kol,R., and Grigoriadis,N. (2003). Effects of proinflammatory cytokines on the growth, fate, and motility of multipotential neural precursor cells. Mol. Cell Neurosci. *24*, 623-631.

Berkeley,M.B., Daussin,S., Hernandez,M.C., and Bayer,B.M. (1994). In vitro effects of cocaine, lidocaine and monoamine uptake inhibitors on lymphocyte proliferative responses. Immunopharmacol. Immunotoxicol. *16*, 165-178.

Besedovsky,H., del Rey,A., Sorkin,E., and Dinarello,C.A. (1986). Immunoregulatory feedback between interleukin-1 and glucocorticoid hormones. Science *233*, 652-654.

Blalock,J.E. (1984). The immune system as a sensory organ. J Immunol *132*, 1067-1070.

Bluthe,R.M., Laye,S., Michaud,B., Combe,C., Dantzer,R., and Parnet,P. (2000). Role of interleukin-1beta and tumour necrosis factor-alpha in lipopolysaccharide-induced sickness behaviour: a study with interleukin-1 type I receptor-deficient mice. Eur. J. Neurosci. *12*, 4447-4456.

Bluthe,R.M., Michaud,B., Kelley,K.W., and Dantzer,R. (1996). Vagotomy attenuates behavioural effects of interleukin-1 injected peripherally but not centrally. Neuroreport *7*, 1485-1488.

Bluthe,R.M., Walter,V., Parnet,P., Laye,S., Lestage,J., Verrier,D., Poole,S., Stenning,B.E., Kelley,K.W., and Dantzer,R. (1994). Lipopolysaccharide induces sickness behaviour in rats by a vagal mediated mechanism. C. R. Acad. Sci. III *317*, 499-503.

Boissier,M.C., Chiocchia,G., Bessis,N., Hajnal,J., Garotta,G., Nicoletti,F., and Fournier,C. (1995). Biphasic effect of interferon-gamma in murine collagen-induced arthritis. Eur. J. Immunol. *25*, 1184-1190.

Borsook,D., Becerra,L., Carlezon,W.A., Jr., Shaw,M., Renshaw,P., Elman,I., and Levine,J. (2007). Reward-aversion circuitry in analgesia and pain: implications for psychiatric disorders. Eur. J. Pain *11*, 7-20.

Brand,D.D. (2005). Rodent models of rheumatoid arthritis. Comp Med. *55*, 114-122.

Brand,D.D., Kang,A.H., and Rosloniec,E.F. (2004). The mouse model of collagen-induced arthritis. Methods Mol. Med. *102*, 295-312.

Brand,D.D., Latham,K.A., and Rosloniec,E.F. (2007). Collagen-induced arthritis. Nat. Protoc. *2*, 1269-1275.

Bremner,J.D., Narayan,M., Anderson,E.R., Staib,L.H., Miller,H.L., and Charney,D.S. (2000). Hippocampal volume reduction in major depression. Am. J. Psychiatry *157*, 115-118.

Brezun,J.M. and Daszuta,A. (1999). Depletion in serotonin decreases neurogenesis in the dentate gyrus and the subventricular zone of adult rats. Neuroscience *89*, 999-1002.

Buczko,W., de Gaetano,G., and Garattini,S. (1975). Effect of fenfluramine on 5-hydroxytryptamine uptake and release by rat blood platelets. Br. J. Pharmacol. *53*, 563-568.

Bull,S.J., Huezo-Diaz,P., Binder,E.B., Cubells,J.F., Ranjith,G., Maddock,C., Miyazaki,C., Alexander,N., Hotopf,M., Cleare,A.J., Norris,S., Cassidy,E., Aitchison,K.J., Miller,A.H., and Pariante,C.M. (2009). Functional polymorphisms in the interleukin-6 and serotonin transporter genes, and depression and fatigue induced by interferon-alpha and ribavirin treatment. Mol. Psychiatry *14*, 1095-1104.

Butovsky,O., Ziv,Y., Schwartz,A., Landa,G., Talpalar,A.E., Pluchino,S., Martino,G., and Schwartz,M. (2006). Microglia activated by IL-4 or IFN-gamma differentially induce neurogenesis and oligodendrogenesis from adult stem/progenitor cells. Mol. Cell Neurosci. *31*, 149-160.

Cacci,E., Claasen,J.H., and Kokaia,Z. (2005). Microglia-derived tumor necrosis factor-alpha exaggerates death of newborn hippocampal progenitor cells in vitro. J. Neurosci. Res. *80*, 789-797.

Cai,W., Khaoustov,V.I., Xie,Q., Pan,T., Le,W., and Yoffe,B. (2005). Interferon-alpha-induced modulation of glucocorticoid and serotonin receptors as a mechanism of depression. J. Hepatol. *42*, 880-887.

Cameron,H.A., Tanapat,P., and Gould,E. (1998). Adrenal steroids and N-methyl-D-aspartate receptor activation regulate neurogenesis in the dentate gyrus of adult rats through a common pathway. Neuroscience *82*, 349-354.

Cannon,D.M., Ichise,M., Rollis,D., Klaver,J.M., Gandhi,S.K., Charney,D.S., Manji,H.K., and Drevets,W.C. (2007). Elevated serotonin transporter binding in major depressive disorder assessed using positron emission tomography and [11C]DASB; comparison with bipolar disorder. Biol. Psychiatry *62*, 870-877.

Capuron,L., Neurauter,G., Musselman,D.L., Lawson,D.H., Nemeroff,C.B., Fuchs,D., and Miller,A.H. (2003a). Interferon-alpha-induced changes in tryptophan metabolism. relationship to depression and paroxetine treatment. Biol. Psychiatry *54*, 906-914.

Capuron,L., Raison,C.L., Musselman,D.L., Lawson,D.H., Nemeroff,C.B., and Miller,A.H. (2003b). Association of exaggerated HPA axis response to the initial injection of interferon-alpha with development of depression during interferon-alpha therapy. Am. J. Psychiatry *160*, 1342-1345.

Capuron,L., Ravaud,A., and Dantzer,R. (2000). Early depressive symptoms in cancer patients receiving interleukin 2 and/or interferon alfa-2b therapy. J. Clin. Oncol. *18*, 2143-2151.

Capuron,L., Ravaud,A., Neveu,P.J., Miller,A.H., Maes,M., and Dantzer,R. (2002). Association between decreased serum tryptophan concentrations and depressive symptoms in cancer patients undergoing cytokine therapy. Mol. Psychiatry *7*, 468-473.

Cavanagh,J., Paterson,C., McLean,J., Pimlott,S., McDonald,M., Patterson,J., Wyper,D., and McInnes,I. (2010). Tumour necrosis factor blockade mediates altered serotonin transporter availability in rheumatoid arthritis: a clinical, proof-of-concept study. Ann. Rheum. Dis.

Chao,H.M., Sakai,R.R., Ma,L.Y., and McEwen,B.S. (1998). Adrenal steroid regulation of neurotrophic factor expression in the rat hippocampus. Endocrinology *139*, 3112-3118.

Chiarugi,A., Calvani,M., Meli,E., Traggiai,E., and Moroni,F. (2001). Synthesis and release of neurotoxic kynurenine metabolites by human monocyte-derived macrophages. J. Neuroimmunol. *120*, 190-198.

Cho,Y.G., Cho,M.L., Min,S.Y., and Kim,H.Y. (2007). Type II collagen autoimmunity in a mouse model of human rheumatoid arthritis. Autoimmun. Rev. *7*, 65-70.

Conover,J.C., Erickson,J.T., Katz,D.M., Bianchi,L.M., Poueymirou,W.T., McClain,J., Pan,L., Helgren,M., Ip,N.Y., Boland,P., and . (1995). Neuronal deficits, not involving motor neurons, in mice lacking BDNF and/or NT4. Nature *375*, 235-238.

Cooper,S.M., Sriram,S., and Ranges,G.E. (1988). Suppression of murine collagen-induced arthritis with monoclonal anti-Ia antibodies and augmentation with IFN-gamma. J. Immunol. *141*, 1958-1962.

Costa,E., Groppetti,A., and Revuelta,A. (1971). Action of fenfluramine on monoamine stores of rat tissues. Br. J. Pharmacol. *41*, 57-64.

Coulter,C.L., Happe,H.K., Bergman,D.A., and Murrin,L.C. (1995). Localization and quantification of the dopamine transporter: comparison of [3H]WIN 35,428 and [125I]RTI-55. Brain Res. *690*, 217-224.

Courtenay,J.S., Dallman,M.J., Dayan,A.D., Martin,A., and Mosedale,B. (1980). Immunisation against heterologous type II collagen induces arthritis in mice. Nature *283*, 666-668.

Cuthill,D.J., Fowler,J.H., McCulloch,J., and Dewar,D. (2006). Different patterns of axonal damage after intracerebral injection of malonate or AMPA. Exp. Neurol. *200*, 509-520.

Dantzer R and Kelley KW (1989). Stress and immunity: an integrated view of relationships between the brain and the immune system. Life Sci *44*, 1992-2008.

Dantzer,R. (2001). Cytokine-induced sickness behavior: mechanisms and implications. Ann. N. Y. Acad. Sci. *933*, 222-234.

Datta,S.C. and Opp,M.R. (2008). Lipopolysaccharide-induced increases in cytokines in discrete mouse brain regions are detectable using Luminex xMAP((R)) technology. J. Neurosci. Methods *175*, 119-124.

Dawson,N., Ferrington,L., Olverman,H.J., Harmar,A.J., and Kelly,P.A. (2009). Sex influences the effect of a lifelong increase in serotonin transporter function on cerebral metabolism. J. Neurosci. Res. *87*, 2375-2385.

Dawson,N., Ferrington,L., Olverman,H.J., and Kelly,P.A. (2008). Novel analysis for improved validity in semi-quantitative 2-deoxyglucose autoradiographic imaging. J. Neurosci. Methods *175*, 25-35.

Dickens,C., McGowan,L., Clark-Carter,D., and Creed,F. (2002). Depression in rheumatoid arthritis: a systematic review of the literature with meta-analysis. Psychosom. Med. *64*, 52-60.

Dinarello,C.A. (2005). Interleukin-1beta. Crit Care Med. *33*, S460-S462.

Drevets,W.C., Price,J.L., and Furey,M.L. (2008). Brain structural and functional abnormalities in mood disorders: implications for neurocircuitry models of depression. Brain Struct. Funct. *213*, 93-118.

Duch,D.S., Woolf,J.H., Nichol,C.A., Davidson,J.R., and Garbutt,J.C. (1984). Urinary excretion of biopterin and neopterin in psychiatric disorders. Psychiatry Res. *11*, 83-89.

Dunbar,P.R., Hill,J., Neale,T.J., and Mellsop,G.W. (1992). Neopterin measurement provides evidence of altered cell-mediated immunity in patients with depression, but not with schizophrenia. Psychol. Med. *22*, 1051-1057.

Ekdahl,C.T., Claasen,J.H., Bonde,S., Kokaia,Z., and Lindvall,O. (2003). Inflammation is detrimental for neurogenesis in adult brain. Proc. Natl. Acad. Sci. U. S. A *100*, 13632-13637.

Elder,G.A., De Gasperi,R., and Gama Sosa,M.A. (2006). Research update: neurogenesis in adult brain and neuropsychiatric disorders. Mt. Sinai J. Med. *73*, 931-940.

Engblom,D., Saha,S., Engstrom,L., Westman,M., Audoly,L.P., Jakobsson,P.J., and Blomqvist,A. (2003). Microsomal prostaglandin E synthase-1 is the central switch during immune-induced pyresis. Nat. Neurosci. *6*, 1137-1138.

Engelhardt,B. and Ransohoff,R.M. (2005). The ins and outs of T-lymphocyte trafficking to the CNS: anatomical sites and molecular mechanisms. Trends Immunol. *26*, 485-495.

Ericsson,A., Liu,C., Hart,R.P., and Sawchenko,P.E. (1995). Type 1 interleukin-1 receptor in the rat brain: distribution, regulation, and relationship to sites of IL-1-induced cellular activation. J. Comp Neurol. *361*, 681-698.

Fiorentino,D.F., Zlotnik,A., Mosmann,T.R., Howard,M., and O'Garra,A. (1991). IL-10 inhibits cytokine production by activated macrophages. J. Immunol. *147*, 3815-3822.

Franklin K.B.J and Paxinos G. (2007). The mouse brain in stereotaxic coordinates. Elsevier).

Frenois,F., Moreau,M., O'Connor,J., Lawson,M., Micon,C., Lestage,J., Kelley,K.W., Dantzer,R., and Castanon,N. (2007). Lipopolysaccharide induces delayed FosB/DeltaFosB immunostaining within the mouse extended amygdala, hippocampus and hypothalamus, that parallel the expression of depressive-like behavior. Psychoneuroendocrinology *32*, 516-531.

Frodl,T., Meisenzahl,E.M., Zetzsche,T., Born,C., Groll,C., Jager,M., Leinsinger,G., Bottlender,R., Hahn,K., and Moller,H.J. (2002). Hippocampal changes in patients with a first episode of major depression. Am. J. Psychiatry *159*, 1112-1118.

Frodl,T., Schaub,A., Banac,S., Charypar,M., Jager,M., Kummler,P., Bottlender,R., Zetzsche,T., Born,C., Leinsinger,G., Reiser,M., Moller,H.J., and Meisenzahl,E.M. (2006). Reduced hippocampal volume correlates with executive dysfunctioning in major depression. J. Psychiatry Neurosci. *31*, 316-323.

Fuller,R.W. (1980). Pharmacology of central serotonin neurons. Annu. Rev. Pharmacol. Toxicol. *20*, 111-127.

Furuzawa-Carballeda,J., Vargas-Rojas,M.I., and Cabral,A.R. (2007). Autoimmune inflammation from the Th17 perspective. Autoimmun. Rev. *6*, 169-175.

Gage,F.H., Kempermann,G., Palmer,T.D., Peterson,D.A., and Ray,J. (1998). Multipotent progenitor cells in the adult dentate gyrus. J. Neurobiol. *36*, 249-266.

Gallagher,B.M., Fowler,J.S., Gutterson,N.I., MacGregor,R.R., Wan,C.N., and Wolf,A.P. (1978). Metabolic trapping as a principle of oradiopharmaceutical design: some factors resposible for the biodistribution of [18F] 2-deoxy-2-fluoro-D-glucose. J. Nucl. Med. *19*, 1154-1161.

Gilbertson,M.W., Shenton,M.E., Ciszewski,A., Kasai,K., Lasko,N.B., Orr,S.P., and Pitman,R.K. (2002). Smaller hippocampal volume predicts pathologic vulnerability to psychological trauma. Nat. Neurosci. *5*, 1242-1247.

Gobbi,M., Frittoli,E., Uslenghi,A., and Mennini,T. (1993). Evidence of an exocytotic-like release of [3H]5-hydroxytryptamine induced by d-fenfluramine in rat hippocampal synaptosomes. Eur. J. Pharmacol. *238*, 9-17.

Gould,E., Cameron,H.A., Daniels,D.C., Woolley,C.S., and McEwen,B.S. (1992). Adrenal hormones suppress cell division in the adult rat dentate gyrus. J. Neurosci. *12*, 3642-3650.

Gould,G.G., Pardon,M.C., Morilak,D.A., and Frazer,A. (2003). Regulatory effects of reboxetine treatment alone, or following paroxetine treatment, on brain noradrenergic and serotonergic systems. Neuropsychopharmacology *28*, 1633-1641.

Grippo,A.J., Francis,J., Beltz,T.G., Felder,R.B., and Johnson,A.K. (2005). Neuroendocrine and cytokine profile of chronic mild stress-induced anhedonia. Physiol Behav. *84*, 697-706.

Gutierrez,E.G., Banks,W.A., and Kastin,A.J. (1993). Murine tumor necrosis factor alpha is transported from blood to brain in the mouse. J. Neuroimmunol. *47*, 169-176.

HARRIS,T.H. (1957). Depression induced by Rauwolfia compounds. Am. J. Psychiatry *113*, 950.

Hart,B.L. (1988). Biological basis of the behavior of sick animals. Neurosci. Biobehav. Rev. *12*, 123-137.

Hebert,C., Habimana,A., Elie,R., and Reader,T.A. (2001). Effects of chronic antidepressant treatments on 5-HT and NA transporters in rat brain: an autoradiographic study. Neurochem. Int. *38*, 63-74.

Henry,J.P. and Scherman,D. (1989). Radioligands of the vesicular monoamine transporter and their use as markers of monoamine storage vesicles. Biochem. Pharmacol. *38*, 2395-2404.

Hestad,K.A., Tonseth,S., Stoen,C.D., Ueland,T., and Aukrust,P. (2003). Raised plasma levels of tumor necrosis factor alpha in patients with depression: normalization during electroconvulsive therapy. J. ECT. *19*, 183-188.

Heyes,M.P., Achim,C.L., Wiley,C.A., Major,E.O., Saito,K., and Markey,S.P. (1996). Human microglia convert l-tryptophan into the neurotoxin quinolinic acid. Biochem. J. *320 (Pt 2)*, 595-597.

Heyes,M.P., Saito,K., Lackner,A., Wiley,C.A., Achim,C.L., and Markey,S.P. (1998). Sources of the neurotoxin quinolinic acid in the brain of HIV-1-infected patients and retrovirus-infected macaques. FASEB J. *12*, 881-896.

Hietala,M.A., Nandakumar,K.S., Persson,L., Fahlen,S., Holmdahl,R., and Pekna,M. (2004). Complement activation by both classical and alternative pathways is critical for the effector phase of arthritis. Eur. J. Immunol. *34*, 1208-1216.

Himmerich,H., Milenovic,S., Fulda,S., Plumakers,B., Sheldrick,A.J., Michel,T.M., Kircher,T., and Rink,L. (2010). Regulatory T cells increased while IL-1beta decreased during antidepressant therapy. J. Psychiatr. Res.

Holmdahl,R., Klareskog,L., Rubin,K., Larsson,E., and Wigzell,H. (1985). T lymphocytes in collagen II-induced arthritis in mice. Characterization of arthritogenic collagen II-specific T-cell lines and clones. Scand. J. Immunol. *22*, 295-306.

Holmes,M.C., French,K.L., and Seckl,J.R. (1995). Modulation of serotonin and corticosteroid receptor gene expression in the rat hippocampus with circadian rhythm and stress. Brain Res. Mol. Brain Res. *28*, 186-192.

Hom,J.T., Cole,H., Estridge,T., and Gliszczynski,V.L. (1992). Interleukin-1 enhances the development of type II collagen-induced arthritis only in susceptible and not in resistant mice. Clin. Immunol. Immunopathol. *62*, 56-65.

Hozumi,H., Asanuma,M., Miyazaki,I., Fukuoka,S., Kikkawa,Y., Kimoto,N., Kitamura,Y., Sendo,T., Kita,T., and Gomita,Y. (2008). Protective effects of interferon-gamma against methamphetamine-induced neurotoxicity. Toxicol. Lett. *177*, 123-129.

Iosif,R.E., Ekdahl,C.T., Ahlenius,H., Pronk,C.J., Bonde,S., Kokaia,Z., Jacobsen,S.E., and Lindvall,O. (2006). Tumor necrosis factor receptor 1 is a negative regulator of progenitor proliferation in adult hippocampal neurogenesis. J. Neurosci. *26*, 9703-9712.

Irwin,M.R. and Miller,A.H. (2007). Depressive disorders and immunity: 20 years of progress and discovery. Brain Behav. Immun. *21*, 374-383.

Jacobs,B.L. and Azmitia,E.C. (1992). Structure and function of the brain serotonin system. Physiol Rev. *72*, 165-229.

Jin,K., Peel,A.L., Mao,X.O., Xie,L., Cottrell,B.A., Henshall,D.C., and Greenberg,D.A. (2004). Increased hippocampal neurogenesis in Alzheimer's disease. Proc. Natl. Acad. Sci. U. S. A *101*, 343-347.

Joosten,L.A., Helsen,M.M., van de Loo,F.A., and van den Berg,W.B. (2008). Anticytokine treatment of established type II collagen-induced arthritis in DBA/1 mice: a comparative study using anti-TNFalpha, anti-IL-1alpha/beta and IL-1Ra. Arthritis Rheum. *58*, S110-S122.

Jordan,G.R., McCulloch,J., Shahid,M., Hill,D.R., Henry,B., and Horsburgh,K. (2005). Regionally selective and dose-dependent effects of the ampakines Org 26576 and Org 24448 on local cerebral glucose utilisation in the mouse as assessed by 14C-2-deoxyglucose autoradiography. Neuropharmacology *49*, 254-264.

Kagari,T., Tanaka,D., Doi,H., and Shimozato,T. (2003). Essential role of Fc gamma receptors in anti-type II collagen antibody-induced arthritis. J. Immunol. *170*, 4318-4324.

Kaneko,N., Kudo,K., Mabuchi,T., Takemoto,K., Fujimaki,K., Wati,H., Iguchi,H., Tezuka,H., and Kanba,S. (2006). Suppression of cell proliferation by interferon-alpha through interleukin-1 production in adult rat dentate gyrus. Neuropsychopharmacology *31*, 2619-2626.

Kapur,S., Meyer,J., Wilson,A.A., Houle,S., and Brown,G.M. (1994). Modulation of cortical neuronal activity by a serotonergic agent: a PET study in humans. Brain Res. *646*, 292-294.

Kasama,T., Strieter,R.M., Lukacs,N.W., Lincoln,P.M., Burdick,M.D., and Kunkel,S.L. (1995). Interleukin-10 expression and chemokine regulation during the evolution of murine type II collagen-induced arthritis. J. Clin. Invest *95*, 2868-2876.

Katsuura,G., Arimura,A., Koves,K., and Gottschall,P.E. (1990). Involvement of organum vasculosum of lamina terminalis and preoptic area in interleukin 1 beta-induced ACTH release. Am. J. Physiol *258*, E163-E171.

Kavelaars,A., Cobelens,P.M., Teunis,M.A., and Heijnen,C.J. (2005). Changes in innate and acquired immune responses in mice with targeted deletion of the dopamine transporter gene. J. Neuroimmunol. *161*, 162-168.

Kenis,G. and Maes,M. (2002). Effects of antidepressants on the production of cytokines. Int. J. Neuropsychopharmacol. *5*, 401-412.

Kent,S., Rodriguez,F., Kelley,K.W., and Dantzer,R. (1994). Reduction in food and water intake induced by microinjection of interleukin-1 beta in the ventromedial hypothalamus of the rat. Physiol Behav. *56*, 1031-1036.

Khachigian,L.M. (2006). Collagen antibody-induced arthritis. Nat. Protoc. *1*, 2512-2516.

Kim,H.Y., Kim,W.U., Cho,M.L., Lee,S.K., Youn,J., Kim,S.I., Yoo,W.H., Park,J.H., Min,J.K., Lee,S.H., Park,S.H., and Cho,C.S. (1999). Enhanced T cell proliferative response to type II collagen and synthetic peptide CII (255-274) in patients with rheumatoid arthritis. Arthritis Rheum. *42*, 2085-2093.

Kim,S.U. and de Vellis,J. (2005). Microglia in health and disease. J. Neurosci. Res. *81*, 302-313.

Kirsch,I., Deacon,B.J., Huedo-Medina,T.B., Scoboria,A., Moore,T.J., and Johnson,B.T. (2008). Initial severity and antidepressant benefits: a meta-analysis of data submitted to the Food and Drug Administration. PLoS. Med. *5*, e45.

Kreiss,D.S., Wieland,S., and Lucki,I. (1993). The presence of a serotonin uptake inhibitor alters pharmacological manipulations of serotonin release. Neuroscience *52*, 295-301.

Kronfol,Z. and House,J.D. (1989). Lymphocyte mitogenesis, immunoglobulin and complement levels in depressed patients and normal controls. Acta Psychiatr. Scand. *80*, 142-147.

Laengle,U.W., Trendelenburg,A.U., Markstein,R., Nogues,V., Provencher-Bollinger,A., and Roman,D. (2006). GLC756 decreases TNF-alpha via an alpha2 and beta2 adrenoceptor related mechanism. Exp. Eye Res. *83*, 1246-1251.

Laye,S., Gheusi,G., Cremona,S., Combe,C., Kelley,K., Dantzer,R., and Parnet,P. (2000). Endogenous brain IL-1 mediates LPS-induced anorexia and hypothalamic cytokine expression. Am. J. Physiol Regul. Integr. Comp Physiol *279*, R93-R98.

Lee,J., Duan,W., and Mattson,M.P. (2002). Evidence that brain-derived neurotrophic factor is required for basal neurogenesis and mediates, in part, the enhancement of neurogenesis by dietary restriction in the hippocampus of adult mice. J. Neurochem. *82*, 1367-1375.

Lehto,S., Tolmunen,T., Joensuu,M., Saarinen,P.I., Vanninen,R., Ahola,P., Tiihonen,J., Kuikka,J., and Lehtonen,J. (2006). Midbrain binding of [123I]nor-beta-CIT in atypical depression. Prog. Neuropsychopharmacol. Biol. Psychiatry *30*, 1251-1255.

Li,Y., Xiao,B., Qiu,W., Yang,L., Hu,B., Tian,X., and Yang,H. (2010). Altered expression of CD4(+)CD25(+) regulatory T cells and its 5-HT(1a) receptor in patients with major depression disorder. J. Affect. Disord. *124*, 68-75.

Linnarsson,S., Willson,C.A., and Ernfors,P. (2000). Cell death in regenerating populations of neurons in BDNF mutant mice. Brain Res. Mol. Brain Res. *75*, 61-69.

Londei,M., Savill,C.M., Verhoef,A., Brennan,F., Leech,Z.A., Duance,V., Maini,R.N., and Feldmann,M. (1989). Persistence of collagen type II-specific T-cell clones in the synovial membrane of a patient with rheumatoid arthritis. Proc. Natl. Acad. Sci. U. S. A *86*, 636-640.

Lopez-Figueroa,A.L., Norton,C.S., Lopez-Figueroa,M.O., Armellini-Dodel,D., Burke,S., Akil,H., Lopez,J.F., and Watson,S.J. (2004). Serotonin 5-HT1A, 5-HT1B, and 5-HT2A receptor mRNA expression in subjects with major depression, bipolar disorder, and schizophrenia. Biol. Psychiatry *55*, 225-233.

Lubberts,E., Koenders,M.I., and van den Berg,W.B. (2005). The role of T-cell interleukin-17 in conducting destructive arthritis: lessons from animal models. Arthritis Res. Ther. *7*, 29-37.

Luheshi,G., Miller,A.J., Brouwer,S., Dascombe,M.J., Rothwell,N.J., and Hopkins,S.J. (1996). Interleukin-1 receptor antagonist inhibits endotoxin fever and systemic interleukin-6 induction in the rat. Am. J. Physiol *270*, E91-E95.

Luross,J.A. and Williams,N.A. (2001). The genetic and immunopathological processes underlying collagen-induced arthritis. Immunology *103*, 407-416.

Maes,M. (2010). Depression is an inflammatory disease, but cell-mediated immune activation is the key component of depression. Prog. Neuropsychopharmacol. Biol. Psychiatry.

Maes,M., Smith,R., and Scharpe,S. (1995). The monocyte-T-lymphocyte hypothesis of major depression. Psychoneuroendocrinology *20*, 111-116.

Maes,M., Stevens,W.J., DeClerck,L.S., Bridts,C.H., Peeters,D., Schotte,C., and Cosyns,P. (1993). Significantly increased expression of T-cell activation markers (interleukin-2 and HLA-DR) in depression: further evidence for an inflammatory process during that illness. Prog. Neuropsychopharmacol. Biol. Psychiatry *17*, 241-255.

Maes,M., Van der,P.M., Stevens,W.J., Peeters,D., DeClerck,L.S., Bridts,C.H., Schotte,C., and Cosyns,P. (1992). Leukocytosis, monocytosis and neutrophilia: hallmarks of severe depression. J. Psychiatr. Res. *26*, 125-134.

Malberg,J.E., Eisch,A.J., Nestler,E.J., and Duman,R.S. (2000). Chronic antidepressant treatment increases neurogenesis in adult rat hippocampus. J. Neurosci. *20*, 9104-9110.

Malison,R.T., Price,L.H., Berman,R., van Dyck,C.H., Pelton,G.H., Carpenter,L., Sanacora,G., Owens,M.J., Nemeroff,C.B., Rajeevan,N., Baldwin,R.M., Seibyl,J.P., Innis,R.B., and Charney,D.S. (1998). Reduced brain serotonin transporter availability in major depression as measured by [123I]-2 beta-carbomethoxy-3 beta-(4-iodophenyl)tropane and single photon emission computed tomography. Biol. Psychiatry *44*, 1090-1098.

Mandyam,C.D., Harburg,G.C., and Eisch,A.J. (2007). Determination of key aspects of precursor cell proliferation, cell cycle length and kinetics in the adult mouse subgranular zone. Neuroscience *146*, 108-122.

Mann,J.J., Malone,K.M., Diehl,D.J., Perel,J., Nichols,T.E., and Mintun,M.A. (1996). Positron emission tomographic imaging of serotonin activation effects on prefrontal cortex in healthy volunteers. J. Cereb. Blood Flow Metab *16*, 418-426.

Manoury-Schwartz,B., Chiocchia,G., Bessis,N., Abehsira-Amar,O., Batteux,F., Muller,S., Huang,S., Boissier,M.C., and Fournier,C. (1997). High susceptibility to collagen-induced arthritis in mice lacking IFN-gamma receptors. J. Immunol. *158*, 5501-5506.

MARSHALL,E.F., STIRLING,G.S., TAIT,A.C., and TODRICK,A. (1960). The effect of iproniazid and imipramine on the blood platelet 5-hydroxytrptamine level in man. Br. J. Pharmacol. Chemother. *15*, 35-41.

Mauri,C., Williams,R.O., Walmsley,M., and Feldmann,M. (1996). Relationship between Th1/Th2 cytokine patterns and the arthritogenic response in collagen-induced arthritis. Eur. J. Immunol. *26*, 1511-1518.

McGregor,I.S., Clemens,K.J., Van der,P.G., Li,K.M., Hunt,G.E., Chen,F., and Lawrence,A.J. (2003). Increased anxiety 3 months after brief exposure to MDMA ("Ecstasy") in rats: association with altered 5-HT transporter and receptor density. Neuropsychopharmacology *28*, 1472-1484.

Mella,L.F., Bertolo,M.B., and Dalgalarrondo,P. (2010). Depressive symptoms in rheumatoid arthritis. Rev. Bras. Psiquiatr.

Mendelson,S.D. and McEwen,B.S. (1992). Autoradiographic analyses of the effects of adrenalectomy and corticosterone on 5-HT1A and 5-HT1B receptors in the dorsal hippocampus and cortex of the rat. Neuroendocrinology *55*, 444-450.

Meyer,J.H., Houle,S., Sagrati,S., Carella,A., Hussey,D.F., Ginovart,N., Goulding,V., Kennedy,J., and Wilson,A.A. (2004). Brain serotonin transporter binding potential measured with carbon 11-labeled DASB positron emission tomography: effects of major depressive episodes and severity of dysfunctional attitudes. Arch. Gen. Psychiatry *61*, 1271-1279.

Meyer,J.H., Kruger,S., Wilson,A.A., Christensen,B.K., Goulding,V.S., Schaffer,A., Minifie,C., Houle,S., Hussey,D., and Kennedy,S.H. (2001). Lower dopamine

transporter binding potential in striatum during depression. Neuroreport *12*, 4121-4125.

Miller,A.H., Maletic,V., and Raison,C.L. (2009). Inflammation and its discontents: the role of cytokines in the pathophysiology of major depression. Biol. Psychiatry *65*, 732-741.

Ming,G.L. and Song,H. (2005). Adult neurogenesis in the mammalian central nervous system. Annu. Rev. Neurosci. *28*, 223-250.

Miura,H., Ozaki,N., Sawada,M., Isobe,K., Ohta,T., and Nagatsu,T. (2008). A link between stress and depression: shifts in the balance between the kynurenine and serotonin pathways of tryptophan metabolism and the etiology and pathophysiology of depression. Stress. *11*, 198-209.

Monje,M.L., Toda,H., and Palmer,T.D. (2003). Inflammatory blockade restores adult hippocampal neurogenesis. Science *302*, 1760-1765.

Mossner,R., Daniel,S., Schmitt,A., Albert,D., and Lesch,K.P. (2001). Modulation of serotonin transporter function by interleukin-4. Life Sci. *68*, 873-880.

Mossner,R., Heils,A., Stober,G., Okladnova,O., Daniel,S., and Lesch,K.P. (1998). Enhancement of serotonin transporter function by tumor necrosis factor alpha but not by interleukin-6. Neurochem. Int. *33*, 251-254.

Munro,J.F., Seaton,D.A., and Duncan,L.J. (1966). Treatment of refractory obesity with fenfluramine. Br. Med. J. *2*, 624-625.

Mussener,A., Litton,M.J., Lindroos,E., and Klareskog,L. (1997). Cytokine production in synovial tissue of mice with collagen-induced arthritis (CIA). Clin. Exp. Immunol. *107*, 485-493.

Nadgir,S.M. and Malviya,M. (2008). In vivo effect of antidepressants on [3H]paroxetine binding to serotonin transporters in rat brain. Neurochem. Res. *33*, 2250-2256.

Nakanishi,M., Niidome,T., Matsuda,S., Akaike,A., Kihara,T., and Sugimoto,H. (2007). Microglia-derived interleukin-6 and leukaemia inhibitory factor promote astrocytic differentiation of neural stem/progenitor cells. Eur. J. Neurosci. *25*, 649-658.

Nandakumar,K.S., Backlund,J., Vestberg,M., and Holmdahl,R. (2004). Collagen type II (CII)-specific antibodies induce arthritis in the absence of T or B cells but the arthritis progression is enhanced by CII-reactive T cells. Arthritis Res. Ther. *6*, R544-R550.

Neeck,G., Renkawitz R, and Eggert M (2002). Molecular aspects of glucocorticoid hormone action in rheumatoid arthritis. Cytokines, Cellular and Molecular Therapy *7*, 61-69.

Neto,F.L., Schadrack,J., Ableitner,A., Castro-Lopes,J.M., Bartenstein,P., Zieglgansberger,W., and Tolle,T.R. (1999). Supraspinal metabolic activity changes in the rat during adjuvant monoarthritis. Neuroscience *94*, 607-621.

Newberg,A.B., Amsterdam,J.D., Wintering,N., Ploessl,K., Swanson,R.L., Shults,J., and Alavi,A. (2005). 123I-ADAM binding to serotonin transporters in patients with major depression and healthy controls: a preliminary study. J. Nucl. Med. *46*, 973-977.

Newman,M.E., Shapira,B., and Lerer,B. (1998). Evaluation of central serotonergic function in affective and related disorders by the fenfluramine challenge test: a critical review. Int. J. Neuropsychopharmacol. *1*, 49-69.

Nibuya,M., Morinobu,S., and Duman,R.S. (1995). Regulation of BDNF and trkB mRNA in rat brain by chronic electroconvulsive seizure and antidepressant drug treatments. J. Neurosci. *15*, 7539-7547.

Niedbala,W., Cai,B., Wei,X., Patakas,A., Leung,B.P., McInnes,I.B., and Liew,F.Y. (2008). Interleukin 27 attenuates collagen-induced arthritis. Ann. Rheum. Dis. *67*, 1474-1479.

Nishioku,T., Matsumoto,J., Dohgu,S., Sumi,N., Miyao,K., Takata,F., Shuto,H., Yamauchi,A., and Kataoka,Y. (2010a). Tumor necrosis factor-alpha mediates the blood-brain barrier dysfunction induced by activated microglia in mouse brain microvascular endothelial cells. J. Pharmacol. Sci. *112*, 251-254.

Nishioku,T., Yamauchi,A., Takata,F., Watanabe,T., Furusho,K., Shuto,H., Dohgu,S., and Kataoka,Y. (2010b). Disruption of the blood-brain barrier in collagen-induced arthritic mice. Neurosci. Lett. *482*, 208-211.

O'Connor,J.C., Lawson,M.A., Andre,C., Moreau,M., Lestage,J., Castanon,N., Kelley,K.W., and Dantzer,R. (2008). Lipopolysaccharide-induced depressive-like behavior is mediated by indoleamine 2,3-dioxygenase activation in mice. Mol. Psychiatry.

O'Keane,V., Dinan,T.G., Scott,L., and Corcoran,C. (2005). Changes in hypothalamic-pituitary-adrenal axis measures after vagus nerve stimulation therapy in chronic depression. Biol. Psychiatry *58*, 963-968.

Ogren,S.O., Eriksson,T.M., Elvander-Tottie,E., D'Addario,C., Ekstrom,J.C., Svenningsson,P., Meister,B., Kehr,J., and Stiedl,O. (2008). The role of 5-HT(1A) receptors in learning and memory. Behav. Brain Res. *195*, 54-77.

Opp,M.R. and Krueger,J.M. (1991). Interleukin 1-receptor antagonist blocks interleukin 1-induced sleep and fever. Am. J. Physiol *260*, R453-R457.

Pettipher,E.R., Higgs,G.A., and Henderson,B. (1986). Interleukin 1 induces leukocyte infiltration and cartilage proteoglycan degradation in the synovial joint. Proc. Natl. Acad. Sci. U. S. A *83*, 8749-8753.

Philip,N.S., Carpenter,L.L., Tyrka,A.R., and Price,L.H. (2010). Pharmacologic approaches to treatment resistant depression: a re-examination for the modern era. Expert. Opin. Pharmacother. *11*, 709-722.

Pierucci-Lagha,A., Covault,J., Bonkovsky,H.L., Feinn,R., Abreu,C., Sterling,R.K., Fontana,R.J., and Kranzler,H.R. (2010). A functional serotonin transporter gene polymorphism and depressive effects associated with interferon-alpha treatment. Psychosomatics *51*, 137-148.

Piguet,P.F., Grau,G.E., Vesin,C., Loetscher,H., Gentz,R., and Lesslauer,W. (1992). Evolution of collagen arthritis in mice is arrested by treatment with anti-tumour necrosis factor (TNF) antibody or a recombinant soluble TNF receptor. Immunology *77*, 510-514.

Plotkin,S.R., Banks,W.A., and Kastin,A.J. (1996). Comparison of saturable transport and extracellular pathways in the passage of interleukin-1 alpha across the blood-brain barrier. J. Neuroimmunol. *67*, 41-47.

Price,J.L., Carmichael,S.T., and Drevets,W.C. (1996). Networks related to the orbital and medial prefrontal cortex; a substrate for emotional behavior? Prog. Brain Res. *107*, 523-536.

Ramamoorthy,S., Ramamoorthy,J.D., Prasad,P.D., Bhat,G.K., Mahesh,V.B., Leibach,F.H., and Ganapathy,V. (1995). Regulation of the human serotonin transporter by interleukin-1 beta. Biochem. Biophys. Res. Commun. *216*, 560-567.

Rang, H. P., Dale, M. M., Ritter, J. M., and Moore, P. K. Pharmacology. [5th Edition]. 2003. Churchill Livingstone.
Ref Type: Generic

Ranges,G.E., Sriram,S., and Cooper,S.M. (1985). Prevention of type II collagen-induced arthritis by in vivo treatment with anti-L3T4. J. Exp. Med. *162*, 1105-1110.

Romanovsky,A.A., Simons,C.T., Szekely,M., and Kulchitsky,V.A. (1997). The vagus nerve in the thermoregulatory response to systemic inflammation. Am. J. Physiol *273*, R407-R413.

Rosloniec,E.F., Brand,D.D., Myers,L.K., Esaki,Y., Whittington,K.B., Zaller,D.M., Woods,A., Stuart,J.M., and Kang,A.H. (1998). Induction of autoimmune arthritis in HLA-DR4 (DRB1*0401) transgenic mice by immunization with human and bovine type II collagen. J. Immunol. *160*, 2573-2578.

Rosloniec,E.F., Brand,D.D., Myers,L.K., Whittington,K.B., Gumanovskaya,M., Zaller,D.M., Woods,A., Altmann,D.M., Stuart,J.M., and Kang,A.H. (1997). An HLA-DR1 transgene confers susceptibility to collagen-induced arthritis elicited with human type II collagen. J. Exp. Med. *185*, 1113-1122.

Rowley,M.J., Nandakumar,K.S., and Holmdahl,R. (2008). The role of collagen antibodies in mediating arthritis. Mod. Rheumatol. *18*, 429-441.

Ruhe,H.G., Mason,N.S., and Schene,A.H. (2007). Mood is indirectly related to serotonin, norepinephrine and dopamine levels in humans: a meta-analysis of monoamine depletion studies. Mol. Psychiatry *12*, 331-359.

Sabol,K.E., Richards,J.B., and Seiden,L.S. (1992). Fluoxetine attenuates the DL-fenfluramine-induced increase in extracellular serotonin as measured by in vivo dialysis. Brain Res. *585*, 421-424.

Sackeim,H.A. (2001). The definition and meaning of treatment-resistant depression. J. Clin. Psychiatry *62 Suppl 16*, 10-17.

Saha,S., Engstrom,L., Mackerlova,L., Jakobsson,P.J., and Blomqvist,A. (2005). Impaired febrile responses to immune challenge in mice deficient in microsomal prostaglandin E synthase-1. Am. J. Physiol Regul. Integr. Comp Physiol *288*, R1100-R1107.

Sahay,A. and Hen,R. (2007). Adult hippocampal neurogenesis in depression. Nat. Neurosci. *10*, 1110-1115.

Saijo,S., Asano,M., Horai,R., Yamamoto,H., and Iwakura,Y. (2002). Suppression of autoimmune arthritis in interleukin-1-deficient mice in which T cell activation is impaired due to low levels of CD40 ligand and OX40 expression on T cells. Arthritis Rheum. *46*, 533-544.

Santarelli,L., Saxe,M., Gross,C., Surget,A., Battaglia,F., Dulawa,S., Weisstaub,N., Lee,J., Duman,R., Arancio,O., Belzung,C., and Hen,R. (2003). Requirement of hippocampal neurogenesis for the behavioral effects of antidepressants. Science *301*, 805-809.

Sarkissian,C.F., Wurtman,R.J., Morse,A.N., and Gleason,R. (1990). Effects of fluoxetine or D-fenfluramine on serotonin release from, and levels in, rat frontal cortex. Brain Res. *529*, 294-301.

Scharfman,H., Goodman,J., Macleod,A., Phani,S., Antonelli,C., and Croll,S. (2005). Increased neurogenesis and the ectopic granule cells after intrahippocampal BDNF infusion in adult rats. Exp. Neurol. *192*, 348-356.

Schildkraut JJ (1965). The catecholamine hypothesis of affective disorders: a review of supporting evidence. J Neuropsychiatry Clin Neurosci *7*, 524-533.

Schmidt,H.D. and Duman,R.S. (2007). The role of neurotrophic factors in adult hippocampal neurogenesis, antidepressant treatments and animal models of depressive-like behavior. Behav. Pharmacol. *18*, 391-418.

Seki,N., Sudo,Y., Yoshioka,T., Sugihara,S., Fujitsu,T., Sakuma,S., Ogawa,T., Hamaoka,T., Senoh,H., and Fujiwara,H. (1988). Type II collagen-induced murine arthritis. I. Induction and perpetuation of arthritis require synergy between humoral and cell-mediated immunity. J. Immunol. *140*, 1477-1484.

Selden,J.R., Dolbeare,F., Clair,J.H., Nichols,W.W., Miller,J.E., Kleemeyer,K.M., Hyland,R.J., and DeLuca,J.G. (1993). Statistical confirmation that immunofluorescent detection of DNA repair in human fibroblasts by measurement

of bromodeoxyuridine incorporation is stoichiometric and sensitive. Cytometry *14*, 154-167.

Shan,X., Chi,L., Bishop,M., Luo,C., Lien,L., Zhang,Z., and Liu,R. (2006). Enhanced de novo neurogenesis and dopaminergic neurogenesis in the substantia nigra of 1-methyl-4-phenyl-1,2,3,6-tetrahydropyridine-induced Parkinson's disease-like mice. Stem Cells *24*, 1280-1287.

Sheline,Y.I., Gado,M.H., and Kraemer,H.C. (2003). Untreated depression and hippocampal volume loss. Am. J. Psychiatry *160*, 1516-1518.

Sheline,Y.I., Wang,P.W., Gado,M.H., Csernansky,J.G., and Vannier,M.W. (1996). Hippocampal atrophy in recurrent major depression. Proc. Natl. Acad. Sci. U. S. A *93*, 3908-3913.

Shibata,H., Yoshioka,Y., Abe,Y., Ohkawa,A., Nomura,T., Minowa,K., Mukai,Y., Nakagawa,S., Taniai,M., Ohta,T., Kamada,H., Tsunoda,S., and Tsutsumi,Y. (2009). The treatment of established murine collagen-induced arthritis with a TNFR1-selective antagonistic mutant TNF. Biomaterials *30*, 6638-6647.

Singh,V.B., Corley,K.C., Phan,T.H., and Boadle-Biber,M.C. (1990). Increases in the activity of tryptophan hydroxylase from rat cortex and midbrain in response to acute or repeated sound stress are blocked by adrenalectomy and restored by dexamethasone treatment. Brain Res. *516*, 66-76.

Sloviter,R.S., Valiquette,G., Abrams,G.M., Ronk,E.C., Sollas,A.L., Paul,L.A., and Neubort,S. (1989). Selective loss of hippocampal granule cells in the mature rat brain after adrenalectomy. Science *243*, 535-538.

Sluzewska,A., Rybakowski,J., Bosmans,E., Sobieska,M., Berghmans,R., Maes,M., and Wiktorowicz,K. (1996). Indicators of immune activation in major depression. Psychiatry Res. *64*, 161-167.

Sluzewska,A., Rybakowski,J.K., Laciak,M., Mackiewicz,A., Sobieska,M., and Wiktorowicz,K. (1995). Interleukin-6 serum levels in depressed patients before and after treatment with fluoxetine. Ann. N. Y. Acad. Sci. *762*, 474-476.

Smith,R.S. (1991). The macrophage theory of depression. Med. Hypotheses *35*, 298-306.

Sokoloff,L. (1977). Relation between physiological function and energy metabolism in the central nervous system. J. Neurochem. *29*, 13-26.

Sokoloff,L. (1981). Localization of functional activity in the central nervous system by measurement of glucose utilization with radioactive deoxyglucose. J. Cereb. Blood Flow Metab *1*, 7-36.

Stahl,S.M. (1998). Mechanism of action of serotonin selective reuptake inhibitors. Serotonin receptors and pathways mediate therapeutic effects and side effects. J. Affect. Disord. *51*, 215-235.

Steele,A.D., Emsley,J.G., Ozdinler,P.H., Lindquist,S., and Macklis,J.D. (2006). Prion protein (PrPc) positively regulates neural precursor proliferation during developmental and adult mammalian neurogenesis. Proc. Natl. Acad. Sci. U. S. A *103*, 3416-3421.

Sternberg,E.M., Hill,J.M., Chrousos,G.P., Kamilaris,T., Listwak,S.J., Gold,P.W., and Wilder,R.L. (1989). Inflammatory mediator-induced hypothalamic-pituitary-adrenal axis activation is defective in streptococcal cell wall arthritis-susceptible Lewis rats. Proc. Natl. Acad. Sci. U. S. A *86*, 2374-2378.

Stockmeier,C.A., Mahajan,G.J., Konick,L.C., Overholser,J.C., Jurjus,G.J., Meltzer,H.Y., Uylings,H.B., Friedman,L., and Rajkowska,G. (2004). Cellular changes in the postmortem hippocampus in major depression. Biol. Psychiatry *56*, 640-650.

Suarez,E.C., Krishnan,R.R., and Lewis,J.G. (2003). The relation of severity of depressive symptoms to monocyte-associated proinflammatory cytokines and chemokines in apparently healthy men. Psychosom. Med. *65*, 362-368.

Svensson,L., Jirholt,J., Holmdahl,R., and Jansson,L. (1998). B cell-deficient mice do not develop type II collagen-induced arthritis (CIA). Clin. Exp. Immunol. *111*, 521-526.

Swiergiel,A.H. and Dunn,A.J. (2007). Effects of interleukin-1beta and lipopolysaccharide on behavior of mice in the elevated plus-maze and open field tests. Pharmacol. Biochem. Behav. *86*, 651-659.

Tagliamonte,A., Tagliamonte,P., Perez-Cruet,J., Stern,S., and Gessa,G.L. (1971). Effect of psychotropic drugs on tryptophan concentration in the rat brain. J. Pharmacol. Exp. Ther. *177*, 475-480.

Takagi,N., Mihara,M., Moriya,Y., Nishimoto,N., Yoshizaki,K., Kishimoto,T., Takeda,Y., and Ohsugi,Y. (1998). Blockage of interleukin-6 receptor ameliorates joint disease in murine collagen-induced arthritis. Arthritis Rheum. *41*, 2117-2121.

Takai,Y., Seki,N., Senoh,H., Yokota,T., Lee,F., Hamaoka,T., and Fujiwara,H. (1989). Enhanced production of interleukin-6 in mice with type II collagen-induced arthritis. Arthritis Rheum. *32*, 594-600.

Taler,M., Gil-Ad,I., Lomnitski,L., Korov,I., Baharav,E., Bar,M., Zolokov,A., and Weizman,A. (2007). Immunomodulatory effect of selective serotonin reuptake inhibitors (SSRIs) on human T lymphocyte function and gene expression. Eur. Neuropsychopharmacol. *17*, 774-780.

Tang,J.S., Qu,C.L., and Huo,F.Q. (2009). The thalamic nucleus submedius and ventrolateral orbital cortex are involved in nociceptive modulation: a novel pain modulation pathway. Prog. Neurobiol. *89*, 383-389.

Taupin,P. (2007). BrdU immunohistochemistry for studying adult neurogenesis: paradigms, pitfalls, limitations, and validation. Brain Res. Rev. *53*, 198-214.

Thomas,A.J., Davis,S., Morris,C., Jackson,E., Harrison,R., and O'Brien,J.T. (2005). Increase in interleukin-1beta in late-life depression. Am. J. Psychiatry *162*, 175-177.

Thomas,C.M. and Morris,S. (2003). Cost of depression among adults in England in 2000. Br. J. Psychiatry *183*, 514-519.

Thorbecke,G.J., Shah,R., Leu,C.H., Kuruvilla,A.P., Hardison,A.M., and Palladino,M.A. (1992). Involvement of endogenous tumor necrosis factor alpha and transforming growth factor beta during induction of collagen type II arthritis in mice. Proc. Natl. Acad. Sci. U. S. A *89*, 7375-7379.

Thornton,S., Duwel,L.E., Boivin,G.P., Ma,Y., and Hirsch,R. (1999). Association of the course of collagen-induced arthritis with distinct patterns of cytokine and chemokine messenger RNA expression. Arthritis Rheum. *42*, 1109-1118.

Toni,N., Laplagne,D.A., Zhao,C., Lombardi,G., Ribak,C.E., Gage,F.H., and Schinder,A.F. (2008). Neurons born in the adult dentate gyrus form functional synapses with target cells. Nat. Neurosci. *11*, 901-907.

Tsao,C.W., Lin,Y.S., Chen,C.C., Bai,C.H., and Wu,S.R. (2006). Cytokines and serotonin transporter in patients with major depression. Prog. Neuropsychopharmacol. Biol. Psychiatry *30*, 899-905.

Tsao,C.W., Lin,Y.S., and Cheng,J.T. (1997). Effect of dopamine on immune cell proliferation in mice. Life Sci. *61*, L-71.

Tuglu,C., Kara,S.H., Caliyurt,O., Vardar,E., and Abay,E. (2003). Increased serum tumor necrosis factor-alpha levels and treatment response in major depressive disorder. Psychopharmacology (Berl) *170*, 429-433.

Vallieres,L., Campbell,I.L., Gage,F.H., and Sawchenko,P.E. (2002). Reduced hippocampal neurogenesis in adult transgenic mice with chronic astrocytic production of interleukin-6. J. Neurosci. *22*, 486-492.

van den Berg,W.B., Joosten,L.A., Helsen,M., and van de Loo,F.A. (1994). Amelioration of established murine collagen-induced arthritis with anti-IL-1 treatment. Clin. Exp. Immunol. *95*, 237-243.

Van Praag,H., Kempermann,G., and Gage,F.H. (1999). Running increases cell proliferation and neurogenesis in the adult mouse dentate gyrus. Nat. Neurosci. *2*, 266-270.

Van Praag,H., Schinder,A.F., Christie,B.R., Toni,N., Palmer,T.D., and Gage,F.H. (2002). Functional neurogenesis in the adult hippocampus. Nature *415*, 1030-1034.

Vermeire,K., Heremans,H., Vandeputte,M., Huang,S., Billiau,A., and Matthys,P. (1997). Accelerated collagen-induced arthritis in IFN-gamma receptor-deficient mice. J. Immunol. *158*, 5507-5513.

Walmsley,M., Katsikis,P.D., Abney,E., Parry,S., Williams,R.O., Maini,R.N., and Feldmann,M. (1996). Interleukin-10 inhibition of the progression of established collagen-induced arthritis. Arthritis Rheum. *39*, 495-503.

Watson,W.C., Brown,P.S., Pitcock,J.A., and Townes,A.S. (1987). Passive transfer studies with type II collagen antibody in B10.D2/old and new line and C57Bl/6 normal and beige (Chediak-Higashi) strains: evidence of important roles for C5 and multiple inflammatory cell types in the development of erosive arthritis. Arthritis Rheum. *30*, 460-465.

Weiland,N.G., Orchinik,M., and Tanapat,P. (1997). Chronic corticosterone treatment induces parallel changes in N-methyl-D-aspartate receptor subunit messenger RNA levels and antagonist binding sites in the hippocampus. Neuroscience *78*, 653-662.

Wichers,M.C., Koek,G.H., Robaeys,G., Verkerk,R., Scharpe,S., and Maes,M. (2005). IDO and interferon-alpha-induced depressive symptoms: a shift in hypothesis from tryptophan depletion to neurotoxicity. Mol. Psychiatry *10*, 538-544.

Williams,R.O., Feldmann,M., and Maini,R.N. (2000). Cartilage destruction and bone erosion in arthritis: the role of tumour necrosis factor alpha. Ann. Rheum. Dis. *59 Suppl 1*, i75-i80.

Willner,P. and Mitchell,P.J. (2002). The validity of animal models of predisposition to depression. Behav. Pharmacol. *13*, 169-188.

Wojtowicz,J.M. and Kee,N. (2006). BrdU assay for neurogenesis in rodents. Nat. Protoc. *1*, 1399-1405.

Wolf,S.A., Steiner,B., Akpinarli,A., Kammertoens,T., Nassenstein,C., Braun,A., Blankenstein,T., and Kempermann,G. (2009a). CD4-positive T lymphocytes provide a neuroimmunological link in the control of adult hippocampal neurogenesis. J. Immunol. *182*, 3979-3984.

Wolf,S.A., Steiner,B., Wengner,A., Lipp,M., Kammertoens,T., and Kempermann,G. (2009b). Adaptive peripheral immune response increases proliferation of neural precursor cells in the adult hippocampus. FASEB J. *23*, 3121-3128.

Wooley,P.H., Luthra,H.S., Stuart,J.M., and David,C.S. (1981). Type II collagen-induced arthritis in mice. I. Major histocompatibility complex (I region) linkage and antibody correlates. J. Exp. Med. *154*, 688-700.

Wu,C., Ying,H., Grinnell,C., Bryant,S., Miller,R., Clabbers,A., Bose,S., McCarthy,D., Zhu,R.R., Santora,L., Davis-Taber,R., Kunes,Y., Fung,E., Schwartz,A., Sakorafas,P., Gu,J., Tarcsa,E., Murtaza,A., and Ghayur,T. (2007). Simultaneous targeting of multiple disease mediators by a dual-variable-domain immunoglobulin. Nat. Biotechnol. *25*, 1290-1297.

Xu,D., Jiang,H.R., Kewin,P., Li,Y., Mu,R., Fraser,A.R., Pitman,N., Kurowska-Stolarska,M., McKenzie,A.N., McInnes,I.B., and Liew,F.Y. (2008). IL-33 exacerbates antigen-induced arthritis by activating mast cells. Proc. Natl. Acad. Sci. U. S. A *105*, 10913-10918.

Yirmiya,R. (1996). Endotoxin produces a depressive-like episode in rats. Brain Res. *711*, 163-174.

Yirmiya,R., Avitsur,R., Donchin,O., and Cohen,E. (1995). Interleukin-1 inhibits sexual behavior in female but not in male rats. Brain Behav. Immun. *9*, 220-233.

Zhao,C., Deng,W., and Gage,F.H. (2008). Mechanisms and functional implications of adult neurogenesis. Cell *132*, 645-660.

Zhu,C.B., Blakely,R.D., and Hewlett,W.A. (2006). The proinflammatory cytokines interleukin-1beta and tumor necrosis factor-alpha activate serotonin transporters. Neuropsychopharmacology *31*, 2121-2131.

Zhu,C.B., Lindler,K.M., Owens,A.W., Daws,L.C., Blakely,R.D., and Hewlett,W.A. (2010). Interleukin-1 Receptor Activation by Systemic Lipopolysaccharide Induces Behavioral Despair Linked to MAPK Regulation of CNS Serotonin Transporters. Neuropsychopharmacology.

Zunszain,P.A., Anacker,C., Cattaneo,A., Carvalho,L.A., and Pariante,C.M. (2010). Glucocorticoids, cytokines and brain abnormalities in depression. Prog. Neuropsychopharmacol. Biol. Psychiatry.

Appendix 1: Details of solutions used.

Cryoprotectant

- 30% glycerol /30% ethylene in 10mM phosphate buffer, stored at -20℃

Poly-L-lysine slides

- Racks of slides were submerged in 1:10 dilution of poly-L-lysine (Sigma-Aldrich) solution for 5 minutes and dried over night in an oven at 65℃

Neutral-buffered formalin (pH 7.0)

- Combine 6.5g anhydrous sodium phosphate dibasic (Na_2HPO_4) and 4.0g acid sodium phosphate monohydrate ($NaH_2PO_4H_2O$, or 4.5g dehydrate) in 500ml distilled water. Once dissolved add 100ml formalin (37-40% formaldehyde) whilst stirring. Adjust to pH7 and add 400ml distilled water.

Abbreviations

2-DG	2-deoxyglucose
ABC	Avidin-biotin complex
AMY	amygdala
ANOVA	analysis of variance
BBB	blood brain barrier
BrdU	5' –bromo-2'-deoxyuridine
CAIA	collagen antibody induced arthritis
Cere	cerebellum
CIA	collagen induced arthritis
cin	cingulate cortex
CNS	central nervous system
CPu	caudate putamen
DAB	diaminobenzidine
DAT	dopamine transporter
DG	dentate gyrus
DRN	dorsal raphe nucleus
GP	globus pallidus
HC	hippocampus
HPA	hypothalamic-pituitary-adrenal
IFN	interferon
IL	interleukin
iLCMRglu	index of local cerebral glucose utilisation
i.p	intraperitoneal
i.v	intravenously
LCMRglu	local cerebral glucose utilisation
LH	lateral hypothalamus
LPS	lipopolysaccharide
N.acc	nucleus accumbens
NRS	normal rabbit serum
NS	non-specific
PAM	4% formaldehyde in phosphate buffer
PBS	phosphate buffed saline

s.c	subcutaneous
SD	standard deviation
SERT	serotonin transporter
SN	substantia nigra
SPECT	single photon emission computed tomography
SQ	semi-quantitative
thal	thalamus
TNF	tumor necrosis factor
VTA	ventral tegmental area
βCIT	β-carbomethoxy-3-β-(4 iodophenyl)tropane